The Characterization of HYA-1, A Hyaluronidase Family Member in *C.elegans*

by

Allison Chatel

A Thesis submitted to the Faculty of Graduate Studies of

The University of Manitoba

in partial fulfilment of the requirements of the degree of

MASTER OF SCIENCE

Department of Biochemistry and Medical Genetics

University of Manitoba

Winnipeg, Manitoba

THE UNIVERSITY OF MANITOBA

FACULTY OF GRADUATE STUDIES

*****

COPYRIGHT PERMISSION

The Characterization of HYA-1, A Hyaluronidase Family Member in *C.elegans*

BY

Allison Chatel

A Thesis/Practicum submitted to the Faculty of Graduate Studies of The University of Manitoba in partial fulfillment of the requirement of the degree

Of

Master of Science

TABLE OF CONTENTS

LIST OF FIGURES

LIST OF TABLES

LIST OF ABBREVIATIONS

β	beta
BLAST	Basic Local Alignment Search Tool
bp	base pair
Ca^{2+}	calcium
$CHCl_3$	chloroform
C.elegans	*Caenorhabditis elegans*
°C	degrees centigrade
CPG	chondroitin proteoglycans
ddH_2O	double distilled water
dH_2O	distilled water
dATP	deoxyadenosine triphosphate
dCTP	deoxycytosine triphosphate
dGTP	deoxyguanosine triphosphate
DIC	differential interference contrast
DNA	deoxyribonucleic acid
dNTP	deoxynucleotide triphosphate
dsRNA	double stranded ribonucleic acid
dTTP	deoxythymidine triphosphate
EBI	European Bioinformatics Institute
E.coli	*Escherichia coli*
ECM	extracellular matrix
EDTA	ethylene diaminetetraacetic acid
EGF	epidermal growth factor
Egl	egg-laying defect phenotype
EtBr	ethidium bromide
EtOH	ethanol
F1	first generation progeny from mating
g	gram
g	earth's gravitational constant
GAG	glycosaminoglycan
GFP	green fluorescent protein
HA	hyaluronan
HSPG	heparan sulfate proteoglycan
IDT	Integrated DNA Technologies
IPTG	isopropylthiogalactoside
kb	kilobase
LB	Luria Bertani
L1	larval stage one
L2	larval stage two
L3	larval stage three
L4	larval stage four
LG	linkage group
M	Molar

µg	microgram
min	minute
µl	microlitre
ml	millilitre
mM	millimolar
NCBI	National Centre for Biotechnology Information
ng	nanogram
NGM	Nematode growth medium
nM	nanomolar
N2	wild type strain of *C.elegans*
PCR	polymerase chain reaction
RNA	ribonucleic acid
Rpm	revolutions per minute
SDS	sodium dodecyl sulfate
SNP	single nucleotide polymorphism
TAE	tris-acetic acid EDTA buffer
Taq	*Thermus aquaticus*

SPECIFIC NOTATION OF GENES AND PROTEINS

Referring to **human**:

Protein	HYAL1
Gene	*HYAL1*

Referring to **mouse**:

Protein	Hyal1
Gene	*Hyal1*

Referring to ***C.elegans***:

Protein	HYA-1
Gene	*Hya-1*

ACKNOWLEDGEMENTS

Dave, thank you very much for all the time you have spent teaching me and helping me prepare over the years with such patience.

To my fellow lab members Cheryl Camia and Ludivine Coudiere, thank you for the help in the lab and friendship over the years.

To the members of the BTR lab: Thank you.
Dianna Martin, I appreciate all the discussions we've had over the years about science and everything else....I wish you the best in your future.
Dr. Rick Hemming, thank you for the time you've spent instructing me and helping me trouble-shoot over the past few years.

To the office staff, Jan, Lil, Tuntun and Gerhard, thank you for the help and guidance along the way.

To my committee members Dr. Triggs-Raine and Dr. Myal: thank you for the time you made available to me and the thought-provoking questions at our meetings.

Finally, to my family:
First of all, thank you Ryan for guiding me in the decision to continue my education.
Thank you Ron and Louise for the moral support you always provided.
And most of all, thank you Mom, Dad, Keith and Ryan for the support I needed to achieve this goal.
It has taken a few years but I am finally done!!! I could not have done this without you....

ABSTRACT

Mammalian hyaluronidases degrade hyaluronan and the related glycosaminoglycan chondroitin. *C.elegans* has one gene encoding a hyaluronidase family member named *hya-1*. A *hya-1* deletion mutant, *hya-1(dm12),* displays both egg-laying deficiency and squashed vulva phenotypes. Enlarged gut granules in the posterior region of the intestine are observed more frequently in *hya-1(dm12)* animals compared to wild type, suggesting an accumulation of HYA-1 substrate within the gut granules or lysosomes. Expression of green fluorescent protein driven by the *hya-1* promoter is detected in the PLM neurons, the intestine, the anal sphincter muscle and amphid neurons in the head. Although total protein extracts display no hyaluronan-degrading activity, chondroitin-degrading activity is detected. Alcian blue staining of *C.elegans* reveals chondroitin distributed in patches in the anterior and posterior section of the animal overlapping the pharynx and anterior section of the intestine and in the intestinal lumen and the germline. *hya-1(dm12)* displays increased Alcian blue staining intensity. The role of *oga-1* was also examined and no redundancy with *hya-1* was observed. Taken together, we propose HYA-1 is a chondroitinase localized to lysosomes in *C.elegans*.

1.INTRODUCTION

Hyaluronidases are enzymes that degrade the glycosaminoglycan hyaluronan (HA), the most abundant glycosaminoglycan in the vertebrate extracellular matrix (ECM). Both hyaluronidase and its substrates have integral roles in embryogenesis (Toole. 2001), wound healing (Li et al. 2000) , inflammation (Sampson et al. 1992) and cancer (Bertrand et al. 1997; Lokeshwar et al. 1996; Pham, Block, and Lokeshwar. 1997). Elevated levels of HA are associated with migrating and proliferating cells during the previously stated processes, while levels of hyaluronidase are elevated during wound healing, inflammation and following differentiation (Toole and Gross. 1971). Furthermore, hyaluronidase and glycosaminoglycans are becoming increasingly important in biotechnology. Glycosaminoglycans are used extensively in the preparation of biomaterials to aid in wound healing and tissue repair and hyaluronidase is used to modulate extracellular material during *in vitro* fertilization, therapeutic drug injections and surgical procedures. The discovery of new functional roles of glycosaminoglycans generates more interest in glycosaminoglycan metabolism, highlighting the importance of glycosaminoglycan degradation.

1.1 Glycosaminoglycans

Glycosaminoglycans are a group of linear polysaccharides composed of repeating disaccharide units. The disaccharide unit consists of a modified sugar which is either N-acetylglucosamine or N-acetylgalactosamine and an uronic acid sugar such as glucuronic acid or iduronate. This group of heteropolysaccharides includes hyaluronan (HA), chondroitin sulfate, dermatan sulfate, keratin sulfate, heparin and heparan sulfate (Table 1)

and can be found throughout the extracellular matrix (ECM). With the exception of HA, glycosaminoglycans form very large polysaccharide chains that attach to a protein backbone, becoming proteoglycans. HA remains unsulfated and is not covalently linked to a protein core but can bind proteoglycans to form large complexes. Glycosaminoglycans are highly acidic molecules due to the presence of the sulfate groups and the carboxyl groups on the saccharides. Both of these groups have a strong negative charge attracting many cations, which in turn attract water molecules and create a gel-like substance that fills the ECM providing resistance to pressure.

Table 1: Dissacharide unit composition of glycosaminoglycans

Glycosaminoglycan	Modified Sugar Unit	Uronic acid
Hyaluronan	N-acetyl-β-glucosamine	Glucuronic acid
Chondroitin	N-acetyl-β-galactosamine	Glucuronic acid
Heparan Sulfate	N-sulfo-D-glucosamine	Glucuronic acid
Dermatan sulfate	N-acetyl-β-galactosamine	Iduronic acid
Keratin sulfate	N-acetyl-α-glucosamine	Galactose

1.2 Hyaluronan (HA)

Within the body, HA is the most abundant in loose connective tissue including skin, synovial fluid and the umbilical cord. A significant amount of HA is also located in tissues of the brain, lungs, kidneys and muscles, with very little amounts in the liver or blood. As previously discussed, the major role of HA within these tissues is mechanical. HA within the ECM binds proteoglycans, attracting cations and water molecules to create a gel-like substance for structural support of the matrix. HA chains within this matrix may

also be bound by cell surface receptors or hyaladherins. This matrix now becomes the scaffold that facilitates cell migration, proliferation and adhesion to other cells.

1.3 HA Metabolism

Levels of HA are very dynamic within vertebrate tissues however the synthesis and degradation of HA is balanced within tissues to maintain a relatively constant amount of HA. Three HA synthases have been identified in humans and mice, HAS1, HAS2 and HAS3. These proteins synthesize HA at the cytoplasmic side of the plasma membrane and the growing HA polysaccharide extends through the membrane into the ECM (Spicer and McDonald. 1998).

HA is degraded in a step-wise process (Roden et al. 1989) by three catabolic pathways (reviewed by Stern, Asari, and Sugahara. 2006). One pathway, at the cellular level, includes binding, internalization and degradation within cells mediated predominately by the HA receptors, CD44 (Lesley et al. 2000; Ponta, Sherman, and Herrlich. 2003) and RHAMM (Cheung, Cruz, and Turley. 1999; Zhang et al. 1998). A second pathway involves the release of HA from the ECM for drainage by vasculature and lymphatics. Receptors involved in this pathway include HARE (Zhou et al. 2000), LYVE-1 (Banerji et al. 1999) and layilin (Bono et al. 2005). Ultimately HA migrates to the liver, kidney and possibly the spleen for degradation. The third pathway of HA degradation is scission by free radicals in the required environmental conditions (Deguine et al. 1998; Myint et al. 1987; Soltes et al. 2005). Once HA is internalized, hyaluronidases function as endoglycosidases; they cleave bonds from within the glycosaminoglycan to release oligosaccharides (mostly hexa- and tetrasaccharides) (Calabro et al. 2001). This differs

from exoglycosidases which cleave from the outside of the glycosaminoglycan to release disaccharide units from the ends of the glycosaminoglycan.

There are two mechanisms of action known for hyaluronidases, hydrolysis and elimination (Calabro et al. 2001). During hydrolysis, a water molecule is added across the bond being cleaved. Hydrolysis is predominately utilized by vertebrate enzymes while the other mechanism, elimination is predominately utilized by bacterial enzymes (Wisniewski, Sweet, and Stern. 2005). An elimination reaction consists of the removal of a water molecule from the hexuronic acid residue.

1.4 Hyaluronidases

Currently, at least six genes encoding hyaluronidase have been identified in humans and mice; *HYAL1, HYAL 2, HYAL3, HYAL4, SPAM1* and *HYALP1*. This family of enzymes share 40% sequence identity and are located in two clusters within the genome (Csoka, Scherer and Stern. 1999). *HYAL1*, *HYAL2* and *HYAL3* are located on human chromosome 3p21.3 with *HYAL4*, *HYALP1* and *SPAM1* located on chromosome 7q31.3 (Lokeshwar et al. 2002). In humans, all of these genes are transcriptionally active and translated except for *HYALP1*, a pseudogene (Stern. 2003). A seventh human gene, meningioma-expressed antigen 5 (*MGEA5*), is proposed to be an additional hyaluronidase. Although *MGEA5* is not related to the hyaluronidase gene family by sequence, its protein product has been reported to degrade HA (Heckel et al. 1998).

HYAL1 is expressed in the human heart, spleen, kidney, lung and liver tissues (Triggs-Raine et al. 1999). The highest levels of expression, in the liver, correspond to the major site of degradation of HA present in blood (Triggs-Raine et al. 1999). *HYAL1*

encodes a 57 kDa protein found in human serum and urine and displays activity at acidic pH (Frost et al. 1997).

HYAL2 is widely expressed throughout many human tissues. Northern blot analysis indicates mRNA expression in heart, skeletal muscles, colon, spleen, kidney, liver, small intestine, placenta, lung and pancreas but not in brain tissue (Lepperdinger, Strobl, and Kreil. 1998b; Triggs-Raine et al. 1999). *HYAL2* encodes a 60 kDa protein GPI-linked to the outer membrane of cells which is active at acidic pH (Lepperdinger, Strobl and Kreil. 1998). HYAL2 degrades high molecular weight HA to approximately 20 kDa fragments and does not hydrolyze chondroitin sulfates A, B or C, heparan sulfate or heparin (Lepperdinger, Strobl, and Kreil. 1998a).

Contrasting the expression patterns of *HYAL1* and *HYAL2*, *HYAL3* is weakly expressed in human brain tissue as well as kidney and liver tissues (Triggs-Raine et al. 1999). No further data is available on HYAL3.

SPAM1 is expressed in sperm (Cherr et al. 1996), epididymis, seminal vesicles, prostate (Deng, He and Martin-Delong. 2000), female reproductive tract (Zhang and Martin-Delong. 2003), placenta, fetal tissue (Csoka, Scherer and Stern. 1999), and breast tissue (Beech, Madan and Stern. 1999). *SPAM1* encodes a 64 kDa protein, PH-20, which is active at neutral pH and GPI-linked to the plasma and acrosomal membranes of sperm (Gmachl. 1993). PH-20 is important in the process of fertilization which will be discussed following (section 1.4.3).

HYALP1 is expressed in a wide range of tissues including the stomach, thyroid, spinal cord, lymph nodes, trachea, adrenal and bone marrow however *HYALP1* is not translated (Csoka, Scherer and Stern. 1999). *HYALP1* is a pseudogene due to a premature stop codon positioned in exon 1 (Csoka, Scherer and Stern. 1999).

HYAL4 is expressed in the placenta and skeletal muscle (Csoka, Scherer and Stern. 1999). HYAL4 is suggested to be a chondroitinase (Stern 2003) however no evidence to support this role is published to date.

1.4.1 Mucopolysaccharidosis IX (MPS IX)

Initially vertebrate hyaluronidase activity was thought to result from a single lysosomal enzyme. Based on this, researchers thought that a deficiency in hyaluronidase would cause a lethal lysosomal storage disorder. Defects in numerous genes encoding lysosomal enzymes can result in an accumulation of their substrates within lysosomes, causing lysosomal storage disorders. One patient was discovered with no detectable serum hyaluronidase (HYAL1) activity (Natowicz et al. 1996). This patient presented with a phenotype consisting of periarticular soft tissue masses, mild short stature and acetabular erosions. Histological examinations of patient tissue revealed macrophages with HA-filled lysosomes and, to a lesser extent, accumulation of HA in lysosomes of fibroblasts. The serum levels of HA were 38-90 fold over normal levels. This non-lethal lysosomal storage disorder was named mucopolysaccharidosis IX (Natowicz et al. 1996).

Typically lysosomal storage disorders cause neurological abnormalities (Online Mendelian Inheritance of Man (OMIM) database), however, *HYAL1* is not expressed in the brain. This fact, combined with the possibility of functional redundancy between the multiple hyaluronidases may account for the mild phenotype seen in MPS IX (Triggs-Raine et al. 1999).

1.4.2 The role of hyaluronidase in venom

Hyaluronidases have been found in venoms of snakes, bees, scorpion and wasps. Gmachl and Kreil (1992) identified the "spreading factor" in honeybee venom that allowed the diffusion of venom components through the tissues of the animal. This "spreading factor" was determined to be a hyaluronidase with a molecular mass of about 43 kDa. They further found that this hyaluronidase gene encodes a precursor form of hyaluronidase that must be cleaved prior to activation. After sequencing this gene, the predicted protein sequence was found to be orthologous to the only mammalian hyaluronidase sequence in EMBL at the time, guinea pig PH-20 (Lathrop et al. 1990). The two hyaluronidase sequences share 36% identity and the PH-20 gene is conserved among many different mammals as assessed by Southern blot analysis (Lathrop et al. 1990). Hyaluronidase in venom degrades HA, which is a major component of the human ECM. Consequently, the presence of this enzyme in venom allows a path to be digested through the ECM to the underlying cells where other venom components can take affect. This "path-clearing" function is also required in the critical biological process of fertilization.

1.4.3 The role of hyaluronidases in fertilization

The mammalian egg is surrounded by a layer of cumulus cells embedded in a HA-rich ECM. The sperm must penetrate this cumulus layer prior to reaching the zona pellucida where the sperm acrosome releases its contents. Subsequently, the sperm must continue clearing a path through the zona pellucida, which also contains HA, to reach the oocyte membrane for fertilization. Due to this function, hyaluronidases are thought to be important for fertilization. Previous studies with guinea pigs suggest that PH-20 not only

degrades the HA of the egg cumulus but may also mediate the binding of the sperm to the underlying zona pellucida (reviewed in Stern. 2003).

PH-20 is GPI-linked to the surface of sperm and the inner acrosomal membrane (Cherr, Yudin, and Overstreet. 2001). GPI-linked PH-20 is a 64 kDa protein which displays activity at neutral pH (Gmachl et al. 1993). The GPI-linked PH-20 is proteolytically processed into a soluble form with a molecular mass of about 53 kDa. This soluble PH-20 is active at acidic pH (Cherr et al 1996). It is not known exactly where the protein is cleaved, by which protease or why (Stern. 2003).

Cherr et al. (2001) support the theory that PH-20 functions as a receptor for HA-induced cell signaling. Their studies showed that GPI-linked PH-20 mediates HA-induced sperm signaling via an HA binding domain separate from the hyaluronidase domains. Further, they suggest that GPI-linked PH-20 appears to initiate intracellular signaling by aggregation in the plasma membrane and linkage to a 92 kDa cell signaling molecule.

The efficiency of fertilization in PH-20 null mice was examined by Baba et al. (2002). Mutant male mice were found to remain fertile. However, the sperm lacking PH-20 had a reduced ability to penetrate the egg cumulus *in vitro*. Further investigation through Western blot analysis revealed that at least one other protein of 55 kDa displays hyaluronidase activity and is present in the sperm lacking PH-20. Recently, Kim et al. (2005) identified a new hyaluronidase, Hyal5, to be the 55 kDa protein present in mouse epididymal sperm. They tested the ability of Hyal5 to disperse the cumulus layer of an oocyte by preparing a Hyal5 enriched sperm sample from PH-20 null mice. This sample did disperse the cumulous layer and furthermore, did not disperse the cumulous layer when in the presence of a hyaluronidase inhibitor, apigenin. The identification of a Hyal5 in

murine sperm confirms the presence of an additional hyaluronidase that may directly be involved in fertilization.

1.4.4 The role of hyaluronidases in cancer

Among the different hyaluronidases, no common pattern of prognosis has emerged. While some hyaluronidases stimulate cancer development, others help inhibit cancer development, yet some hyaluronidases can display both tendencies depending on the type of cancer involved (Lin and Stern. 2001; Rai et al. 2001; Udabage et al. 2005a; Udabage et al. 2005b). A comprehensive review of hyaluronan metabolism and its role in cancer biology (Stern. 2005) discusses findings suggesting HYAL1 and HYAL2 can both stimulate and inhibit cancer. *HYAL1* is deleted in many tobacco-related tumours (those of lungs, head, neck and upper airways (Frost et al. 2000; Lerman and Minna. 2000) while levels of *HYAL1* correlate with tumour aggressiveness and poor prognosis for bladder and prostate cancers (Hautmann et al. 2001; Lokeshwar et al. 2001). *HYAL2* also displays opposing affects. In human lung cancers and murine astrocytoma cells, overexpression of *HYAL2* accelerates tumor formation (Novak et al. 1999; Rai et al. 2001). However, under different circumstances, *HYAL2* can accelerate apoptosis which protects cells against cancer (Chang. 2002). Additionally, overexpression of *SPAM1* correlates with breast (Madan et al. 1999b), prostate (Madan et al. 1999a) and laryngeal cancers (Godin et al. 2000). Taken all together, the role of hyaluronidases in cancer is not well understood at this time.

1.4.5 MGEA5 as a seventh hyaluronidase?

MGEA5 was discovered during an immunological screen designed to identify naturally occurring IgG antibodies in the serum of human patients (Comtesse et al. 2000). This involved screening of a meningioma cDNA expression library with normal sera and comparing the antigens identified with those identified when probing the library with serum from the patient bearing the original tumor. This screen uncovered eight different antigens (termed *MGEA1-8*) that were reactive to the autologous serum. *MGEA5* was encoded by 4 different clones which had almost identical sequences. The consensus sequence consists of 5147 base pairs and the protein product is predicted to contain 916 amino acids. One of these four clones represents a splice variant producing a truncated product, MGEA5s (Comtesse et al. 2000).

The human *MGEA5* nucleotide sequence does not contain significant sequence similarity to any human hyaluronidase genes (Comtesse et al. 2000). However, MGEA5 protein sequences revealed a significant sequence similarity with the *C.elegans* protein OGA-1 that is described as "similar to hyaluronoglucosaminidase" (gi 861300) in the Wormbase database (Comtesse et al. 2000). The protein sequences share 31.2% identity and 45.8% conservation of residues versus MGEA5 (Heckel et al. 1998). Heckel *et al.* (1998) constructed a phylogenetic tree using a computer program (PHYLIP- Phylogeny Interference Package v 3.5) and demonstrated that *MGEA5* belongs to a different evolutionary group than human hyaluronidases. The authors located *MGEA5* in human chromosomal band 10q24.1- q24.3 and demonstrated expression in the brain, cranial skin, skeletal muscles, stomach, liver, placenta and heart. Through the use of an in-gel zymogram and a microtitre plate turbidity assay, hyaluronan degrading activity was detected at pH 7.0 and 37°C. The splice variant, MGEA5s, displayed reduced hyaluronan degrading activity as measured with the turbidity assay. Consequently it was proposed by

Heckel et al. (1998) that *MGEA5* likely represents a novel member of the human hyaluronidase family. However, due to both the lack of *in vivo* evidence of HA-degrading activity and the lack of sequence conservation which all other hyaluronidases share, the designation of *MGEA5* as a hyaluronidase remains controversial.

1.4.5.1 The connection between *MGEA5* and diabetes mellitus type 2

Diabetes mellitus is a human metabolic disorder usually caused by disrupted carbohydrate metabolism leading to increased blood sugar levels. The World Health Organization has recognized three types of diabetes mellitus. Type 2 results from a combination of defective insulin secretion and defective insulin responsiveness of cells. Under normal conditions, insulin enables cells to absorb glucose from blood to use as fuel and for conversion of glucose and lipids to glycogen and triglycerides for storage within cells.

Diabetes is a wide-spread disease around the world with increased prevalence in developed countries. In North America prevalence rates are even higher, so high that the WHO has declared diabetes an epidemic and predict one third of the population will develop it within their lifetime (http://en.wikipedia.org/wiki/Diabetes).

In 2005, a single nucleotide polymorphism (SNP) in ***MGEA5*** was determined to be associated with type 2 diabetes in a Mexican-American population in the United States (Lehman et al. 2005). This group had previously mapped linkage of type 2 diabetes to a region of chromosome 10q which includes the ***MGEA5*** locus (Duggirala et al. 1999). Sequencing of ***MGEA5*** from 44 subjects revealed 24 SNPs present within the gene. After extensive statistical analysis, one SNP (#14) was determined to have strong association with onset of diabetes. SNP14 consists of an A/T within intron 10 which contains an

alternative stop codon in a 130 kDa isoform produced. Although the SNP does not cause a nonsense or missense mutation, it may decrease expression of the 130 kDa isoform of MGEA5. Lehman et al. (2005) propose ***MGEA5*** is a susceptibility locus for type 2 diabetes in humans.

1.5 *C.elegans*

Caenorhabditis elegans is a small, non-parasitic, soil nematode. Sydney Brenner first used *C.elegans* beginning in 1965 to study the development and function of the nervous system (Brenner. 1974). Since then, *C.elegans* has become a model organism for the study of genetics, anatomy, development and behavior. In the last 30 years, research has elucidated the complete cell lineage of *C.elegans* for both male and hermaphrodite worms, and the complete genome has been sequenced. The genome sequence and the cell lineage are available as an on-line database at www.wormbase.org.

C.elegans is easily maintained in the laboratory and has many features that increase its appeal for use as a model organism. Worms are kept in Petri plates containing Nematode Growth Medium (NGM) agar where they feed on a lawn of OP50 *Escherichia coli (E.coli)*. On the agar the worms move on their lateral sides in either a forward or backward motion. The surface tension of water in the agar is enough to keep the worms confined to the surface. These worms have a very short reproduction time of three to four days with approximately 300 offspring per generation. The small size (about 1 mm in length) allows for storage of large numbers and relatively simple experimental techniques. However, they are not too small for visual inspection at a cellular and sub-cellular level using a dissecting microscope. Additionally, *C.elegans* is a transparent organism.

Therefore, many developmental events can be observed directly within a living organism which is quite a unique feature of this animal.

The basic anatomy of this worm consists of an outer tube covering an inner intestinal tract and gonad, separated by a fluid filled space called the psuedocoelom, which maintains shape through hydrostatic pressure. A protective cuticle, primarily composed of collagen, covers the outer tube. The cuticle is shed at each larval stage with a new cuticle secreted by the underlying hypodermis. The basement membrane is a specialized type of ECM and serves to cover most internal organs and separate them from the psuedocoelomic cavity. The major components of the basement membrane are type IV collagen, laminin, nidogen and proteoglycans. Also found within this organism is a nervous system, excretory/secretory system, muscles and rectum.

1.5.1 Reproduction

C.elegans has two sexes, male and hermaphrodite. A hermaphrodite has two X chromosomes and a male (XO) will arise spontaneously from an X chromosome non-disjunction at a frequency of 0.1%. The hermaphrodite produces both sperm and oocytes and is capable of self-fertilization. The life cycle of the worm includes 4 larval stages, L1-L4. Late in the fourth larval stage sperm is produced and stored in the spermathecum. Oocytes are produced once the worm is an adult. The oocytes form in the proximal arm of the gonad and move through towards the uterus (Figure 1). During this movement, oocytes pass into the spermatheca where fertilization occurs. Fertilized eggs then leave the spermatheca and enter the uterus, forming a single row of eggs. The eggs are laid by expulsion through the vulva at roughly the same rate at which they enter into the uterus so there is not an accumulation of eggs. Hermaphrodite worms are also capable of cross-

fertilization using sperm provided by a male. When males successfully mate with a hermaphrodite, the sexes of the resulting progeny are in a 1:1 ratio.

1.5.2 The vulva

The vulva, composed of 22 cells, creates a very important passage between the outside environment and the uterus for both male sperm entry and laying of fertilized eggs. Vulval development is a very important and regulated process comprised of multiple steps (reviewed in Sternberg and Horvitz. 1986). The initial step required is the birth of vulval precursor cells (VPCs) from the six hypodermal cells P3.p-P8.p during larval stages 1 and 2 (Figure 2-A) (Kimble and White. 1981; Sternberg and Horvitz. 1986; Sulston and White. 1980). Prior to late larval stage 3, correct vulval morphogenesis and patterning relies on the anchor cell (AC) (Kimble and White. 1981; Sulston and White. 1980). The AC is part of the somatic gonad positioned dorsally to the VPCs in the ventral hypodermis. Here the AC induces underlying VPCs P5.p-P7.p to adopt vulval fates during larval stage 3 while many other cell-cell interactions specify P3.p, P4.p and P8.p to adopt non-vulval fates including inductive, lateral and inhibitory signaling pathways. Three major signaling pathways identified in patterning of the vulva and uterus are the epidermal growth factor (EGF) (Hill and Sternberg. 1992), Notch (Koga and Ohshima. 1995; Simske and Kim. 1995) and Wnt (Gleason, Korswagen, and Eisenmann. 2002) pathways. During larval stage 4 vulval cells invaginate, the AC fuses with a multinucleate uterine cell (Cinar et al. 2003; Hanna-Rose and Han. 1999; Newman et al. 1999) while the vulval cells fuse to generate seven toroidal rings (Figure 2-B) (Sharma-Kishore et al. 1999). Finally, at the larval stage 4 molt vulval invagination everts to form the mature vulva (Sharma-Kishore et al. 1999).

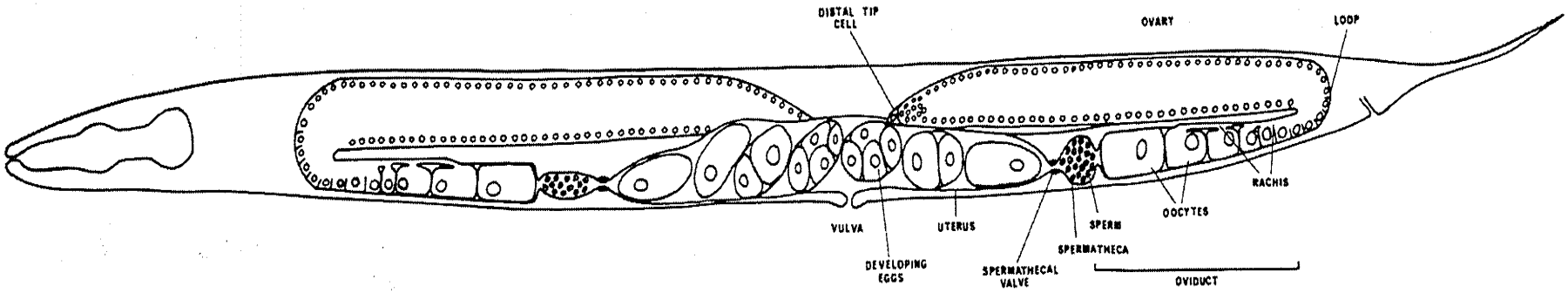

Figure 1: Gonad structure of adult hermaphrodite in *C.elegans.* The gonad is a symmetric structure which consists of two C-shaped gonad arms which extend to the anterior and posterior of a central and common vulva. Each gonad arm is comprised of a distal tip cell and syncitial area followed by an oviduct, spermatheca and a uterus. Oocytes migrate through the gonad arms. Here they pass through the spermathecum where sperm develops and the oocytes are fertilized prior to entering the uterus. The fertilized eggs begin to develop within the uterus prior to passing through the vulva when they are laid.

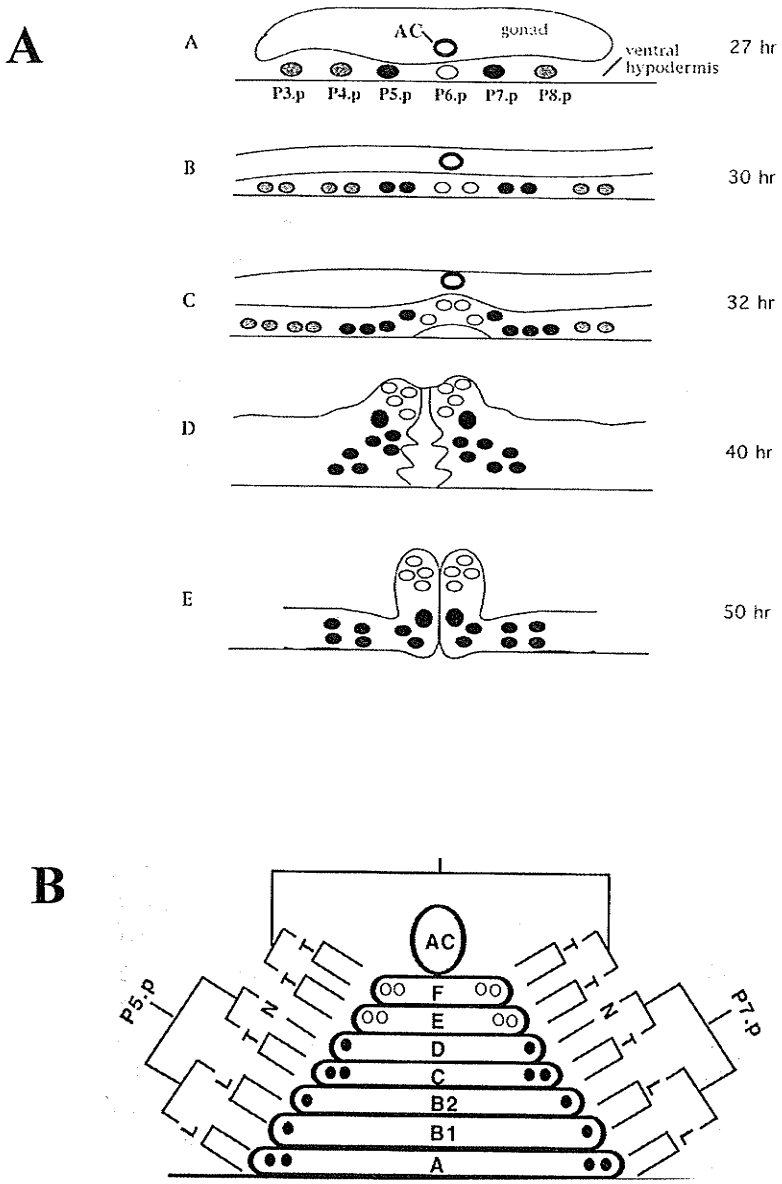

Figure 2: Vulval development displaying cell fates and migration patterns. (A) The anchor cell (AC) in the gonad induces the underlying ventral hypodermal cells P5.p-P7.p to adopt vulval fates. These cells divide and migrate forming distinct invagination patterns (B, C, D) as shown prior to evagination to form the mature vulval lips (E). (B) At mid-L4 stage, the vulval cells (as seen above in A-D (40 hr)) fuse to generate seven toroidal rings.

1.5.3 Muscles

C.elegans has 95 striated muscles as adults, 81 of which are body wall muscles that develop during embryogenesis (Moerman and Williams. 2006). These body wall muscles are organized into four quadrants running the length of the worm with two located dorsally and two ventrally (Hresko, Williams, and Waterston. 1994). Nonstriated muscles within the worm include the pharyngeal, intestinal, anal, vulval, uterine, contractile sheath and the male muscles required for mating. Due to the dominance of body wall muscles within this organism, these muscles are the best characterized to date. Striated muscles contain multiple contractile units called sacromeres as nonstriated muscles have only one contractile unit. Nematode and vertebrate muscles are very similar in their basic structure and function; however there are a few differences. Both systems consist of alternating myosin-containing thick filaments and actin-containing thin filaments, but, in nematodes the filaments are over five times longer then the vertebrate filaments and the thick filament contains an extra protein called paramyosin (Epstein, Casey, and Ortiz. 1993; Francis and Waterston. 1985). Another divergence is that nematode striated muscle cells remain mononucleate and pack in tightly with neighbouring muscle cells, underlying ECM and hypodermis, unlike vertebrate cells which fuse to create multinucleate myotubes (Moerman and Williams. 2006).

1.5.4 Lysosomes

C.elegans contains birefringent gut granules which are intestine specific sub-cellular organelles (Chitwood and Chitwood, 1974). The gut granules can be labeled with lysosomal markers and thus are identified as lysosomes (Hermann et al. 2005). Early embryos display a granular cytoplasmic distribution of lysosomes which become restricted

to the intestinal granules in later embryogenesis (Hersh, Hartwieg, and Horvitz. 2002). The gut granule loss (Glo) mutants are defective in lysosome biosynthesis and the Glo genes are homologous to genes involved in generation of specialized lysosome-related organelles such as the melanosomes in mammals or the pigment granules in Drosophila (Hermann et al. 2005). Therefore, it is unresolved whether the gut granules are lysosomes or lysosome-related organelles. Either way, the gut granules in *C.elegans* are acidic sub-cellular organelles.

Additionally, lysosomes are located in coelomocytes. *C.elegans* contains 6 coelomocyte cells which function as scavenger cells and are highly active in endocytotic removal of fluid phase molecules (Fares and Greenwald. 2001a). The process of endocytosis is required to reform endo-lysosomal organelles into lysosomes within coelomocyte cells (Fares and Greenwald. 2001a; Fares and Greenwald. 2001b; Hersh, Hartwieg, and Horvitz. 2002; Treusch et al. 2004).

1.6 Glycosaminoglycans in *C.elegans*

Unlike higher organisms which produce many different types of glycosaminoglycans, *C.elegans* synthesizes only two: unsulfated chondroitin and heparan sulfate (Morio et al. 2003; Suzuki et al. 2006; Toyoda, Kinoshita-Toyoda, and Selleck. 2000; Yamada et al. 2002). Chondroitin and HA are structurally similar. Both glycosaminoglycans have glucuronic acid as one saccharide unit but HA contains N-acetylglucosamine and chondroitin contains N-acetylgalactosamine which differs from N-acetylglucosamine by the position of a hydroxyl group on C4.

The glycosaminoglycan biosynthesis machinery in *C.elegans* was discovered when Herman et al. (1999) utilized the vulva as an *in vitro* model to explore epithelial

invagination. During this study a genetic screen identified eight genes, *squashed vulva (sqv) 1-8,* which disrupt vulval invagination. Mutations in *sqv1-8* cause a partial collapse in vulval invagination as detected by a reduced size and a slight decrease in the height of the vulval space at a mid fourth larval stage (when the space between invaginating vulval cells and the cuticle should be the largest). Patterns of vulval cell divisions in the mutant animals remained the same as in wild type animals with the correct number and overall pattern of vulval cells forming. The *sqv1-8* mutant strains also experienced a defect in laying eggs which was visible in older adult worms as the retention of eggs in the uteri and often protruding vulvae. *sqv-5* mutants were an exception to this phenotype. *sqv-5* mutants did not accumulate eggs in their uteri and laid very few eggs. The authors suggested that this mutant may exhibit this phenotype due to reduced production of oocytes. Further examination of *sqv1-8* mutants indicated a possible defect in oocyte formation and furthermore, a role for *sqv1-8* in embryonic development.

Over the next three years the molecular identities of *sqv1-8* were determined as well as their functional roles. *sqv1-4 & 6-8* are responsible for the formation of a tetrasaccharide link required on proteins for glycosaminoglycans to build onto. Their respective roles summarized in Figure 3 and are as follows (Bulik et al. 2000; Hwang and Horvitz. 2002a; Hwang and Horvitz. 2002b; Hwang et al. 2003a; Hwang et al. 2003b):

"SQV-4 (UDP-glucose dehydrogenase) synthesizes UDP-glucuronic acid (UDP-GlcA) in the cytoplasm, which is translocated into the lumen of the Golgi apparatus by the SQV-7 nucleotide-sugar transporter. SQV-7 also translocates UDP-galactose and UDP-acetylgalatosamine. SQV-1 catalyzes the decarboxylation of UDP-GlcA, forming the first nucleotide-sugar donor required for glycosaminoglycan biosynthesis, UDP-xylose. In the lumen of the Golgi apparatus, UDP-xylose, UDP-galactose and UDP-GlcA are used as

substrates of the SQV-6 xylosyltransferase, the SQV-3 galactosyltransferase I, the SQV-2 galactosyltransferase II and the SQV-8 glucuronyltransferase I to build onto the protein core the glycosaminoglycan linkage tetrasaccharide (GlcAβ1,3Galβ1,3Galβ1,4Xylβ-O-serine) on which glycosaminoglycan backbones polymerize" (Hwang et al. 2003a).

The next step required for glycosaminoglycan biosynthesis after generation of the tetrasaccharide link is initiation and elongation of the repeating disaccharide chain. Together, rib-1 and rib-2 may be responsible for the generation of heparan sulfate in *C.elegans*. Whereas rib-2 has displayed GlcNAc transferase activity involved in the generation of heparan sulfate, rib-1 is only proposed to have GlcUA transferase activity based solely on homology to a mammalian protein EXT1 (Kitagawa et al. 2001).

For the generation of chondroitin in humans, both chondroitin synthase (ChSy) and chondroitin polymerizing factor (ChPF) are necessary. ChSy displays both GlcUA and GalNAc transferase activity (Kitagawa et al. 2001). However, until chondroitin polymerizing experiments were executed *in vitro*, ChSy was thought to act alone in chondroitin biosynthesis. Upon expression within COS-1 cells, a soluble recombinant ChSy displayed very little GlcAT-II or GalNcT-II activity. Following co-expression with ChPF, the glycosyltransferase activities were greatly improved. Furthermore, both proteins display similar expression patterns in human tissues (Kitagawa et al. 2003).

Miziguchi et al. (2003) investigated the role of chondroitin in development and morphogenesis by preventing chondroitin synthesis through RNA interference (RNAi) in *C.elegans*. Chondroitin synthase is the protein product of *sqv-5* (Hwang et al. 2003b). Although no orthologue of ChPF is present within the *C.elegans* genome (Mizuguchi et al. 2003), a genetic screen unveiled a necessary cofactor, MIG-22, which is required with SQV-5 for chondroitin biosynthesis (Suzuki et al. 2006). RNA interference for *sqv-5*

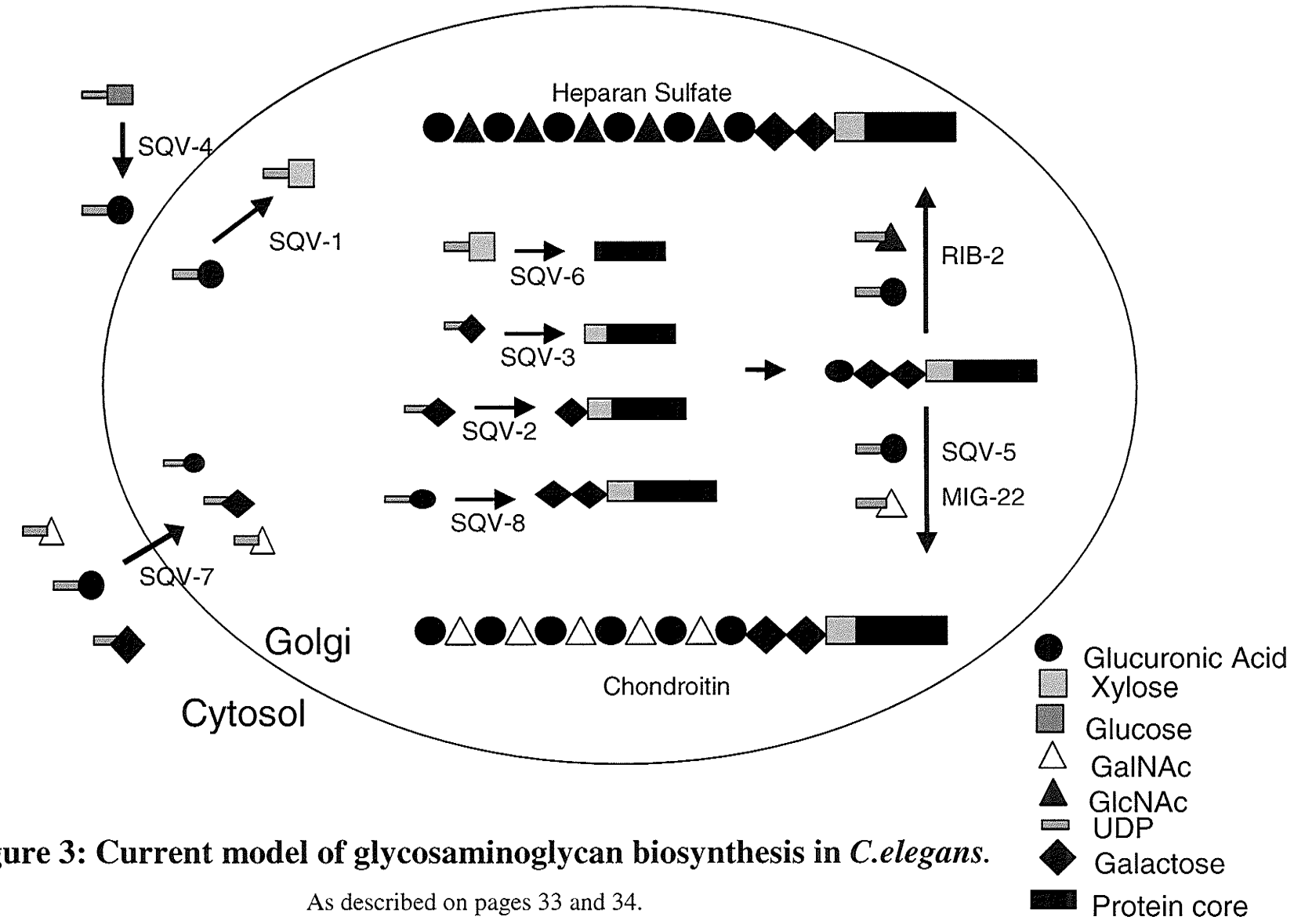

Figure 3: Current model of glycosaminoglycan biosynthesis in *C.elegans*.

As described on pages 33 and 34.

produces a distinct phenotype consisting of oocyte and fertilized egg death in utero for the initial worm exposed to RNAi. Most of the F1 generation were not viable and those which did survive had poor gonad formation with a very reduced amount of eggs laid. Any worms that developed to L4 developed morphologically abnormal oocytes and eggs resulting in abnormal positioning of eggs. A closer inspection of embryogenesis revealed defects in cytokinesis with a correlation between the time eggs were hatched and the severity of cytokinesis defects. To further demonstrate this correlation, an egg hatched within 12 hours of RNAi treatment displays a cytokinesis reversal pattern of 2 cell embryo to 4 cells to 6 cells and then to 4 cells. 70% of eggs hatched 20 hours after RNAi treatment did not undergo cytokinesis at all. These embryos became multinucleated and died. Overall, these results strongly indicate that chondroitin is essential for normal cytokinesis and nuclear division in *C.elegans*. The authors suggest that chondroitin may have a role in structure or be involved in a critical signaling pathway to illicit this effect.

Chondroitin is synthesized in the Golgi apparatus in cells in the vulva, uterus and oocytes (Hwang et al. 2003b) with weak expression detected in gonad arms and strong expression detected in the gonad, uterus, oocytes, spermatheca and fertilized eggs. Upon closer inspection, abundant chondroitin was evident in the fertilized egg shell and at the cell surface of cleavage stage embryos (Mizuguchi et al. 2003).

Suzuki et al. (2006) found mutant *mig-22* and *sqv-5* strains had weak phenotypes similar to the other *sqv* mutants. However, double mutant strains displayed much stronger phenotypes. Further support of the role of MIG-22 in chondroitin biosynthesis is its overlapping expression pattern with SQV-5. Both proteins are expressed in the proximal arm of the gonad, oocytes, adult gonads, developing vulval epithelium and the seam cells. The only difference is that MIG-22 is expressed in distal tip cells of the gonad arms where

SQV-5 is not expressed. Altogether, it is well established that both SQV-5 and MIG-22 are required for chondroitin synthesis (Suzuki et al. 2006).

1.7 Proteoglycans in *C.elegans*

1.7.1 Heparan sulfate proteoglycans

Heparan sulfate proteoglycans (HSPG) have an important role in structure adhesion and signaling. HSPGs can either increase signaling by sequestering signaling molecules near a cell surface receptor or inhibit signaling by sequestering signaling molecules and preventing diffusion across distances (Beauvais and Rapraeger. 2004; Merz et al. 2003; Rhiner et al. 2005b). This signaling, in turn, affects many developmental and biological processes from cell migration and adhesion to axon guidance (Beauvais and Rapraeger. 2004; Minniti et al. 2004; Rhiner et al. 2005a). The *C.elegans* genome contains at least four HSPGs, syndecan (SDN-1) (Minniti et al. 2004; Rhiner et al. 2005a) and glypican (Hudson et al. 2006) which are cell surface-anchored; and perlecan (UNC-52) (Rogalski et al. 2001) and CLE-1 (a homolog of collagen XVIII) which are extracellular HSPGs (Ackley et al. 2001).

1.7.1.1 Perlecan

In mammals, the proteoglycan perlecan is the major HSPG in the ECM. The homologue of perlecan in *C.elegans* is the protein product of *unc-52*. Normally UNC-52 is present in the basement membrane which lies between the body wall muscles and the underlying hypodermis with the myofilament lattice attached to the muscle cell membranes and further attached to the underlying basement membrane. A complete deficiency of UNC-52 in a *C.elegans* knock-out model is embryonic lethal due to

paralyzed and arrested elongation of worms during embryogenesis (Rogalski et al. 2001). This phenotype is a result of incorrect myofilament lattice assembly in muscles (Rogalski et al. 2001).

UNC-52 is generally expressed in body wall muscles of embryos, the basement membrane associated with the body wall, pharyngeal, anal and sex-specific muscles in larvae and adults (Merz et al. 2003; Rogalski et al. 2001). However, spatial and temporal expression patterns of UNC-52 isoforms may be unique or overlapping and this remains to be determined.

1.7.1.2 Syndecan

Minniti et al. (2004) identified syndecan (SDN-1) by RT-PCR and cDNA sequencing and determined its apparent molecular weight to be 50 kDa by Western blot analysis. Amino acid sequence analysis predicts four structural domains: a signal peptide, an ectodomain with glycosylation sequences, a hydrophobic transmembrane domain and a cytoplasmic domain; which are also present in mammalian syndecans. The authors investigated the mutant strain, *sdn-1(ok449),* which contains a deletion in the ectodomain where two putative glycosaminoglycan attachment sites are located. This mutant displayed an egg-laying deficient phenotype consisting of an accumulation of twice the number of eggs in the uterus as compared to wild type. However, all the eggs are eventually laid. A heparan sulfate-specific antibody showed HSPGs localized to the nerve ring, nerve cords and the vulva in wild type worms.

Further investigations into the role of syndecan in cell migration and axon guidance in *C.elegans* found that animals null for syndecan are viable but have defects in backwards locomotion, are variably egg-laying deficient and produce slightly reduced brood sizes

(Rhiner et al. 2005a). Within this knock-out strain, specific neurons displayed migratory defects and non-neuronal coelomcytes also migrated far from their normal positions. The authors tried to rescue the cell migration and axon guidance defects by expressing syndecan in either a cell autonomous or cell non-autonomous fashion. When syndecan was expressed in a nervous system-specific manner, significantly reduced defects in the neurons were observed. A transgenic strain expressing a C-terminally tagged SDN-1::GFP fusion protein displayed early developmental (embryos and L1) expression in neurons, pharynx and hypodermis later changing to strong expression in the nervous system, nerve ring and VNC motorneurons with weaker expression in the hypodermis and vulval cells. The authors concluded that SDN-1 is likely to act cell autonomously in neurons to promote cell migration and axon guidance. The authors further explored the role of syndecan in the known axon guidance pathway, Slit/Robo. Briefly, the severity of defects caused by the deletion of SLT-1 (a protein required for the correct migration of neurons; and whose deletion causes defects similar to those seen in the syndecan knock-out strain) does not increase when expressed with a syndecan deletion suggesting that the two proteins are disrupting the same pathway. Based on these observations, it was concluded that syndecan was required for axon guidance in *C.elegans*.

1.7.2 Chondroitin proteoglycans

Unlike heparan sulfate proteoglycans, there were no identified chondroitin proteoglycans until very recently. To identify possible chondroitin proteoglycans Olson et al. (2006) began with a bioinformatic analysis of the *C.elegans* genome. However this search did not identify any mammalian chondroitin sulfate proteoglycan core protein homologs. Chondroitin proteoglyans were later identified through a biochemical mass

screening procedure. First proteoglycans were isolated from a mixed-stage worm population and subjected to chondroitinase treatment followed by Western blot analysis. Detection of chondroitin proteoglycan candidates was achieved using an antibody which recognizes the neotope generated by chondroitinase digestion of chondroitin proteoglycans. When the chondroitinase digestion pattern was compared to the pattern generated by a heparan lyase digest, band patterns and intensities were not altered suggesting that mixed proteoglycans containing both heparan sulfate and chondroitin chains may not exist in *C.elegans*. Subsequently, chondroitin proteoglycan candidates were tagged and analyzed by mass spectrophotometry. Full length sequences of candidates were obtained from a protein database and designated as chondroitin proteoglycan core proteins if it had at least one glycosaminoglycan attachment site and a hydrophobic signal peptide. This screen resulted in the identification of nine novel chondroitin proteoglycan core proteins termed CPG-1-9. The authors proposed that the effect of depleting CPG-1 and CPG-2 should be similar to the effect seen for depleting SQV-5, chondroitin synthase, thus they inspected brood sizes. Further, RNAi for either CGP-1 or CPG-2 expressed alone showed no phenotypic changes however, expression together resulted in an embryonic lethal phenotype. Closer inspection of embryogenesis revealed failed polar body extrusion, absence of membrane ruffling and absence of space normally located between the embryonic plasma membrane and the egg shell during cell division. During cytokinesis, the cleavage furrow failed to form an ingress to separate the daughter cells. Instead the daughter nuclei fused and repeatedly attempted cell division without cytokinesis. Since depletion of CPG-1 and CPG-2 causes a similar embryonic defect as the depletion of SQV-5, CPG-1 and CPG-2 must be functionally important chondroitin proteoglycans

required at this early developmental stage (Olson et al. 2006) and others are likely to be involved in other functions like vulval development.

1.8 Glycosaminoglycan degradation in *C.elegans*

C.elegans has one gene, *hya-1*, which is identified as a member of the hyaluronidase family based on sequence similarity. However, no published evidence is available for the role of *hya-1* in *C.elegans*. As previously mentioned, *C.elgans* also has an orthologue of MGEA5, *oga-1*, which is proposed to be a novel hyaluronidase member.

In 2006, Forsythe et al reported that an *oga-1* deletion mutant, *oga-1(ok1207),* impacts O-linked glucosamine (O-GlcNAc) cycling, metabolism and dauer formation in *C.elegans*. The authors had previously shown that the hexosamine (O-GlcNAc)-signaling pathway affected the insulin-like signaling pathway in *C.elegans* (Hanover et al. 2005; Lubas et al. 1997). In humans, the hexosamine-signaling pathway has been implicated in diabetes mellitus and neurodegeneration (McClain et al. 2002; Wells, Vosseller, and Hart. 2003). More recent studies reveal linkage between MGEA5 and diabetes mellitus (Duggirala et al. 1999; Lehman et al. 2005).

Oga-1(ok1207) animals displayed altered levels of O-GlcNAc on nuclear pore proteins which did not interfere with nuclear transport; and elevated stores of glucose and trehalose with decreased lipid storage within a subset of gut granules (Forsythe et al. 2006). Additionally, *oga-1(ok1207)* generated a significant increase in dauers when expressed in a temperature-sensitive constitutive dauer allele background. Dauers are an alternative L3 development stage developed for survival within harsh environmental conditions such as high population density, lack of food and high temperatures (Cassada and Russell. 1975; Golden and Riddle. 1984a; Golden and Riddle. 1984b). The insulin-like

signaling pathway affects nutrient storage in *C.elegans* and regulates dauer development (Gottlieb and Ruvkun. 1994; Kimura et al. 1997; Rea and Johnson. 2003). In conclusion, OGA-1 functions in a pathway which normally inhibits the dauer formation signaling pathway (Forsythe et al. 2006).

The role of OGA-1 in glycosaminoglycan degradation and the issue of redundancy between *oga-1* and *hya-1* has not yet been addressed in a *C.elegans* model.

1.9 Aims of this study

1. Generate and characterize a *hya-1* deletion mutant in *C.elegans*

2. Examine possible redundancy between *hya-1* and *oga-1* through the generation and characterization of:

    i. A *oga-1* deletion mutant and

    ii. A *hya-1;oga-1* double mutant strain

3. Establish cellular expression patterns of *hya-1* and *oga-1*

4. Determine substrate degradation by HYA-1 in *C.elegans*

2. MATERIALS AND METHODS

2.1 Maintenance and handling of *C.elegans*

Worms were cultured, handled and manipulated using standard methods for *C.elegans* (Brenner, 1974). Briefly, worms were maintained on Nematode Growth Medium (NGM) agar (50 mM NaCl, 2.5% peptone, 5 uM cholesterol in ethanol, add 17% agar, after autoclaved add 1 mM $CaCl_2$, 1 mM $MgSO_4$, 25 mM potassium phosphate, pH 6.0) covered with a lawn of OP50 *E.coli,* in Petri plates, unless otherwise noted. The OP50 strain of *E.coli* is a uracil auxotroph with limited growth and NGM agar is uracil limiting, preventing *E.coli* overgrowth on the agar plates. Worms feed on the lawn of *E.coli.* A platinum wire pick was used to transfer worms from the plate. Between uses the pick was sterilized by flaming with an ethanol burner until the pick was red hot to prevent cross contamination. Bulk transfer of strains was performed by using a sterile toothpick and aseptic technique to transfer a small piece of agar with worms on it onto a new agar plate. The worms crawl off the piece of agar onto the new plate. Worms were maintained at room temperature unless noted otherwise. The N2 Bristol strain (N2) was the wild type strain used for comparison in the following experiments.

2.2 DNA and molecular biology methods

2.2.1 DNA isolation

2.2.1.1 Single worm lysis

To isolate and prepare DNA to be used as template for polymerase chain reactions (PCR), one or more worms were placed in a 100 µl PCR tube containing 10 µl of single worm lysis buffer (SWLB) (50 mM KCl, 100 mM Tris-HCl pH 8.3, 2.5 mM $MgCl_2$, 0.45% NP-40, 0.45% Tween-20, 0.01% gelatin and 60 µg/ml proteinase K). The tube was

then placed in a dry ice and ethanol bath for 15 minutes. Mineral oil was layered on top of the sample and it was placed in an Eppendorf gradient temperature cycler. The sample was incubated at 60°C for 60 minutes, then 95°C for 15 minutes, and finally held at 4°C. At this point 1 µl was removed for use as PCR template. The remaining sample was stored at 4°C.

2.2.1.2 Genomic DNA

To obtain the maximal number of healthy and growing animals, they were grown on five plates of Rich Agarose (50 mM NaCl, 0.75% BactoPeptone, 5 µg/ml cholesterol, 1.5% agarose and [the following were added after autoclaving, 1 mM $CaCl_2$, 1 mM $MgSO_4$ and 25 mM KPO_4 pH 6.0]), until just before starvation as visually assessed by depletion of *E.coli.* The worms were harvested by washing the plates with dH_20. The dH_20 was collected in a 15 ml conical tube and the worms were pelleted by centrifugation for 30 s at 400 x g. The supernatant was discarded and the pellet was washed twice with water. The pellet was re-suspended in 1 ml of H_20 and transferred to a 1.5 ml Eppendorf tube containing 500 uL of worm lysis solution (100 mM Tris pH 8.5, 100 mM NaCl, 50 mM EDTA, 1% SDS, 1% beta-mercaptoethanol and 100 µg/ml proteinase K). The sample was placed at -80°C for 30 minutes, thawed and then placed at 60°C for 45 minutes. The solution was then transferred to a new tube leaving behind large debris such as egg shells and worm carcasses. Extraction of genomic DNA was performed using 500 µl of phenol/$CHCl_3$ (1:1 v/v). The aqueous phase was then extracted with an equal volume of $CHCl_3$. The DNA was precipitated by adding 2.5 volumes of ethanol to the final aqueous phase and then collected by centrifugation for 10 minutes at 16, 000 x g. The resulting

pellet was washed with 70% ethanol and resuspended in 500 µl Tris-EDTA (10 mM Tris, 1 mM EDTA, pH 8.0) by rotating overnight at 4°C.

2.2.2 Oligonucleotide primer design

Primers were designed considering the following requirements to optimize primer specificity to the target DNA sequence. The primer length was approximately 20 base pairs and the G/C composition was approximately 50%. The last six 3' bases had 50% G/C composition, and the last two 3' bases were a C or G. Once candidate primer sequences were designed they were entered into the Oligo Analyzer 3.0 application available on the IDT website http://www.idtdna.com/analyzer/Applications/OligoAnalyzer/ to screen for homodimer formation (primers binding to other primers consisting of the same sequence), heterodimer formation (primers to be used together in a PCR reaction binding to each other) and hairpin formation (primers binding to themselves in a possible hairpin configuration). Primer sequences were optimal if no heterodimers, homodimers or hairpins were predicted to form, however, many primers did form some weak dimers or hairpins. All primers used in this project are listed in Appendix 5.1.

2.2.3 PCR

A standard PCR reaction consisted of template DNA, 1 X PCR buffer, 1.5 mM $MgCl_2$, 200 µM dNTPs (equal mix of dATP, dCTP, dGTP and dTTP), 100 ng of each primer and 5 units of recombinant *Taq* polymerase (Invitrogen) for a total reaction volume of 50 µl. The reaction proceeded in an Eppendorf Mastercycler Gradient PCR machine.

All cycle conditions, including temperatures, are listed specifically in methods sections describing the use of a PCR reaction.

2.2.4 Agarose gel electrophoresis

Agarose gel electrophoresis was used to separate DNA produced by PCR methods or by restriction digests based on size for analysis or further manipulations using the Fisherbrand horizontal units (mini or midi). Agarose gels consisted of 1% molecular biology grade agarose (Promega) dissolved in 1 X TAE (40 mM Tris-acetate and 1 mM EDTA) and 0.001% ethidium bromide. DNA samples were mixed 6:1 with 6 X Orange G loading dye (0.25% Orange G, 30% glycerol and 2 mM EDTA). A one kilobase ladder (Invitrogen) was loaded onto the gel and run out in addition to the samples to obtain a DNA fragment size reference. Samples were separated using 1 X TAE as running buffer, at approximately 100 volts with a Fisher FB300 power supply. The resulting gels were visualized with an AlphaImager2200 transilluminator and documented with AlphaEase FC software.

2.2.5 Extraction of DNA from gels

Extractions of DNA fragments from gels were performed utilizing the QIAquick Gel Extraction kit from Qiagen according to the manufacturer's instructions

.

2.2.6 DNA sequencing

To prepare PCR products for sequence analysis, multiple PCR reactions were prepared to obtain a sufficient quantity of each product, Platinum *Taq* (Invitrogen) was used to minimize the errors generated during amplification. PCR products were separated

on agarose gels and extracted using a Qiagen Gel Extraction Kit (see 2.2.5) for sequencing. Gel extraction products were combined. If the DNA fragment to be sequenced was longer then 2 kilobases, a concentration of 200 ng/µl was required. If the DNA fragment was shorter then 2 kilobases, a concentration of 50 ng/µl was required. The mass of DNA in 2 µl of gel extraction product was determined by visual assessment in comparison a mass ladder in an agarose gel (see 2.2.10.1). If the concentration was insufficient, more PCR product was made, gel extracted and added to the existing DNA sample. Once the required concentrations were achieved, a minimum of 50 µl of DNA sample was sent to the DNA Sequencing Facility at The Centre For Applied Genomics in Toronto, Ontario. Results from sequencing provided by email.

2.2.7 Miniprep of plasmid DNA

Plasmid DNA was purified from 4 ml of overnight *E.coli* culture grown in Luria-Bertani (LB) broth using a QIAprep Spin Miniprep Kit (Qiagen) according to the maufacturer's instructions.

2.2.8 Quantification of DNA

2.2.8.1 Mass ladder

DNA concentrations were estimated by visual comparison to a standard low mass ladder (Invitrogen) after separation by agarose gel electrophoresis

2.2.8.2 Spectrophotometric analysis

The concentration of DNA in samples was using a UV spectrophotometer (Pharmacia Biotech Ultrospec 1000). Five µl of the DNA sample was added to 995 µl of

autoclaved dH_2O. The spectrophotometer was blanked at 260 nm with a quartz cuvette containing autoclaved dH_2O. The diluted DNA sample was then transferred to the same quartz cuvette to obtain an absorbance reading. DNA with a concentration of 50 µg/ml has an established absorbance reading of 1.0 at 260 nm in a 1 cc cuvette. Based on this relationship, the obtained absorbance reading is multiplied by a factor of 50 to obtain the concentration of DNA in the cuvette in µg/ml. Finally, this concentration of DNA in the cuvette was divided by 5 to calculate the concentration of the undiluted DNA.

2.3 Mutant strains

2.3.1 WP777

In collaboration with Dr. J. G. Culotti (University of Toronto), the deletion mutant of T22C8.2, *T22C8.2(dm12),* was generated by mutagenizing a N2 worm population with trimethyl psoralen and UV radiation (TMP-UV) (as described by Gengyo-Ando and Mitani. 2000) and subsequent screening for a deletion using a PCR-based assay with gene specific primers for T22C8.2 (performed in Toronto). Upon receiving this strain in Winnipeg, new PCR primers were specified and reaction conditions were optimized to genotype T22C8.2. Due to the random mutagenesis technique used to generate this strain, outcrossing to N2 was required to eliminate undesired background mutations. To perform the outcross, a *T22C8.2(dm12)* hermaphrodite was crossed with a wild type male (Figure 4). Resulting progeny were isolated and cloned. Clones were then genotyped (see single worm lysis 2.1.2.1) using primers O & P (detected wild type alleles) and primers DM121 & DM12B (detected both wild type and deletion alleles) with DM12OP PCR program (95°C for 5 minutes followed by 32 cycles of 95°C for 45 seconds, 60°C for 45 seconds and 72°C for 45 seconds with a final step of 72°C for 5 minutes). Next, a hermaphrodite

worm heterozygous for *T22C8.2(dm12)* was selected and allowed to self fertilize. Again the resulting progeny was isolated and cloned. The clones were genotyped and at this point a hermaphrodite worm homozygous for the deletion mutation was selected for further use. Outcrossing of the deletion mutant was comprised of three repetitions of crossing with N2 followed by genotype selection.

2.3.2 WP667

This strain was obtained from the *C.elegans* Gene Knockout Project at OMRF which is part of the International *C.elegans* Gene Knockout Consortium. The deletion mutant of T20B5.3, *T20B5.3(ok1207),* was generated by mutagenizing a N2 worm population with trimethyl psoralen and UV radiation (TMP-UV) and subsequent screening for a deletion using a PCR-based assay with gene specific primers for T20B5.3. Upon receiving this strain in Winnipeg, new PCR primers were specified and reaction conditions were optimized to genotype T20B5.3. Due to the random mutagenesis technique used to generate this strain, outcrossing to N2 was required to eliminate undesired background mutations. To perform the outcross, an *oga-1(ok1207)* hermaphrodite was crossed with a wild type male (Figure 5). Resulting progeny were isolated and cloned. Clones were then genotyped (see single worm lysis 2.1.2.1) using primer pair MGEA2 & MGEAD and primer pair MGEAA2 & MGEA1 and the PCR program MGEA (Initial step of 95°C for 10 minutes followed by 36 cycles of 95°C for 45 seconds, 60°C for 45 seconds and 72°C for 45 seconds with a final step of 72°C for 10 minutes). Next, a hermaphrodite worm heterozygous for *oga-1(ok1207)* was selected and allowed to self fertilize. Again the resulting progeny was isolated and cloned. The clones were genotyped and at this point a hermaphrodite worm homozygous for *oga-1(ok1207)*

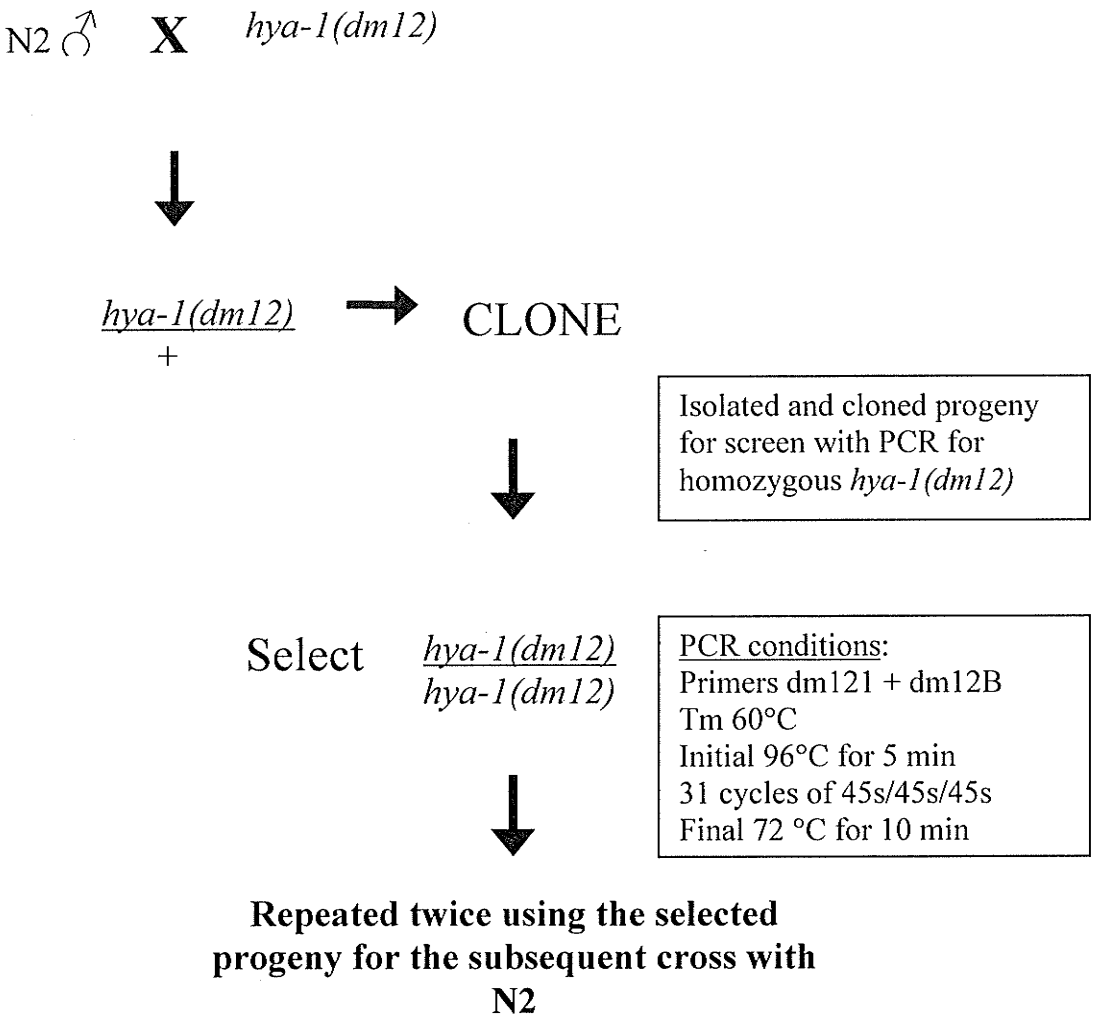

Figure 4: Outcross of *hya-1(dm12)* with N2 wild type flowchart.

was selected for further use. Outcrossing of the deletion mutant was comprised of three repetitions of crossing with N2 followed by genotype selection.

2.3.3 WP668

The outcrossed strains homozygous for *hya-1(dm12)* and *oga-1(ok1207)* were crossed to generate *hya-1(dm12);oga-1(ok1207)*. The resulting progeny were isolated and cloned. Clones were then genotyped at both alleles as previously described (see above). A worm heterozygous at both alleles was then allowed to self fertilize. Resulting progeny were isolated and cloned, with genotyping performed on the cloned worms. A worm homozygous for the deletion mutations at both alleles was selected for further use.

2.4 Microscopy and phenotypic analysis

A Leica MZ6 dissecting microscope (0.63-4.0X magnification) was utilized to visualize worms for most techniques such as picking worms to transfer to other plates or generating DNA template for single worm lysis, sex determination and initial gross morphological and movement phenotype assessments. If a higher magnification was required for phenotype analysis, a Zeiss Stemi M2BIO QUAD stereomicroscope with 10X and 20X objectives was utilized (9.6-660X magnification). This Zeiss stereomicroscope also had an ebq 100 isolated fluorescent lamp and filters required to enable visualization of green fluorescent protein expression.

2.4.1 Vulval phenotype analysis

A Zeiss imager.A1 AxioImager compound microscope with a 63X objective was utilized for the detailed phenotypic analysis of worms, including the vulval phenotypes

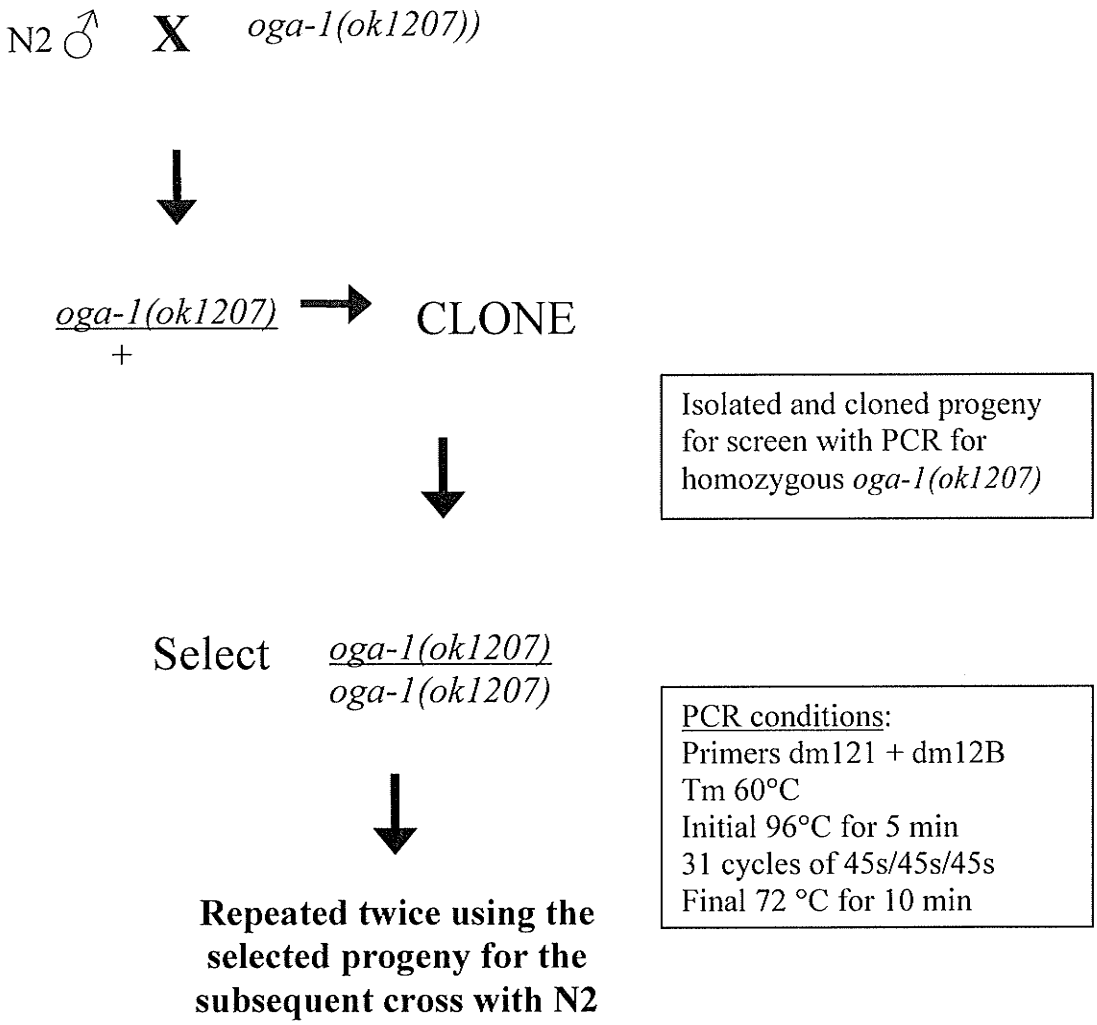

Figure 5: Outcross of *oga-1(ok1207)* with N2 wild type flowchart.

(630X magnification). The microscope had an Axiocam MRc camera and an X-cite 120 Fluorescence Illumination System. Differential interference contrast (DIC) optics were used with the 63X objective.

2.4.2 Still imaging

Agarose pads were made by placing a drop of agarose (2% agarose in dH_20) on a glass slide positioned between two other slides which had a small piece of masking tape on them. These three slides were positioned in parallel. A fourth slide was then placed on top of the agarose drop so it was positioned across the three other slides and resting on top of the flanking slides with the masking tape. The masking tape was the spacer to create the thickness of the agarose pad. After the agarose had cooled and hardened (approximately 5 seconds minimum), the two slides sandwiching the agarose pad were slid apart to maintain the agarose pad on one of the slides. Worms were then transferred onto this pad using a platinum worm pick. A drop of 5 mM levamisole (in M9, see appendix) was placed on the worms. After the worms had stopped moving (approximately 15 minutes) a cover slip was placed on top of the agarose pad and worms could be visualized with a microscope.

2.5 RNA interference (RNAi)

2.5.1 RNA vectors

RNA vectors were from the Ahringer *C.elegans* cDNA Expression Library (Timmons and Fire. 1998) and were obtained from Dr. Peter Roy (University of Toronto). These vectors contained a tetracycline resistance gene for selection. For these studies, the vectors X4-N19 containing *oga-1* cDNA and II6-EO2 containing *hya-1* cDNA were used.

2.5.2 Transformation of HT115(DE3) *E.coli* cells

To make competent HT115(DE3) *E.coli* cells, the calcium chloride method was utilized. A 25 ml overnight culture of HT115(DE3) *E.coli* cells (in LB and 12.5 μg/ml tetracycline) was centrifuged at 3000 rpm for 10 minutes at 4°C. The pellet was resuspended in 0.5 X original volume of cold, sterile 50 mM $CaCl_2$ by gently pipetting. The cells were incubated on ice for 30 minutes followed by centrifugation as described previously. The pellet was resuspended in 0.1 X the original volume of cold, sterile 50 mM $CaCl_2$ by gently pipetting. Cells are now competent for transformation. To transform, 50-200 μl of competent cells were added to a cold, sterile tube on ice. 1-100 ng of plasmid DNA was added to the cells and the tube was incubated in an ice bath for 30 min. The tube was then immersed in a 37°C water bath for 1 min followed by incubation in an ice bath for 2 min. 1 ml sterile SOC (2% Bacto Tryptone, 0.5% Bacto Yeast Extract, 0.05% NaCl, 2.5 mM KCl, 20 mM glucose [added after autoclaving], pH 7.0)
media was added to the tube with incubation at 37°C for 1 h. Cells were then plated on LB agar (12.5 μg/ml tetracycline) and incubated overnight at 37°C.

2.5.3 Expression of RNA

RNAi was performed by the feeding method (as described in Kamath et al. 2001). The feeding method consists of plating the transformed HT115(DE3) *E.coli* cells on NGM agar (with 50 μg/ml carbinicillin and 0.4 mM IPTG). The plates sat at room temperature overnight prior to seeding with transformed HT115(DE3) *E.coli*, at which point the plates were then stored at room temperature overnight prior to use. The IPTG in the plate induces transcription of the RNA vector. Once the plates were ready for use, a L4

hermaphrodite worm was placed on a plate and stored at 20°C until the resulting progeny were analyzed approximately three days later (see phenotype analysis 2.3).

2.6 Integrated reporter strain

The first attempt at generating an integrated reporter strain used *unc47*::GFP. unc-47::GFP is expressed in all GABAergic neurons including 19 ventral nerve cords and four specific neurons in the head and tail (Eastman, Horvitz, and Jin. 1999) . The second attempt used *unc73;evIs111*. *unc73;evIs111* worms appeared uncoordinated (Unc phenotype) and display pan neuronal GFP expression (Hutter et al. 2005). As illustrated in Figure 6, the generation of this strain consisted of multiple steps. First, a N2 male was crossed with *unc73;evIs111*. The resulting progeny were heterozygous for all three genes and a male was selected for the next step, to cross with a *hya-1(dm12)* hermaphrodite. Progeny resulting from this step were all heterozygous at *hya-1* and selected for by weak GFP expression and non-Unc representing heterozygosity of the GFP *evIs111* and homozygosity of wild type alleles at *unc73*. These selected worms were isolated on new plates and allowed to self-fertilize. The resulting progeny were screened for homozygosity of *evIs111* as assessed by visualization of strong GFP expression and genotyped at *hya-1* to select worms homozygous for *hya-1(dm12)*. Ultimately, this progeny is the integrated reporter strain. Inspection of neuron structure and patterning was performed utilizing a stereomicroscope (see 2.3). RNAi (see 2.4) was also performed on the integrated reporter strain using *oga-1* RNA to investigate the effects of loss of both *oga-1* and *hya-1* on neuronal structure and patterning.

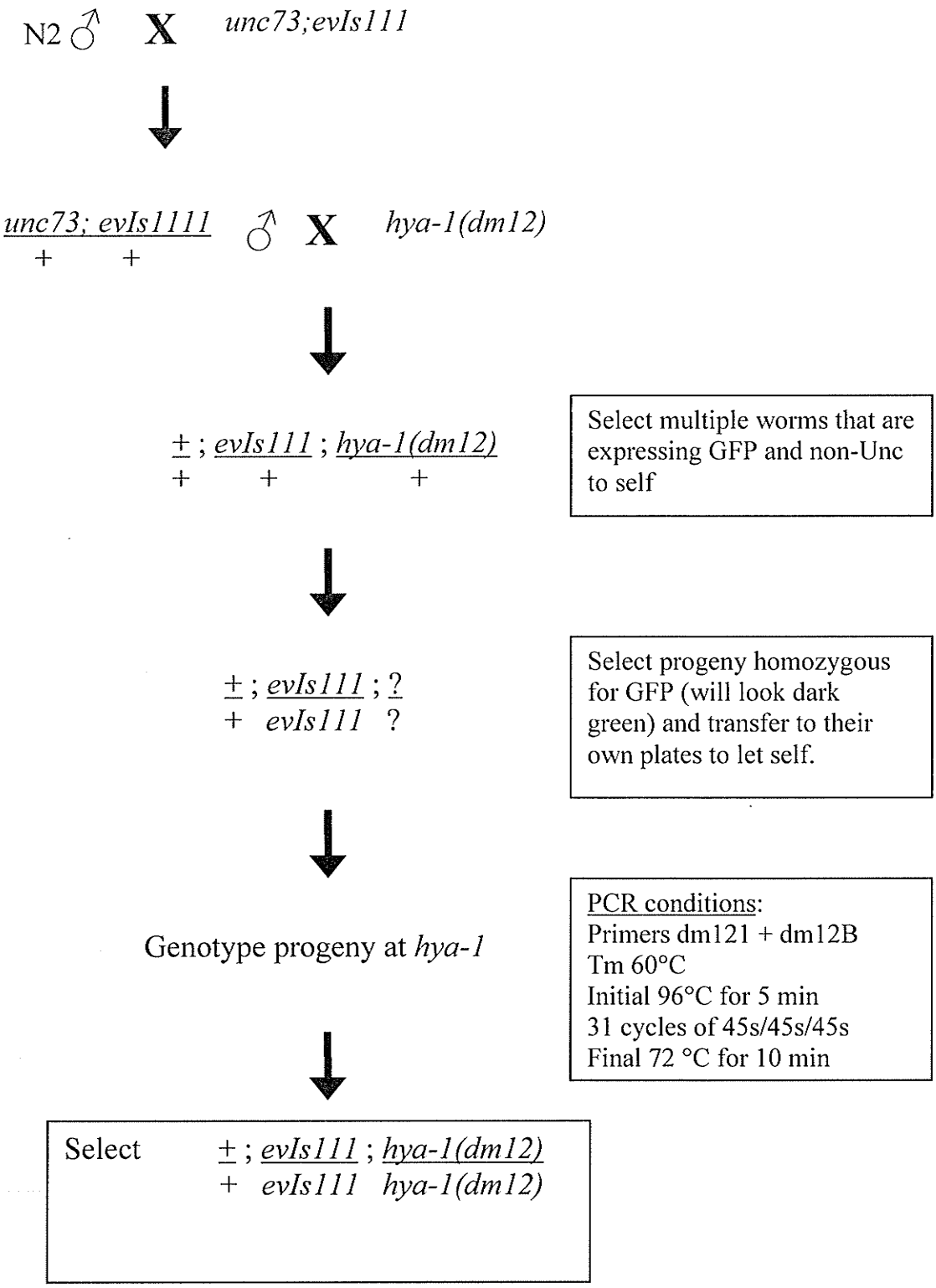

Figure 6: Generation of integrated reporter strain flowchart. The resulting strain was used for *oga-1* RNAi.

2.7 Brood size inspection

To analyze brood sizes, a single L4 hermaphrodite worm was transferred onto an NGM agar plate. After three days, the resulting progeny was counted and removed from the plates leaving only the original parental worm on the plate (and possibly eggs). This process of counting and removing the progeny continued each day following until all progeny was counted. The resulting brood sizes were statistically analyzed using a Student's T-test.

2.8 Worm protein isolation

2.8.1 Liquid cultures

N2, *hya-1(dm12), oga-1(ok1207)* and *hya-1(dm12); oga-1(ok1207)* strains were grown separately in liquid culture to obtain large quantities of worms. To do this, approximately five plates of worms were washed off with M9 (22 mM KH_2PO_4, 42 mM Na_2HPO_4, 86 mM NaCl and 1 mM $MgSO_4$) and added to 1 L of NGM broth. Approximately 50 ml of OP50 *E.coli* overnight culture (in LB) was allowed to settle, the supernatant was withdrawn and discarded. This concentrated bacteria was added to the liquid worm culture as a source of food. Cultures were placed on a shaker (New Brunswick Scientific) at room temperature and low speed for 5- 14 days. During this period concentrated OP50 *E.coli* was added aseptically as food was needed. Visual assessment determined the need for food to be when the liquid culture began to clear. To harvest the worms in the culture, 250 ml aliquots were centrifuged at 5000 rpm for 10 minutes at 4°C (Beckman J2-HS Centrifuge with a JA-14 Rotor). The supernatant was discarded and the pellets were reconstituted using 15 ml of ice cold PBS. At this point the pellets were cleaned with a sucrose gradient (see below).

2.8.2 Sucrose gradient

The four pellets were combined into two 50 ml conical centrifuge tubes. The centrifuge bottles were rinsed with 10 ml ice cold PBS and added to the tubes. The tubes were then centrifuged at 3500 rpm at 4°C for 5 minutes in a (Beckman Coulter Allegra 21R) countertop centrifuge. At this stage the pellets were soft so the supernatant was removed with a pipette. The tubes were placed on ice and an equal amount of 80% sucrose was added. The tubes were quickly mixed and spun again at 3500 rpm for 5 minutes. The resulting top brown layer contained worms and was therefore removed (about 20 ml) and combined with 30 ml of ice cold PBS in a new tube on ice. Both tubes were mixed and spun at 3100 rpm for 3 minutes. The supernatants were removed and pellets were resuspended in 50 ml of PBS. Again samples were mixed and spun at 3100 rpm for 3 minutes. Supernatants were removed and the pellets were either French pressed immediately or stored at -80°C until further use.

2.8.3 Protein extraction with a French Pressure cell press

The frozen pellets were thawed on ice and the remaining supernatant was removed and discarded. PBS (0.125 M NaCl, 17 mM Na_2HPO_4 and 8 NaH_2PO_4) was added to the sample, additionally, a general protease inhibitor cocktail (Sigma, 1 in 100 concentration) was added to the sample to prevent protein degradation. The sample was then French pressed under high pressure (16,000 cell pressure) according to the instructions provided by the manufacturer (American Scientific Co.). The sample was pre-chilled and collected on ice. Approximate 300 µl aliquots were made and stored at -80°C. An aliquot of total protein lysate (as prepared by the French Press) was thawed on ice and then mixed with 10% Triton-X 100 to a final concentration of 1%. The sample was then sonicated (Braun-

sonic 1510) for 15 stokes with the probe up and down in the sample and put on ice (while the other samples were sonicated) prior to repeating. Subsequently, samples were centrifuged for 10 minutes at 13,200 rpm at 4°C. The supernatant was aliquoted and stored at -20°C.

2.9 Protein quantification

Protein was quantified in the total protein lysates with the Bio-Rad Protein Assay, based on the method of Bradford (Bradford. 1976). Bio-Rad reagent is an acidic solution of Coomassie Brilliant Blue G-250 dye and generates different color changes correlating to different concentrations of protein. The color change can be assessed by measuring absorbance at 595 nm with a spectrophotometer. For each quantification assay, a standard curve was generated using samples containing 0, 5, 10 and 15 µg of gamma-globulin protein in 800 µl ddH_2O, 200 µl of 5 X BIORAD reagent (Bio-Rad) and 2 µl of 1% Triton-X. Samples consisted of 2 µl of total protein lysate (in 1% Triton-X 100 in PBS) in 800 µl ddH_2O and 200 µl BIORAD reagent. As with the standard samples, the protein samples incubated at room temperature for about 15 minutes before the absorbance values were obtained using a plastic cuvette in a spectrophotometer (Pharmacia Biotech Ultrospec 1000). The standard curve values were used to calculate a linear relationship between the protein quantity and absorbance reading. The linear relationship ($y=mx+b$, where m is the slope of the line and b is the Y intercept) was used to then calculate the quantity of protein present in the samples based on their absorbance values.

2.10 Hyaluronan zymography

Native discontinuous poylacrylamide systems (0.75 mm thick) were prepared as follows: The stacking gel consisted of 4% polyacrylamide, 0.3M TRIS pH 6.8, 0.04% N,N,N',N'-tetramethylethylenediamine (TEMED) and 0.4% ammonium persulfate (APS). The 7% polyacrylamide resolving gel contained 0.4M TRIS pH 8.8, 0.18 mg/ml hyaluronan, 0.1% TEMED and 0.8% APS. Protein samples were made to 20 µl with 25% 4 X native sample prep buffer (40% glycerol, 250 mM Tris pH 6.8 and 0.002% bromophenol blue) and loaded into the gel. Samples were separated by electrophoresis at 10 mA until the dye front reached the bottom of the gel. The running buffer (25 mM Tris, 192 mM glyciene) and gel system was pre-chilled and electrophoresis was performed at 4°C. Gels were rinsed with dH_2O and then equilibrated in 100 mM formic acid (pH 3.7) or PBS (pH 7.0) for 30 minutes with one change of buffer. The gels were then incubated at either 20°C or 37°C in the same buffer overnight to allow for potential hyaluronan degradation. Hyal1 from human serum was used as a positive control. Hyal1 displays hyaluronan-degrading activity at acidic pHs. Subsequently, the gels were rinsed with water and then equilibrated in 20 mM Tris (pH 8) for 30 minutes with one change of buffer. The gels were then incubated overnight at 37°C in 0.2 mg/ml protease (Sigma) in 20 mM Tris (pH 8). Gels were subsequently rinsed with dH_20 for 15 minutes twice, fixed in 7% acetic acid for at least 30 minutes and then stained with 0.5% alcian blue for at least 2 hours (in 3% acetic acid). Following this the gels were destained (10% acetic acid, 30% methanol) and then stained with 0.1% coomassie blue for at least 2 hours (in 10% acetic acid, 30% methanol). Finally, after destaining the gel once more (in 10% acetic acid, 30% methanol) a picture was obtained with an Epson Perfection 1650 scanner.

2.11 Chondroitinase assay

To assess chondroitinase activity in *C.elegans*, 250 μg of total protein was combined with 7.5 μg chondroitin (Seikagaku) and brought to 65 μl with incubation buffer. The incubation buffers were 100 mM formic acid pH 4 or 50 mM Tris pH 7 and 8.8. Samples were incubated overnight at 20°C. Chondroitinase ABC (Sigma) was used as a positive control. Samples were made to 1 X with modified 3 X Laemmli's loading buffer (30% glycerol, 16% beta-mercaptoethanol, 6% SDS, 0.24 M Tris pH 6.8, 0.0006% Orange G dye), boiled for 3 min, cooled and then briefly centrifuged. Samples were then loaded in a 4% polyacrylamide stacking gel (0.75 M Tris pH 8.45, 0.075% SDS, 0.05% APS, 0.01% TEMED) with a 16.5% polyacrylamide resolving gel (1 M Tris pH 8.45, 0.1% SDS, 0.03% APS, 0.13% TEMED) and a tris tricine buffer system (0.2 M Tris pH 8.9 anode buffer and 0.1 M Tris, 0.1 M tricine, 0.1% SDS, pH 8.25 cathode buffer). Following electrophoresis, the gel was incubated for 1 hour in 20 mM Tris pH 8.8 followed by a protease digest (0.2 mg/ml protease (Sigma), 20 mM Tris pH 8.8) overnight at 37°C with gentle agitation. Subsequently the gel was fixed in 25% isopropanol for 1 hour and stained overnight (0.005% Stains-All [Kodak], 25% isopropanol [Fisher Scientific, HPLC grade], 0.05% formamide [Fisher Scientific, molecular biology grade]). To visualize undegraded chondroitin within the gel, the gel was destained in water and by exposure to light. Once the background of the gel was destained an image of the gel was scanned with an Epson Perfection 1650 scanner.

2.12 Transgenic strains

2.12.1 BC10915

The BC10915 strain was constructed as part of the Baillie Lab Genome Project at Simon Fraser University (British Columbia, Canada). A *dpy-5* homozygous mutant (CB907) was microinjected with a plasmid containing 2 kb of the 5' upstream region of T20B5.3 fused to a DNA cassette encoding a green fluorescent protein (GFP) along with a *dpy-5* rescuing construct. A stable transgenic line was identified among rescued wild type worms by the presence of GFP expression from the fusion construct.

2.12.2 WP759

The *hya-1* transcriptional reporter construct, pAC3, consisted of 860 base pairs upstream of the codon coding for the initiator methionine in *hya-1*, the transcriptional start site. This DNA fragment was ligated in frame, into the Fire vector p95.77, encoding for a green fluorescent protein. This procedure required two subcloning steps as described in the following section. Subsequently, pAC3 was microinjected into the distal gonad arm of a hermaphrodite worm (described following) and progeny were inspected for GFP expression.

2.12.2.1 Generation of pAC2

The 860 bp DNA fragment to be subcloned was amplified using the T22C8 cosmid as template, primers AHT22-MSC and AHT22-SPH and the PAC2 PCR program (96°C for 30 s followed by 32 cycles of 94°C for 45 s, 57°C for 45 s and 72°C for 30 s followed by final extension of 72°C for 5 min). Both of these primers contained engineered restriction sites for enzymes MscI and SphI respectively. Immediately following PCR

amplification, the fresh PCR product was ligated into a TOPO vector (TOPO/TA Cloning Kit, Invitrogen), transformed, and selected with spectinomycin according to the manufacturer's instructions. The TOPO vector is linearized and contains a 3'-thymidine (T) overhang. Taq polymerase has a terminal transferase activity which adds a single deoxyadenosine (A) to the 3' end of PCR products. Therefore, the TOPO vector and PCR product are compatible for ligation without any further sequence manipuation. This subcloning step was performed for two reasons: 1) to allow the visualization of two distinguishable digestion products (DNA fragments) and 2) to ensure the engineered restriction sites had a sufficient length of flanking base pairs for the enzymes to restrict the recognition sites. Spectinomycin resistant colonies were grown up in 4 ml of LB broth overnight at 37°C in a shaking incubator. The plasmids were then isolated and purified from the bacterial cultures using a Qiagen miniprep kit. A sample of miniprep product was run out on an agarose gel to verify the prescence of a plasmid and determine if it was the anticipated size. To verify the plasmids contained the desired insert, 5 µl of the purified plasmid was digested with 1 µl of each Msc I and Sph I enzymes (New England Biolabs (NEB), 1 µl 10 X buffer 4 (NEB) and 2 µl autoclaved dH_2O at 37°C overnight. Samples producing a 860 bp and a 2.8 kb fragment were combined and designated pAC2.

2.12.2.2 Generation of pAC3

The second subcloning step begins with the digestion of pAC2 with Msc I and Sph I to obtain the 860 bp insert. The FIRE vector p95.77 was digested with both Msc I and Sph I overnight at 37°C. Both double digested samples were separated by agarose gel electrophoresis and the desired DNA fragments (860 bp from pAC2 and 4.4 kb from p95.77) were isolated with a Qiagen gel extraction kit. The concentrations of the purified

DNA fragments were estimated by comparison to a DNA mass ladder (Invitrogen) and a ligation was prepared with approximately 500 ng insert DNA and 400 ng vector DNA (1 µl ligase, 1 X ligase buffer in 20 µl reaction volume). Ligation proceeded at 25°C for 1 h in the PCR machine with a final hold at 4°C. DH5α cells (Invitrogen) were thawed on ice prior to transformation by the heat shock method. 5 µl of ligation mix was added to the cells and gently mixed by tapping. The tube was incubated on ice for 30 min, then heat shocked at 42°C for 30 sec and returned to ice for 2 min. 500 µl of SOC (2% bactotryptone, 0.5% yeast extract, 0.1 M NaCl, 2.5 mM KCl and added after autoclaving are 0.1M MgCl, 0.1M $MgSO_4$ and 0.2M glucose) at room temperature was added to the cells and then incubated at 37°C for 1 h in an incubator shaker (C25 New Brunswick Scientific). 50, 100 and 200 µl were spread on LB-AMP (100 µg/ml AMP) plates and incubated overnight at 37°C.

Following transformation, ampicillin resistant colonies were grown in 4 ml of LB broth overnight at 37°C in a shaking incubator. The plasmids were then isolated and purified from the bacterial cultures using a Qiagen miniprep kit (see appendix). A sample of miniprep product was electrophoresed on an agarose gel to verify the prescence of a plasmid and determine if it was the anticipated size. To verify the plasmids contained the desired insert, 1 µl of the purified plasmid was digested with 0.3 µl Msc I and 0.6 µl Sph I enzymes (New England Biolabs (NEB)), 1 µl 10 X buffer 4 (NEB) in 10 µl reaction volume at 37°C overnight. Samples producing a 860 bp and a 4.4 kb fragment were combined for further use and named pAC3.

2.12.2.3 Microinjection of pAC3 into *C.elegans*

An L4 hermaphrodite worm was transferred onto an agarose pad (2% agarose dried on a glass microscope slide) covered with a thin layer of mineral oil. A few small marks were made on the reverse side of the slide with a thin marker for spatial orientation reference. Once the worm had adhered to the agarose pad, the slide was placed on the stage of an inverted microscope (Leica DMIL DIC). The microscope had a movable stage and injection needle micromanipulator. Injection needles were generated from glass capillaries using a needle puller. The plasmid injection mix (80 ng/µl pAC3 and 20 ng/µl *rol-6*) contained a co-transfection marker, *rol-6*, that causes worms to roll when they move forward or backwards. Therefore, transgenic animals could be easily identified and selected. A small volume of the injection mixture was loaded into the needle using capillary action. The needle was then mounted on the micromanipulator. The worm was aligned with the needle and quickly but carefully moved into the needle allowing the needle to enter the distal arm of the gonad. A very brief expulsion of compressed nitrogen gas propelled the solution within the needle into the gonad of the worm. This area of the gonad is syncytial allowing the plasmid mixture to be incorporated into the nucleolus of oocytes during division. The DNA mixture creates random copy number, extra-chromosomal arrays expressed using endogenous machinery. After injection, the worm was swiftly moved away from the needle and then transferred onto a new NGM agar plate to recover and eventually lay eggs. Progeny were then screened for rol-6 and GFP expression. The extra-chromosomal arrays vary in stability and have a 5-95% transmission frequency.

2.12.3 Generation of WP770

The pAC3 transgene (as described above) was microinjected into an L4 *hya-1(dm12)* hermaphrodite animal (as above). A resulting stable line with GFP expression visible was named WP770.

2.13 Alcian blue staining of animals

Poly-L-lysine slides were prepared in our lab as follows (performed by L.Coudiere): Pre-cleaned slides with frosted edges were wiped thoroughly with kim wipes and then placed back to back with the frosted sides out in a Coplin jar slot. Slides were shaken for 30 minutes in dilute ionic detergent such as dishwashing liquid followed by a rinse in running water for 4 minutes. Subsequently the slides were rinsed for an additional four minutes with running distilled water. The slides were shaken in 70% ethanol and 1% HCl for almost five minutes prior to rinsing with running distilled water for 5 minutes. Slides were then removed from the Coplin jar and dried at 60°C in an oven for 10 minutes. Finally the slides were shaken in poly-L-lysine solution (0.2% poly-L-lysine (high molecular weight, Sigma) and 0.1% sodium azide) for 5 minutes followed by a final drying in the 60°C oven overnight. Slides were cracked apart by sliding a scalpel between slides and stored at 4°C.

To prepare worms on the slide, worms were washed off plates using M9 buffer and transferred to a microcentrifuge tube. The tube was centrifuged at 200 rpm for 2 minutes. The supernatant was withdrawn and discarded. This wash step was repeated three times with M9 buffer and twice with ddH_20 to remove bacteria. After the final supernatant was removed the tube was placed on ice for 2 minutes to reduce movement. A drop of worms was placed on a lab-made poly-lysine slide. Using a pipette tip, worms were spread out

carefully to reduce overlapping (as visualized with a dissecting microscope). A second poly-L-lysine slide was carefully pressed face down onto the first slide containing the worms. The sandwiched slides were placed in a metal container which was immersed in a dry ice/ethanol bath to conduct temperature for the slides for 45 minutes.

To fix the worms, the slide sandwich was cracked apart by gently twisting apart the two slides followed by immediate immersion into ice cold methanol for four minutes. Next, the slides were immersed in ice cold acetone for four minutes. To re-hydrate worms, slides were immersed for two minutes in each 90% ethanol in PBS, 60% ethanol in PBS, 30% ethanol in PBS and finally PBS.

To stain the worms, slides were immersed in Alcian blue (in 3% acetic acid) overnight with gentle agitation. Subsequently slides were rinsed with dH_20 approximately five times or until no more stain was evident in the rinse water. Slides were gently dried and a drop of mounting medium was applied followed by a cover slip. Slides were inspected utilizing a Zeiss imager.A1 AxioImager compound microscope and documented with AxioVision software.

2.14 Bioinformatic analysis and other internet references

The following websites were used for bioinformatic analysis during this project:

Wormbase http://www.wormbase.org/

-database for C.elegans information including gene and protein information summaries

National Centre for Biotechnology Information (NCBI) http://www.ncbi.nlm.nih.gov/

Basic Local Alignment Search Tool (BLAST) http://www.ncbi.nlm.nih.gov/BLAST/

-this resource was utilized to perform nucleotide and amino acid sequence alignments

Wormbook http://www.wormbook.org/

-contains literature reviews about *C.elegans*

Simple Modular Architectural Research Tool (SMART) http://smart.embl-heidelberg.de/

Expert Protein Analysis System (ExPASy) Proteomics Serverhttp://expasy.org/

-server with links to bioinformatics tools

ClustalW http://www.ebi.ac.uk/clustalw/

-used to align multiple protein sequences

NetNGlyc http://www.cbs.dtu.dk/services/NetNGlyc/

-used for the prediction of N-glycosylation sites in proteins

Pfam http://www.sanger.ac.uk/Software/Pfam/

-a large collection of multiple sequence alignments and hidden Markov models covering many common protein domains and families

Sequence Manipulation Suite http://bioinformatics.org/sms2/

-used to analyze nucleotide sequences including identification of restriction sites

3. RESULTS

3.1 Characterization of *hya-1*

As part of the *C.elegans* Genome Sequencing Project, the gene T22C8.2 was sequenced (*C.elegans* Sequencing Consortium. 1998) and identified as a putative hyaluronidase based on sequence similarity to other known hyaluronidases. *C.elegans* has only one gene encoding hyaluronidase, which we have named *hya-1*. *hya-1* is located on chromosome II and produces a 3058 bp unspliced transcriptional product containing 9 exons. The spliced transcript is comprised of 1377 bp of coding sequence (Figure 7).

Predictions of HYA-1 structure are divergent from structural characteristics of the GPI-linked guinea pig PH-20 (gpPH-20). gpPH-20 displays features typical of a membrane-bound protein including a N-terminal signal sequence, a membrane anchoring signal and six sites for N-glycosylation at residues 46, 130, 144, 218, 333 and 366. HYA-1 is comprised of 458 aa which encode a N-terminal signal sequence (residues 1-22, SMART) and contains four sites for N-glycosylation (NetNGlyc 1.0 Server) but no membrane anchoring sequence. The N-glycosylation sites are on residues N34, N92, N119 and N433. HYA-1 is also predicted to contain a glycosyl hydrolase domain (residues 25-360) and an epidermal growth factor-like (EGF) domain (residues 361-401) by SMART analysis. Glycosyl hydrolases are widespread and function to hydrolyze the glycosidic bond between two or more monosaccharides or a carbohydrate and a non-carbohydrate substance. HYA-1 is specifically identified as a member of glycosyl hydrolase family 56 in the Pfam database. Family 56 is specific for enzymes with only one known function, that of hyaluronidase activity. EGF domains contain a repeating pattern involving a number of conserved cysteine residues thought to be important for the three dimensional

A

B

458 aa

C

MVIVWYHQLLLVLLIFIGAAKGAQYIGSGASQPNRTDVVW-
M V P S W T C K N E Y S I D V E -
KYGILQNEDQHFVGGKQFAIFYEHSFGKIPYFKAQNESDPKN
GGLPQMGDLEAHLIQAEKDINETIPDENFNGIAVIDIEEFRPM
WELSWGPFSVYKTESIRLTRQQHPYWSTKQIEWQAERDYEK
ACQKFFIETLRLGKRLRPNAKWGYYLFPKCNGDVGQKSDTD
CSTLFQKFNDNLHWLWGESTALFPSIYLYPSQKQNPEYNFVNS
GALITETKRIKRNYCPSCEIHVFTKIEYNPYYTPDDFYSKQNLA
STLDLAIKMNANSVVIWSTSQSIGSRCGSLQTYVDNTLGPYLQ
LTDRNLDKCRMERCEGRGECYLPRPKTNPAIYNFACRCERPY
FGKSCEYRGRRMGVSMPKASQTPQVIPDVTAYFSTSSNGTKK
Y N A P N Q F Y S R T G G D I K L A R K L

Figure 7: Schematic of *C.elegans* hyaluronidase gene structure, protein domains and sites of predicted N-glycosylation. (A) Schematic of *hya-1* depicting the 9 exons within the 3078 bp transcript. (B) Schematic representation of HYA-1 predicted domains including a N-terminal signal sequence (SP), a catalytic glycosyl hydrolase domain and an epidermal growth factor-like domain (EGF). (C) Predicted protein sequence of HYA-1. The signal sequence is in green, the glycosyl hydrolase domain is in blue and the EGF domain is in yellow. Sites of possible N-glycosylation are highlighted in red.

structure of proteins. Furthermore, EGF domains are commonly found in extracellular proteins.

Sequence alignments between human hyaluronidases and the predicted HYA-1 sequence revealed a significant amount of conservation ranging between 20-30% identity with a further 10-20% similarity as shown in Figure 8. This amount of sequence conservation is typical for human-worm homologues, although it can vary. The area of highest sequence conservation corresponds to the glycosyl hydrolase domain while both the N-terminal and C-terminal regions have highly divergent sequences with almost no conservation of residues.

Structural comparisons of HYA-1 were performed with bee venom hyaluronidase (bvHYA). The structure of bvHYA has been determined by X-ray crystallography including all protein sequence except for residues 1-33. The structure of bvHYA resembles a classic TIM barrel $(beta/alpha)_8$ but with only seven strands (Markovic-Housley et al. 2000). A long substrate binding groove extends across the C-terminal end of the barrel and active site residues were identified from co-crystallization with a hyaluronan tetramer analog. An alignment of protein sequences from bvHYA and *C.elegans* HYA-1 shows a 29% identity and 24% similarity as shown in Figure 9. Closer inspection of sequences reveals that *C.elegans* HYA-1 shares four conserved cysteine residues (C47, C212, C224 and C337) identified in disulfide bridges in bvHYA. One disulfide bridge formed in bvHYA (C212 and C224 in HYA-1) stabilizes the base of a long loop at the C-terminal end of beta strand 4 and the other disulfide bridge (C47 and C337 in HYA-1) joins distant secondary structures. A substrate binding groove forms on the protein surface, running perpendicular to the barrel axis with loops from beta strands 2, 3 and 4 forming one wall and loops of strands 1, 5, 6 and 7 forming the opposing wall

of the groove. The binding groove is large enough to accommodate a HA tetramer. The active site within this groove is proposed to function through an acid-base catalytic mechanism with Glu113 positioned to act as the proton donor. Asp111 and Glu247 were identified as the other active site residues which produce a disaccharide product. Additional support of a role for Glu113 in the active site comes from the patient identified with MPS IX. This patient had a nonconservative amino acid substitution of the putative active site glutamic acid to a lysine residue and displayed reduced serum hyaluronidase activity with elevated levels of hyaluronan within the serum (Triggs-Raine et al. 1999). *C.elegans* also shares conservation of these three active site residues. Furthermore, it is important to recognize that the active site residues as well as the cysteine residues are also conserved in mammalian hyaluronidases as shown in Figure 8.

As shown in Figure 9, HYA-1 has significant amount of conservation with the bvHYA sequence within areas of secondary strucuture formation. All alpha helices and 3_{10} helices share significant amounts of sequence conservation as do all of the beta strands except for two very small beta strands (consisting of three residues each). However, most of the secondary structures are also flanked by sequence conservation.

Based on the sequence conservation at the active site residues, the cysteine residues and throughout the secondary structures, it is very likely that HYA-1 has similar structure to bvHYA and also functions through an acid-base catalytic mechanism.

3.2 Generation of *hya-1(dm12)* and identification of deletion region in *hya-1*

hya-1(dm12) was generated by the TMP-UV method of mutagenesis (as described in section 2.3.1) in the lab of Dr.J. Cullotti (U of T). A deletion mutation in *hya-1* was detected with a molecular based PCR assay using gene specific primers. Upon receiving

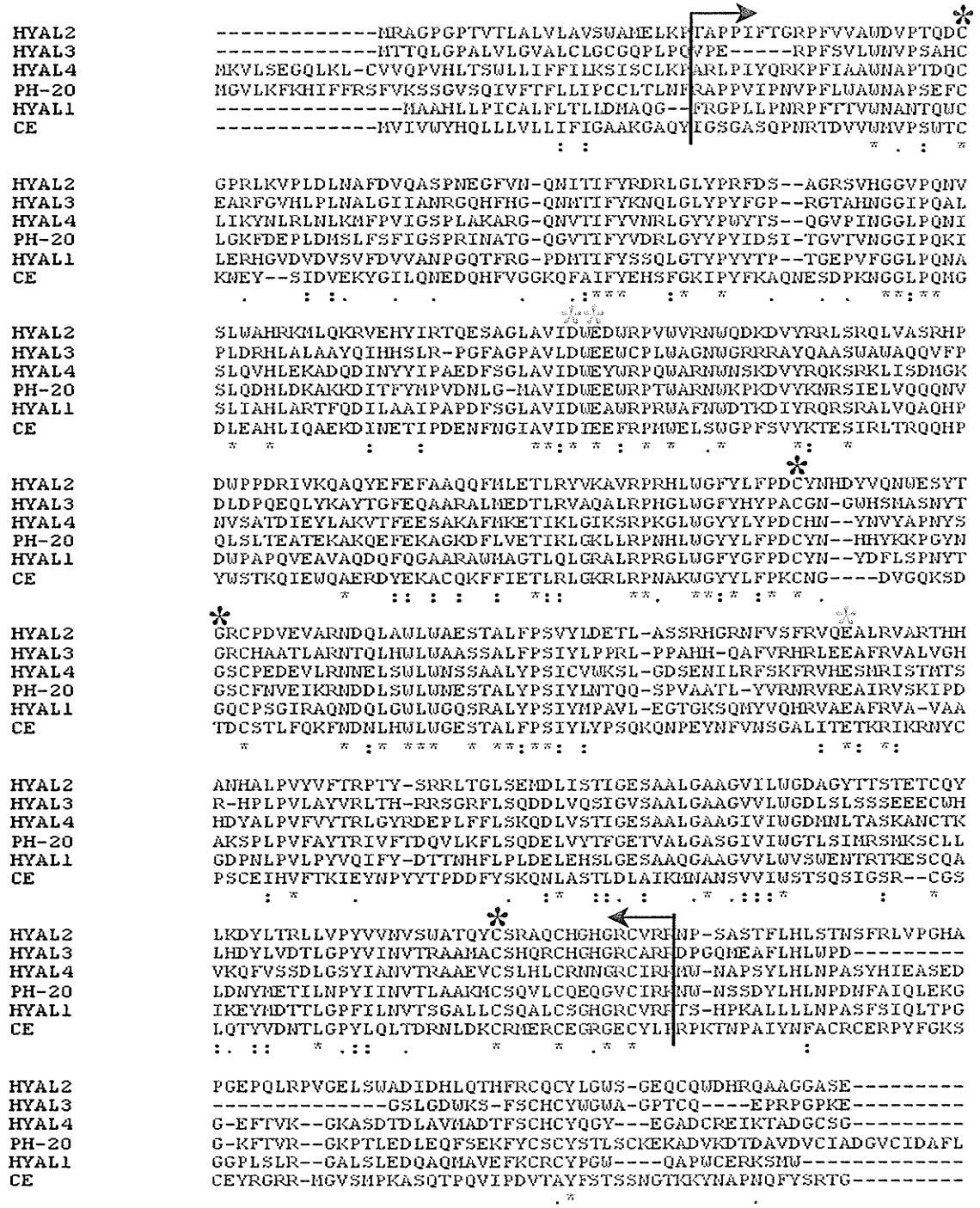

Figure 8: Protein sequence alignments of human hyaluronidases and *C.elegans* hyaluronidase. Each human sequence shares between 20-30% identity (*), 10-20% strong sequence similarity (:) and additional weak sequence similarity (.) with the HYA-1 protein sequence. The catalytic glycosyl hydrolase domain is the sequence contained within the black arrows above. This catalytic domain contains almost all of the sequence conservation. All of these hyaluronidase sequences display conserved residues identified to be in the active site in bee venom hyaluronidase and are thought to act in an acid-base catalytic mechanism (*). Also, cysteine residues 47, 212, 224 and 337 are conserved (*) from bee venom hyaluronidase and form two disulfide bridges. One bridge is formed between residues 47 and 337, the other bridge is between residues 212 and 224.

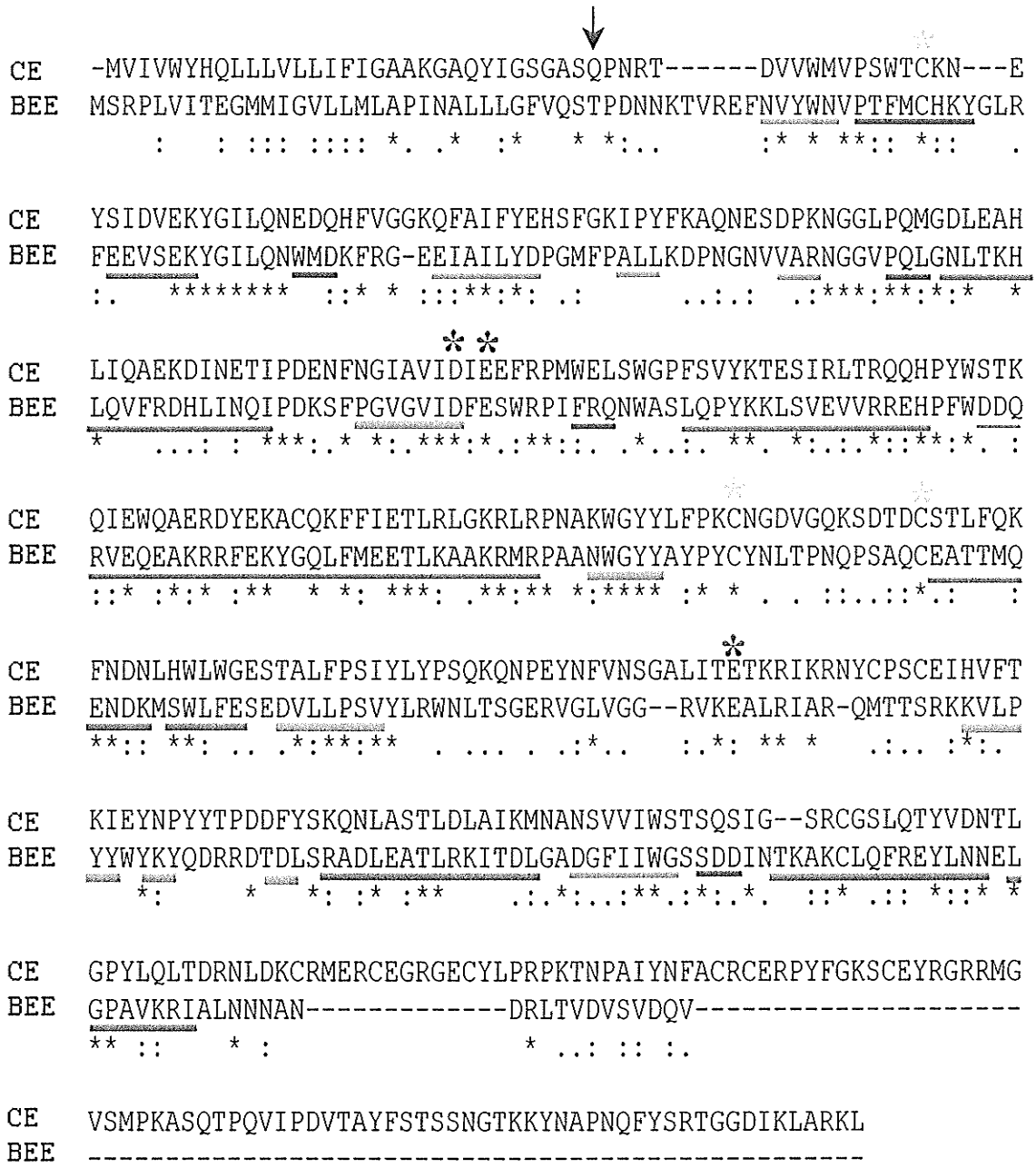

Figure 9: ClustalW protein alignment with *C.elegans* hyaluronidase and bee venom hyaluronidase. The sequences share 29% identity (*), 24% strong sequence similarity (:) and a further 17% weak sequence similarity (.). *C.elegans* has conserved residues which were identified to be in the active site in bee venom hyaluronidase and are thought to act in an acid-base catalytic mechanism (*). Also, cysteine residues 47, 212, 224 and 337 are conserved ( ) from bee venom hyaluronidase and form two disulfide bridges (residues C47 and C337 form a bridge and C212 and C224 form the other bridge). Secondary structures formed in bee venom hyaluronidase as identified by X-ray crystallography are β-strands (underlined in green), α-helices (underlined in red) and 310 helices (underlined in blue). The sequence identified during crystallography with bee venom hyaluronidase begins at the black arrow and extends to the end of the sequence listed here.

this strain, it was necessary to outcross it with N2 wild type to remove any undesired background mutations. Background mutations may be generated due to the random nature of this mutagenesis method. Primers were designed randomly along *hya-1* because although our collaborators in Toronto suggested the deletion region was approximately 1.7 kb in size, the exact size and position of the deletion was unknown. Many different primer pairs were utilized with the single worm lysis method of template preparation in an attempt to amplify regions of *hya-1*. The primer pair X+S produced the first successful PCR with a resulting band of approximately 300 bp. Sequencing of this product revealed that the band was not a product from amplification of *C.elegans* DNA, rather a product from the amplification of *E.coli* DNA. As described in section 1.3, animals are maintained and fed on a lawn of *E.coli* on NGM agar plates. To circumvent this problem, genomic DNA from *C.elegans* was prepared for future use as template for molecular biology techniques. This method involves washing of the animal pellet three times and includes a transfer of extracted DNA to a new tube which separates the large egg shell and worm carcass debris. Both of these steps physically remove bacteria from the DNA preparation.

Using the genomic DNA as template, primer pair A+D resulted in an approximately 3 kb band for wild type DNA and a 2.2 kb band for *hya-1(dm12)*. The products differ in size by approximately 800 bp which is significantly different than what had been suggested by our collaborators in Toronto. Sequencing of the 2.2 kb band from *hya-1(dm12)* was successful in identification of an 848 bp deletion region spanning exons 1-4 (Figure 10). The sequencing technique used has a limitation of sequencing approximately 600 bp extending from the primer and therefore primers A+D were too far apart to obtain overlapping sequences. To confirm the deletion region, primers E+H were selected to use for subsequent amplification and sequencing of the region because these

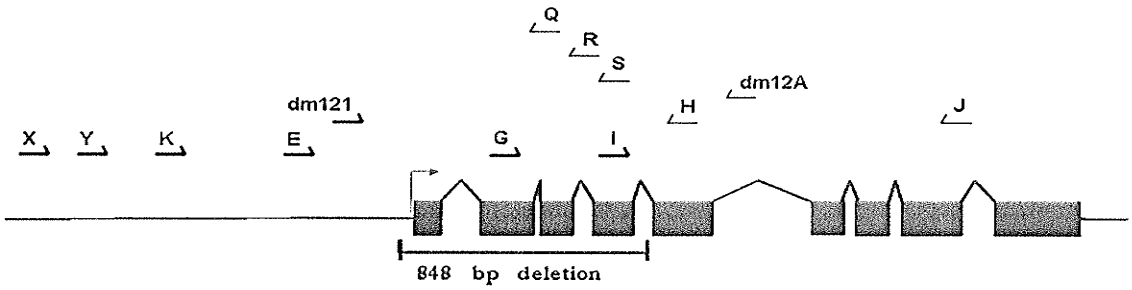

Figure 10: Schematic of primer locations along *hya-1*. Primer sequence locations are approximated by the black arrows in the direction indicated by arrowhead positioning. Exons are represented by boxes along genomic DNA sequence indicated as blue lines. The region deleted in *hya-1(dm12)* is represented by the bar below the gene schematic. The transcriptional start site is indicated by the red arrow.

primers flanked the deletion region. Primer pair E+H amplified a 607 bp product spanning the deleted region and confirmed the 848 bp deletion was positioned from -28 to 820 bp. This deletion spans exons 1-4, deleting most of the catalytic glycosyl hydrolase domain (Figure 10). This deletion is presumed to be a null allele.

3.3 Preliminary observations of *hya-1(dm12)*

The resulting animals of *hya-1(dm12)* were viable. Examination at larval and adult stages with low magnification did not reveal any obvious difference in movement or gross morphology when compared to wild type animals. However, while growing *hya-1(dm12)* animals in large liquid cultures it appeared that this strain exhibited a very slight difference in growth perhaps either due to production of reduced brood sizes or a slower growth rate. At this point the animals may contain random background mutations contributing to this very slight growth difference and therefore the strain was outcrossed before further investigation.

3.4 Outcross of *hya-1(dm12)*

Following the identification of the deletion region, new primers were designed to improve PCR amplification quality of *hya-1(dm12)*. These primers incorporated intronic regions of *hya-1* into their sequences to reduce mispriming of *E.coli* DNA. Primers E+H were utilized to identify and recover *hya-1(dm12)* during outcrossing with wild type as described in section 2.3.1. The detection of wild type alleles at *hya-1* was confirmed by an additional PCR amplification with primers O+P. The resulting strain is named WP777 and will be referred to as *hya-1(dm12)* hereafter.

3.5 Investigation into possible redundancy between *hya-1* and *oga-1* with RNAi

Having observed no significant phenotypic change after deleting a region of *hya-1* in *C.elegans*, the question of possible redundancy arose. There are at least six hyaluronidase genes in humans with a seventh proposed hyaluronidase, MGEA5. As previously discussed, in *C.elegans* there is only one hyaluronidase gene, however there is an orthologue of MGEA5, *oga-1*. To address the issue of possible redundancy between *hya-1* and *oga-1*, RNAi was performed.

An RNAi vector containing the *oga-1* double stranded gene fragment was generously provided by P.Roy (University of Toronto) and transformed into the appropriate *E.coli* strain in our lab as described in section 2.5.2. Mid-L4 stage animals were picked and cloned onto separate plates seeded with *E.coli* expressing *oga-1* dsRNA. After 3 days the resulting F1 progeny were visually examined. RNAi was performed with wild type and *hya-1(dm12)* animals. The animals would experience a knock-down of *oga-1* RNA expression with *hya-1(dm12)* animals becoming a double mutant. If *oga-1* and *hya-1* are redundant, animals would be expected to show an increase in severity or penetrance in the double mutant compared to any defect observed in either single mutant.

Observation of the F1 progeny revealed N2 animals that had injested *oga-1* dsRNA appeared normal. However when *hya-1(dm12)* injested *oga-1* dsRNA, F1 progeny appeared to be egg-laying deficient (Egl), possibly slightly uncoordinated, locomotion defects (Unc), and slighty dumpy body shape (Dpy), as assessed from at least six parental animals. Also, vulvas were slightly different in appearance, although the difference was difficult to assess at this point because of the low magnification that a compound microscope allows, and due to the movement of the animals. In conclusion, we observed

what we considered to be a definite synthetic phenotype and decided to obtain an *oga-1* deletion mutant to investigate redundancy with *hya-1*.

The possible Unc phenotype seen in *hya-1(dm12)* animals exposed to *oga-1* dsRNA could be due to neuronal defects or caused by physical limitations due to the observed egg laying deficiency. To investigate the possible neuronal defect, an integrated reporter strain was generated with an *unc-47*::GFP transgenic strain. However, upon crossing the *unc-47*::GFP and *hya-1(dm12)* strains, a non-Mendelian pattern of inheritance was observed (0/8 of progeny were heterozygous for both *hya-1(dm12)* and *unc-47*::GFP; Mendelian pattern of inheritance predicts 1/4). Therefore, these genes displayed linkage and will not be used further. A second strain, *unc-73;evIs111,* was used to cross into *hya-1(dm12)*. This strain contains a pan-neuronal expressed GFP. To generate the reporter strain, *unc-73;evIs111* was crossed with *hya-1(dm12)* and both alleles were recovered to homozygosity using a PCR based assay with primers specific to *hya-1(dm12)* and by assessing *evIs111* GFP expression. No defect was observed in morphology or patterning of neurons in *hya-1(dm12),* indicating the Unc phenotype observed in the animals treated with RNAi was due to the physical limitations caused by the accumulation of eggs within the uterus.

The other phenotypes observed in the RNAi experiments were investigated further following the generation of an *oga-1* deletion mutant strain and a *hya-1;oga-1* double mutant strain.

3.6 Acquisition of *oga-1(ok1207)* and identification of deletion region in *oga-1*

oga-1(ok1207) was provided by the *C.elegans* Gene Knock-out Project at OMRF. This deletion mutant was also generated by the TMP-UV method of mutagenesis and

therefore required outcrossing to a wild type background. Again, primers were designed randomly along the gene and optimized for PCR analysis. Primers 3+C were successful in PCR amplification of the gene across the deletion region generating a 3.2 kb band for wild type and a 1.8 kb band for *oga-1(ok1207).* Amplified DNA was prepared and sent for sequence analysis (section 2.2.6). The resulting sequence was used for a nucleotide BLAST (NCBI) that revealed a deletion of 1442 bp in *oga-1(ok1207).* However, a region of the gene remained unsequenced because the primers were situated too far apart to obtain an overlap in sequence. A second set of primers, 2+C, were utilized to PCR-amplify *oga-1(ok1207).* This PCR amplification resulted in a 400 bp band for *oga-1(ok1207)* and a 1.8 kb band for wild type. The sequencing results confirmed the previous results. In conclusion, the deletion in *oga-1* consists of 1442 bp as shown in Figure 11. This deletion spans the entire catalytic domain and is a presumed null allele. Recently a paper was published which identifies the deletion region in *oga-1(ok1207)* as spanning from 10 bases into exon 3 to the beginning of intron 7 (Forsythe et al. 2006), confirming the deletion region identified here.

3.7 Preliminary observations of *oga-1(ok1207)*

oga-1(ok1207) animals were viable and did not exhibit any obvious gross morphological or movement abnormalities when observed with low magnification.

3.8 Outcross of *oga-1(ok1207)*

After the deletion region was identified, new primers were designed to improve PCR amplification quality of *oga-1(ok1207).* Primers pairs 3+C and A2+1 were utilized to identify and recover *oga-1(ok1207)* during outcrossing with wild type as described in

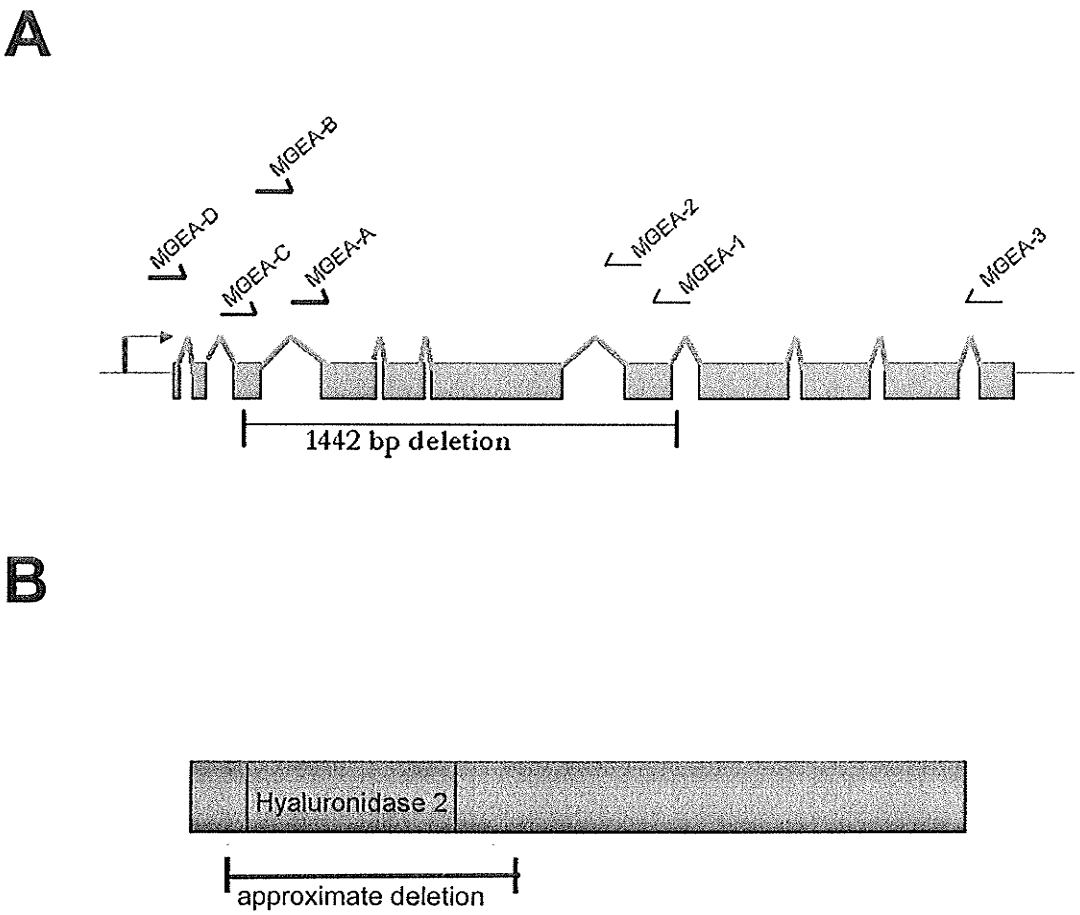

Figure 11: Schematics of deletion location in *oga-1* and its protein product. (A) Oligonucleotide primer locations are approximated by the black arrows in the direction indicated by the arrowhead. The gene produces an unspliced transcript of 3927 base-pairs with 2562 base pairs of coding sequence in the spliced transciption product. Exons are represented by boxes along the genomic DNA sequence indicated by the green line. The region deleted in *oga-1(ok1207)* is represented by the bar below the gene schematic. The transriptional start site is indicated by the red arrow. (B) Schematic of OGA-1 depicting the predicted domain and the sequence deleted in *oga-1(ok1207)*. The deletion spans the entire catalytic hyaluronidase domain.

section 2.3.2. Primer pair 3+C produced bands of 3.2 kb and 1.8 kb for wild type and *oga-1(ok1207)* alleles respectively while primer pair A2+1 produced a band of 1.7 kb for wild type only. The resulting outcrossed strain is named WP667 and will be referred to as *oga-1(ok21207))* hereafter.

3.9 Generation of *hya-1(dm12);oga-1(ok1207)*

To generate the double mutant strain, *hya-1(dm12)* and *oga-1(ok1207)* were crossed. The resulting progeny were isolated and cloned. Clones were then genotyped for the presence of deletion alleles for *hya-1* and *oga-1* utilizing primer pairs dm121+B, O+P, 2+C and 1+A (as described previously). Primer pair dm121+B generated a 1.6 kb product for wild type *hya-1* and an approximately 800 bp band for the mutant allele. A clone identified as heterozygous for both deletion alleles was then cloned and the resulting progeny were isolated and cloned. These resulting progeny were subsequently genotyped and an animal homozygous for both deletion alleles at *hya-1* and *oga-1* was selected for further use. The resulting strain is named WP668 and will be referred to as *hya-1(dm12);oga-1(ok1207)* hereafter.

3.10 Phenotypic analysis of *hya-1(dm12), oga-1(ok1207)* and *hya-1(dm12);oga-1(ok1207)*

During the RNAi assays with *oga-1* dsRNA, the Egl phenotype was displayed by *hya-1(dm12).* Thus, all the mutants were inspected specifically for this phenotype and the Egl phenotype was observed in at least 50% of each *hya-1(dm12), oga-1(ok1207)* and *hya-1(dm12); oga-1(ok1207).* The accumulation of eggs within the uterus occurred throughout with no obvious correlation to a particular region of the uterus as seen in

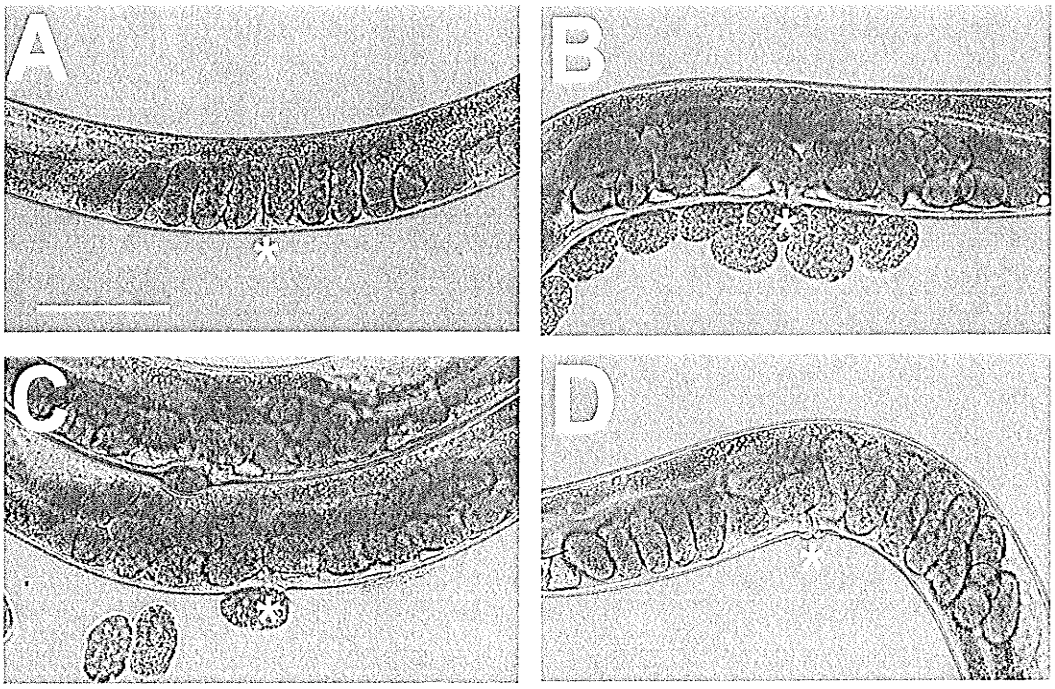

Figure 12: Mutants display strong egg laying deficiencies. Nomarski DIC micrographs displaying (A) wild type with a single row of eggs within the uterus and the egg laying deficiency observed in (B) *hya-1(dm12)*, (C) *oga-1(ok1207)* (two animals are positioned in parallel) and (D) *hya-1(dm12); oga-1(ok1207)*. Normally in young adults, eggs are generated and move into the uterus at the same rate at which they are laid, forming a single ventral row of eggs within the uterus as they pass through. Egg laying deficient (egl) mutants are detected by an accumulation of eggs within the uterus. The egl phenotype is detected in at least 50% of *hya-1(dm12)*, *oga-1(ok1207)* and *hya-1(dm12); oga-1(ok1207)*. Animals are oriented such that ventral is down, dorsal is up, the asterick represents the vulva and the scale bar in (A) represents 100 microns.

Figure 12. The three general components of the egg laying system include the vulva, sex muscles (vulval and uterine) and neurons (specifically HSN). Many different mutations involving these components result in egg laying deficiencies. To investigate the possible cause of the Egl phenotype in these mutants, vulvas were inspected utilizing DIC optics.

Vulvas of wild type animals were observed to establish key stages formed during development. As previously discussed, vulval development is a dynamic process including cell division and migration, invagination and evagination to form a mature vulva. Figure 13 shows the representative successive stages of vulval development. Observation of the mutants revealed a defect at the mid-L4 toroidal stage when the vulval space between the invaginating cells and the cuticle is largest. The mutants exhibited a reduction in vulval space thus displaying a squashed vulva (Sqv) phenotype. Animals were documented at mid-L4 stage and a set of three measurements were determined. As shown in Figure 14-A, the measurements included the width of the toroidal cells, the height of the toroidal cells invagination and the height of the anchor cell membrane.

The mean and standard deviations were calculated for each set of measurements as shown in Table 2 (following). The Sqv vulva phenotype was not fully penetrant therefore mutants were assessed as Sqv if any of the vulval measurements were below the range of the wild type measurement. The range of wild type vulval measurements were determined based on one standard deviation above and below the mean value and a list of all vulval measurements can be found in appendix 2 (and Figure 15). The Sqv phenotype was observed with a similar frequency in all three mutants, 60% in *oga-1(ok1207)*, 52% in *hya-1(dm12)* and 64% in *hya-1(dm12);oga-1(ok1207)*. This frequency of the Sqv phenotype includes all variably sized reductions of vulval measurements. Some of the

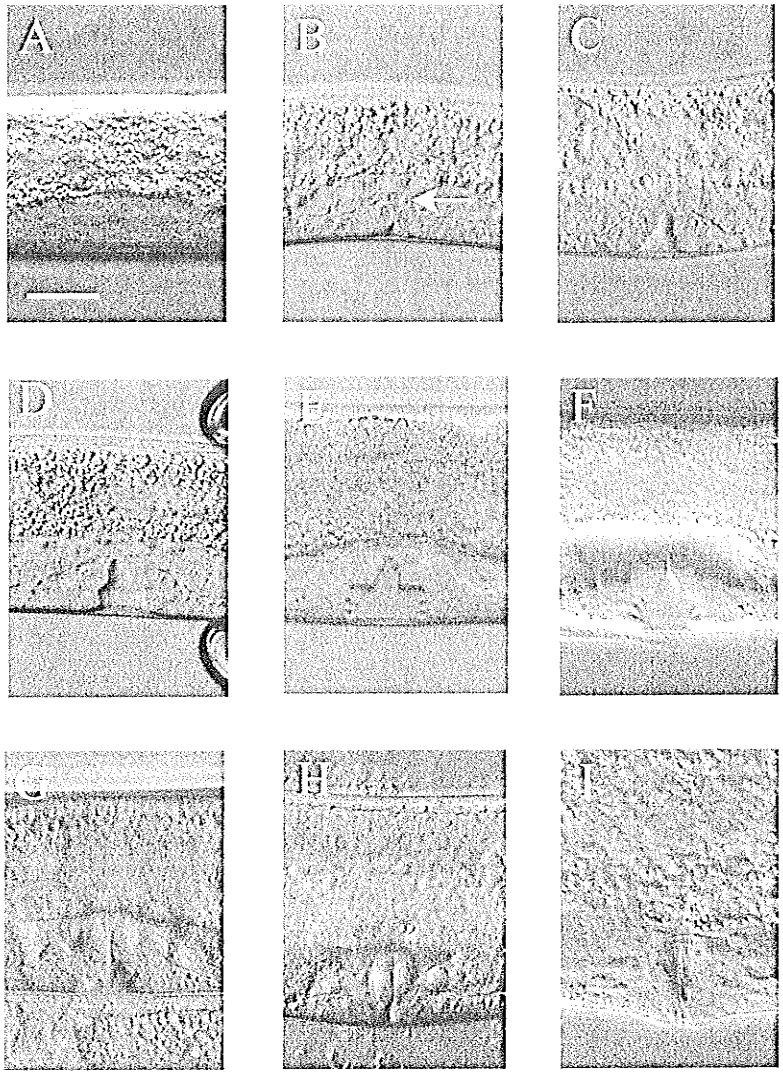

Figure 13: Successive stages of vulval development in wild type animals. Micrographs using DIC optics. Dorsal is up and ventral is down. (A) L3 stage showing vulval precursor cells and descendants. (B) Late L3 stage showing early invagination of vulval cells towards the anchor cell (arrow). (C) L3-L4 molt stage further invagination towards the anchor cell. (D) Early L4 showing a distinct shape formed by the vulval cells as invagination continues. (E) Mid L4 stage showing the toroidal cell shapes formed by fusing vulval cells. (F) Late L4 stage shows a characteristic maple leaf-like shape. Vulval cells begin to evert by migration to the center of the vulval space. (G-I) Eversion continues with vulval cells migrating ventrally and forming the mature vulval lips. (I) Adult animal. Scale bar in (A) represents 15 microns.

vulvas displaying a Sqv phenotype could easily be visualized due to large reductions (Figure 14).

Table 2: Mean and standard deviation values of vulval measurements.

Measurement	N2 wild type	*oga-1(ok1207)*	*hya-1(dm12)*	*hya-1(dm12); oga-1(ok1207)*
Height of anchor cell membrane	24.0 +/- 3.2 n=19	19.9 +/- 5.6 n=19	22.2 +/- 4.0 n=23	20.9 +/- 2.4 n=24
Height of toroidal cells	12.7 +/- 3.1 n=19	12.0 +/- 2.5 n=19	10.8 +/- 2.5 n=23	10.8 +/- 1.9 n=25
Width of toroidal cells	26.5 +/- 2.7 n=19	23.2 +/- 3.2 n=19	23.2 +/- 2.8 n=23	23.9 +/- 3.4 n=25
Width of worm	72.9 +/- 5.6 n=19	69.9 +/- 7.0 n=19	58.8 +/- 21.7 N=17	55.2 +/- 25.9 n=19

A significant difference exists between the toroidal width measurement of wild type animals and each of the mutant strains as calculated by the statistical method of analyis of variance (p= 0.0001). This suggests that the variance between strains is a true difference and not due to chance. A significant difference is also detected between wild type with *oga-1(ok1207)* and *hya-1(dm12);oga-1(ok1207)* for the height of the anchor cell membrane measurements (p=0.0051) but no significant difference is observed for the height of the toroidal cell measurement. The width of animals was also measured at a

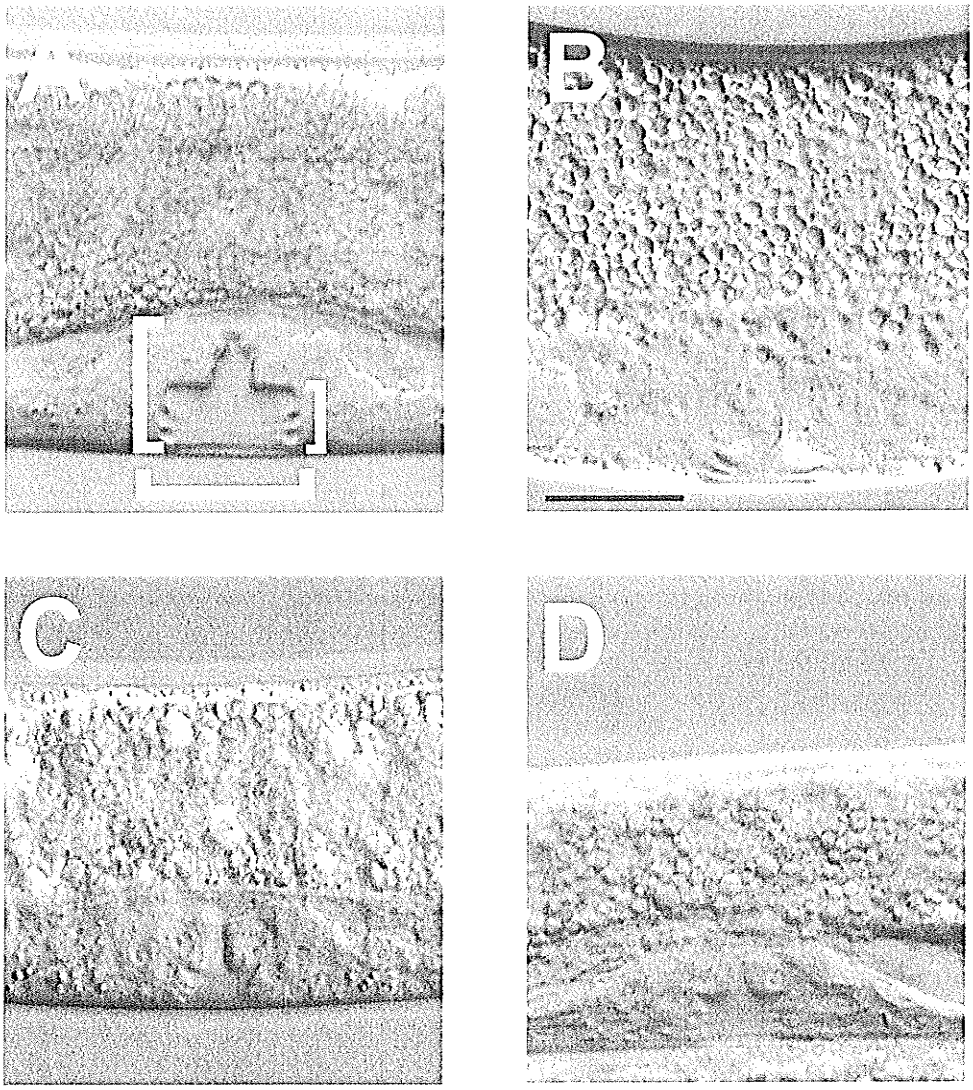

Figure 14: Mutants display squashed vulva phenotype. Nomarski DIC micrographs of a mid-L4 wild type vulva (A), and the squashed vulvas (sqv) observed at the same stage in *oga-1(ok1207)* (B), *hya-1(dm12)* (C) and *hya-1(dm12); oga-1(ok1207)* (D). The developing vulva is formed by cell division of the epithelial vulval precursor cells P5.p, P6.p and P7.p followed by a distinct pattern of invagination. At mid-L4 stage the space between the vulval cells and ventral cuticle is largest. Squashed vulvas are defined by considerably smaller vulval spaces and appear to extend less dorsally then wild type vulvas. Measurements of vulvas used for assessing reduced vulval space are represented by bars in (A). Animals are oriented such that ventral is down, dorsal is up and the scale bar in (B) represents 15 microns.

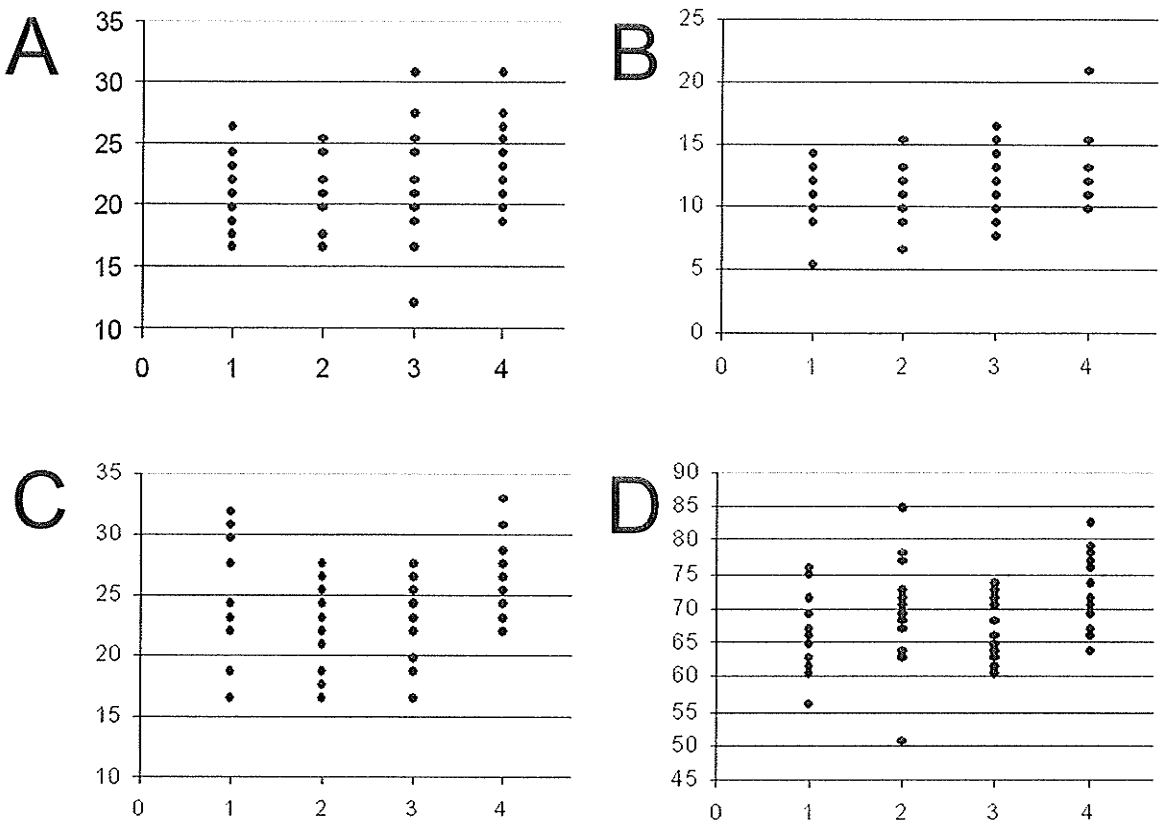

Figure 15: Graphs of vulval measurements obtained. Graphs represent measurements in microns along the Y-axis. Along the X-axis, (1) is *hya-1(dm12);oga-1(ok1207),* (2) is *oga-1(ok1207)*, (3) is *hya-1(dm12)* and (4) is wild type (N2). (A) Measurements of vulval height from the cuticle to the anchor cell membrane (the highest point). (B) Measurements of the vulva from the cuticle to the height of the toroidal rings. (C) Measurements of the width of the toroidal opening of the vulva. (D) Measurements of the width of the animals across the midbody. Visual representation of these measurements in a micrograph of the vulva can be seen in Figure 14-A.

point close to the vulva. Again, a significant difference in measurements was detected between wild type animals with *oga-1(ok1207)* and *hya-1(dm12);oga-1(ok1207)*.

During the course of inspection of vulvas in *C.elegans*, protruding vulvas were often observed in mature adult animals. This has been reported as an associated phenotype which often occurs in animals displaying an Egl phenotype (Bulik et al. 2000; Hwang and Horvitz. 2002a; Hwang and Horvitz. 2002b; Hwang et al. 2003a; Hwang et al. 2003b). Additionally, possible defects were observed during the evagination process consisting of atypically large vulval spaces or space present between the maturing vulval lips and the cuticle. These were not investigated further at this point.

Furthermore, we observed an enlargement of gut granules present in the posterior region of the intestine in *hya-1(dm12)* animals (Figure 16) correlating directly to the phenotype detected in MPS IX. An MPS IX patient, who is deficient in serum hyaluronidase activity, displayed an accumulation of hyaluronan within lysosomones of macrophages and fibroblasts (Triggs-Raine et al. 1999). Gut granules in *C.elegans* are intestine-specific lysosomes and therefore an enlargement of gut granules could represent an accumulation of substrate, very likely chondroitin due to the HYA-1 deficiency.

3.11 Inspection of brood sizes and timing

Preliminary observations of *hya-1(dm12)* (not outcrossed) showed what we interpreted as a slight difference in growth when compared to wild type animals. To assess if this difference was indeed caused by the deletion in *hya-1* or due to a background mutation, the number of embryos produced were determined by quantifying brood sizes. To do this, an L4 stage animal was isolated on an agar plate and cloned. After three days the resulting progeny were removed from the plate and counted until no more progeny

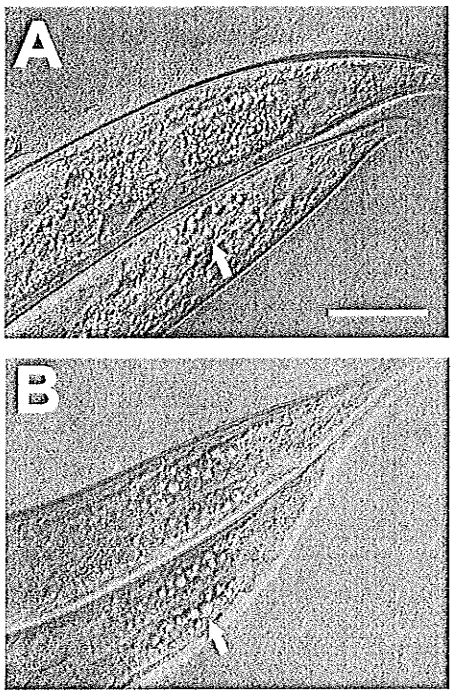

Figure 16: Enlarged gut granules are more frequent in the posterior region of the intestine in *hya-1(dm12)*. (A) Wild type animals and (B) *hya-1(dm12)* animals. Arrows demonstrate a gut granule in each micrograph. Scale bar in (A) represents 50 microns.

remained (usually day 5). Although all mutant strains produced mean brood sizes smaller then wild type brood sizes, they were not significantly different (Figure 17). The brood sizes for each strain were highly variable producing large standard deviations.

Another possible cause of difference in growth of *hya-1(dm12)* may have been due to the retention of eggs within the uterus, so brood sizes were quantified at time points for *hya-1(dm12)* animals for comparison to wild type animals. Normally all progeny are counted by day five with the majority of eggs laid at day three, counting day one as the day the L4 stage animal was isolated. *hya-1(dm12)* did not produce an obvious difference from the patterns of brood timing observed in wild type animals.

To assess whether the partially penetrant Sqv phenotype correlated to timing of producing broods, double mutants were estimated as to being Sqv or non-Sqv and then cloned. The resulting brood sizes were assessed at different time points. Unfortunately this assessment of Sqv has a low degree of confidence associated with it because the animals were inspected with low magnification while moving. This was necessary because the animals can not be recovered after exposure to levamisole, a paralyzing agent necessary to fix the animals on a slide. From the small sample size observed, no obvious correlation emerged. Overall, any difference thought to be observed for the growth of *hya-1(dm12)* (not outcrossed) was most likely due to a background mutation.

3.12 Analysis of cellular expression pattern of *hya-1* *in vivo*

The cellular localization pattern of *hya-1* was established in a transgenic strain expressing a transcriptional reporter construct. As described in section 2.12.2, the reporter construct contained 860 bp of genomic sequence upstream to *hya-1* ligated into a vector containing a GFP cassette. This construct was microinjected into the syncytial gonad of a

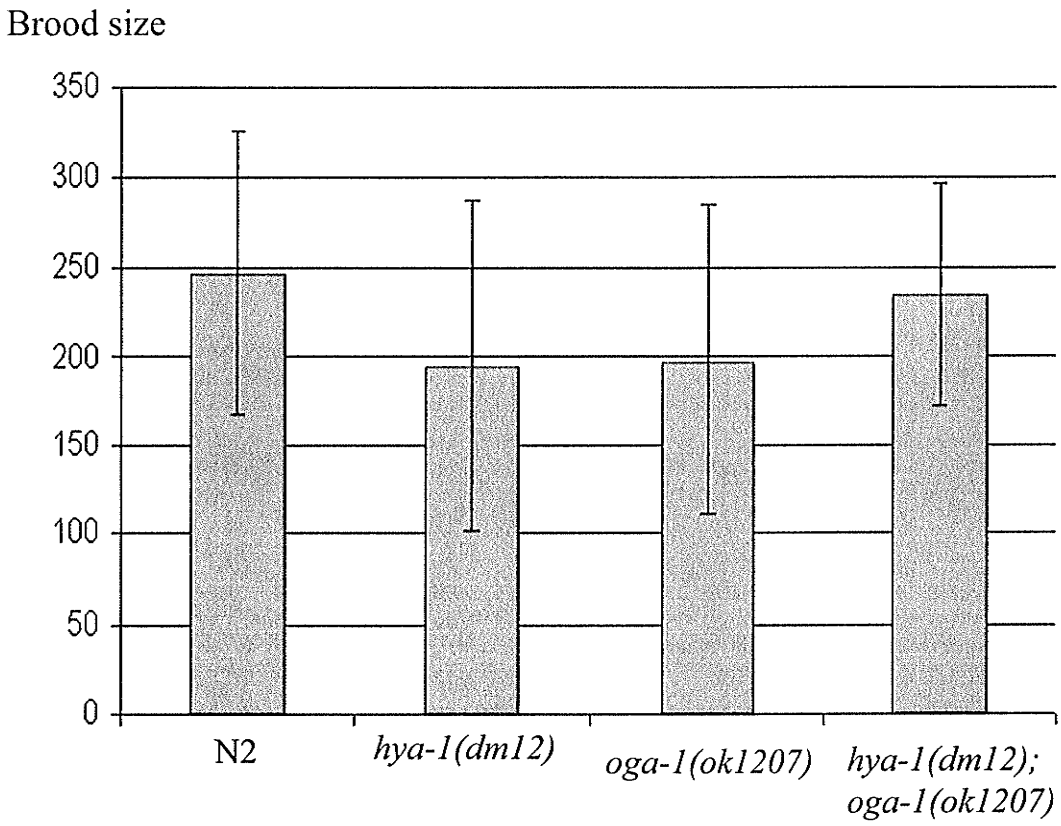

Figure 17: Illustration of mean brood sizes and standard deviations. Brood sizes were quantified by counting progeny produced by cloning of a hermaphrodite animal. Blue bars represent the mean brood size and the error bar represents standard deviation for each stain. Although all three mutant strains have reduced mean brood sizes compared to that produced by wild type (N2), they are not significantly different.

hermaphrodite animal where the exogenous DNA can be incorporated into the developing germ cell nuclei. Three stable lines expressing *hya-1*::GFP were generated. In wild type animals the *hya-1* promoter drove expression of the GFP in the posterior lateral microtubule (PLM) neurons, the intestine, the anal sphincter muscle, amphid neurons in the head and in the area of vulval cells (Figure 18).

Expression was detected early in embryos after the developmental stage of gastrulation. Inspection of L1 stage animals showed expression in the intestine, PLM neurons and cells in the head. Detection of other expression at this time point was difficult due to both the small size of animals and weak expression in other cells.

A total of six microtubule neurons exist in *C.elegans* with PLM neurons accounting for two (Chalfie and Sulston. 1981). Microtubule neurons are mechanosensory neurons which function as touch receptors allowing animals to move away from gentle stimuli (Chalfie and Sulston. 1981). PLM neurons are present at hatching and comprise of a pair of bilaterally symmetric neurons located posterior to the anus laterally on the right and left (Chalfie and Sulston. 1981). The neuron processes run anteriorly, lying close to the cuticle separated only by a thin layer of specialized ECM with periodic attachments to the cuticle (Chalfie and Sulston. 1981; Emtage et al. 2004).

Amphid neurons in the head are required for chemosensation, responsible for the detection of olfactory and gustatory cues (Bargmann. 2006). These neurons are also present as bilaterally symmetric pairs with one positioned laterally on the right and then other on the left (Bargmann. 2006).

One of the major organs in *C.elegans* is the intestine, accounting for almost one third of the somatic tissue mass (McGhee. 2007). The intestine is responsible for digestion however it is also the primary source of synthesis and storage of macromolecules

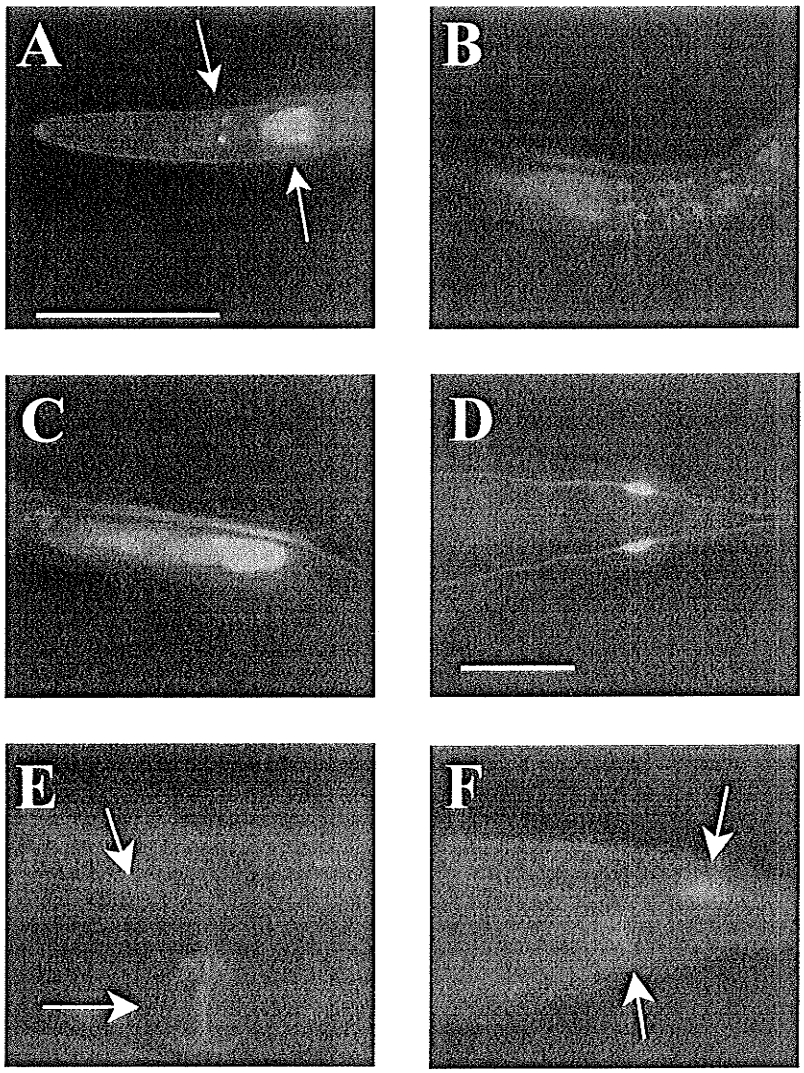

Figure 18: *hya-1*::GFP expression pattern *in vivo*. Microphotographs are oriented such that dorsal is up, ventral is down, anterior is left and posterior is right. Scale bars represent 50 microns (A-C) and 20 microns (D-F). (A) The head displays expression in amphid neurons and in the anterior region of the intestine. (B) Anterior region of intestine to midbody. (C) Midbody to posterior of animal shows expression within the intestinal cells. (D) Dorsal view of animal showing both PLM neurons with processes running anterior. (E) Animal is rotated to produce a slight ventral veiw of the vulval cell expression (bottom arrow) and PLM neuron processes. (F) Anal sphincter muscle (bottom arrow) and PLM neuron.

(McGhee. 2007). At the posterior end of the intestine lies the anus. Here the anal sphincter and anal depressor muscles work in tandem to control defecation in *C.elegans*.

3.13 Analysis of PLM neurons in *hya-1(dm12)*

As PLM neurons are mechanosensory receptors responsible for touch sensitivity in the head and tail (Chalfie and Sulston. 1981), we tested their function by gently stroking animals of the head and tail with a human eyelash. The animals responded appropriately by moving backwards or forwards, respectively, representing functioning PLM neurons.

The PLM neuron cells are located posterior to the anus with processes extending anteriorly to just anterior of the vulva where they turn ventrally. Although PLM neuron function seems to be unaffected by the deletion of *hya-1*, morphology was investigated by injecting the *hya-1*::GFP reporter construct into the *hya-1(dm12)* mutant. Inspection of the resulting transgenic *hya-1(dm12)* animals revealed no significant morphological deviations from that observed within a wild type background.

3.14 Analysis of cellular expression pattern of *oga-1 in vivo*

A transgenic strain, BC10915, expressing an *oga-1*::GFP transcriptional reporter construct (described in 2.12.1) was kindly provided by Dr. D. Baillie (Simon Fraser University). Overall, *oga-1*::GFP expression is early in development (seen in embryos and throughout larval stages) and produces a strong and broad expression pattern (Figure 19). Specifically, *oga-1*::GFP expression was detected in the pharynx, head and tail neurons, vulval cells, the spermatheca, distal tip cell, body wall muscles (hypodermis), excretory canal, rectal muscles and the seam cells.

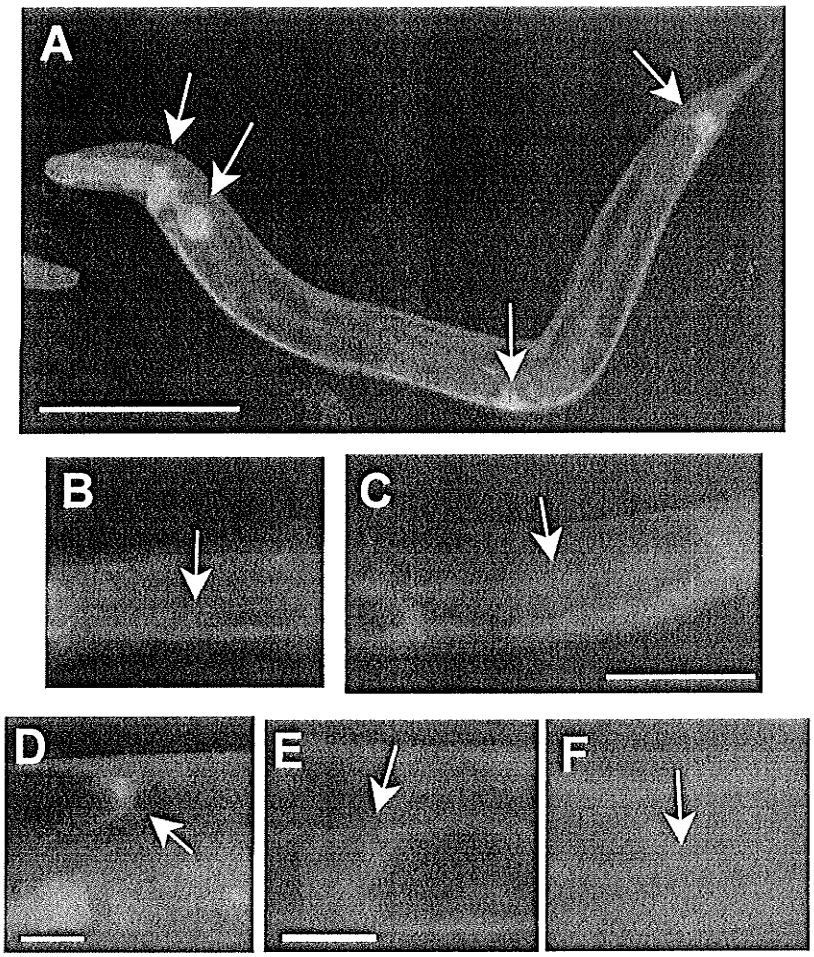

Figure 19: Expression of *oga-1*::GFP *in vivo*. Micrographs are oriented such that dorsal is up, ventral is down, anterior is left and posterior is right. (A) Arrows point out, from left to right, the nerve ring, the pharynx, vulval cells, rectal muscles in an adult animal. Scale bar in (A) represents 100 microns in (A) and (B). (B) Arrow points out a body wall muscle in an adult animal. (C) The seam cell (scale bar represents 40 microns), (D) the distal tip cell of the gonad arm (scale bar represents 20 microns) (E) the spermathecum (scale bar represents 50 microns) and (F) the excretory canal (scale bar from (E)).

Our inspection of BC10915 confirms the expression initially reported by McKay et al. (2004) within the pharynx, hypodermis, head neurons and tail neurons during larval stages. Additionally, adult expression was reported in the pharynx, vulval muscle, spermatheca, gonad sheath cells, hypodermis, tail neurons and other unidentified cells in the body. We were unable to detect expression in the gonad sheath cells and we identified the vulval expression in the cells as opposed to muscles. We have also identified cells which may have been reported as "unidentified cells in the body" including the distal tip cell, excretory canal and the seam cell.

3.15 Analysis of GAG-degrading activity in *C.elegans* protein lysate samples

In mammals, hyaluronidases primarily degrade HA. To determine if either HYA-1 or OGA-1 had HA degrading activity, HA zymography was preformed. The assay involved fixing the substrate, HA, within a polyacrylamide gel and using it for the separation of the total protein samples isolated from N2, *hya-1(dm12)*, *oga-1(ok1207)* and *hya-1(dm12);oga-1(ok1207)* (section 2.10). Once the samples were separated within the gel, the gel was pH equilibrated and incubated in a pH specific buffer overnight to allow for any enzymatic activity. The ability to degrade HA was detected as a clear patch visible in the gel after staining with Alcian blue and Coomassie blue.

The enzymatic activity of the protein samples were tested with four sets of conditions based on the known pH optima of mammalian hyaluronidases as well as the temperatures commonly used for human and *C.elegans'* enzyme assays. A neutral (pH 7.0) and an acidic (pH 3.7) pH were tested at both 20°C and 37°C. Gels incubated at both temperatures with pH 3.7 clearly display activity present in the positive control consisting of human HYAL1 (Figure 20-A, 20-B). However, no activity is detected from any of the

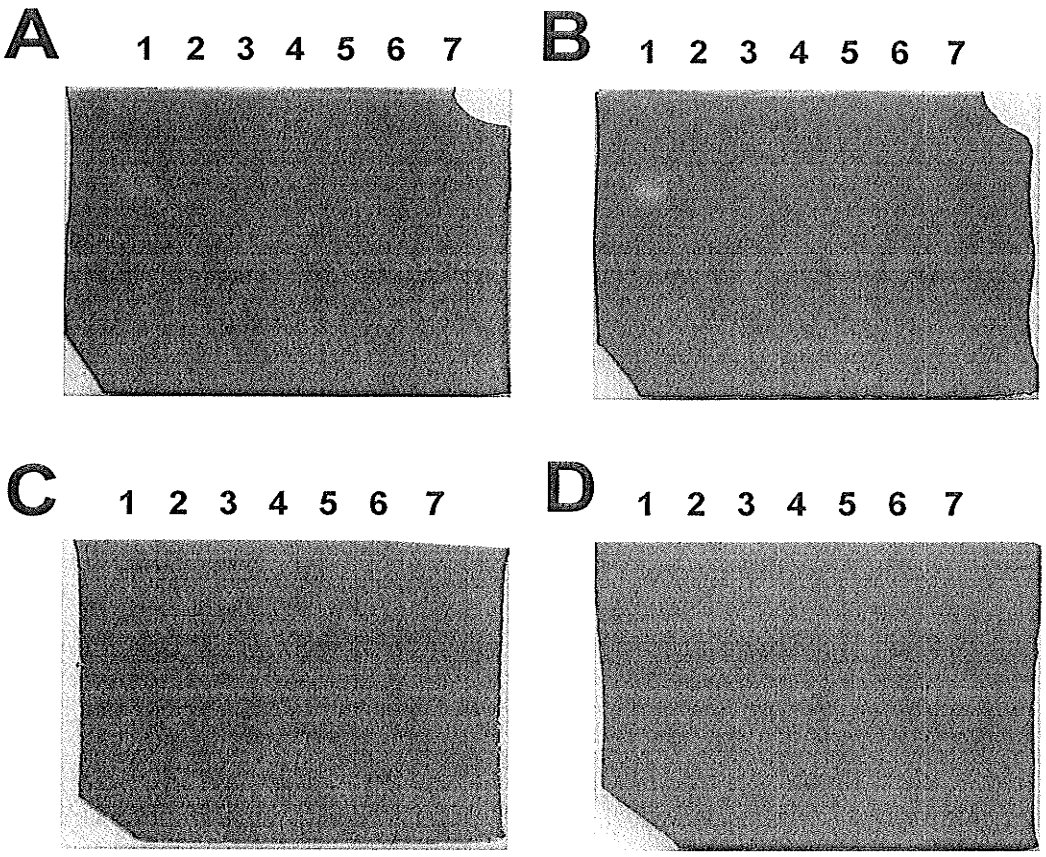

Figure 20: Analysis of HA-degrading activity. Samples were separated in a hyaluronan-embedded polyacrylamide gel. Gels were loaded as follows: (1) positive control, human HYAL1 (2) negative control (blank), and 60 ug total protein lysate from each (3) *hya-1(dm12); oga-1 (ok1207)* (4) *oga-1(ok1207)* (5) *hya-1(dm12)* (6) wild type and (7) OP50 E.coli. After electrophoresis, gels were incubated in either PBS (pH 7.0) or formic acid (pH 3.7) to allow for possible enzymatic activity. Subsequently gels were treated with proteases, stained with Alcian Blue which binds to undegraded hyaluronan and counterstained with Coomassie Blue to detect false positives due to areas of high protein concentration. Hyaluronidase activity is detected as a clear patch. The positive control displays activity while no activity is detected with the *C.elegans* protein samples (A) at pH 3.7 and 20°C and (B) at pH 3.7 and 37°C. No hyaluronidase activity is detected with *C.elegans* protein samples at (C) pH 7.0 and 20° C or (D) pH 7.0 and 37°C. Additionally, the positive control is inactive at pH 7.0.

C.elegans protein samples. At pH 7.0 both temperatures show no activity for human HYAL1 (Figure 20-C, 20-D) which is an expected result because this enzyme is only active at acidic pH. Again, both temperatures at pH 7.0 result in no activity detected for any of the *C.elegans* protein samples. In conclusion, no HA-degrading activity was detected for *C.elegans*.

These findings are not unexpected when the fact that *C.elegans* does not synthesize HA is taken into account. Additionally, some hyaluronidases have been reported to also degrade chondroitin (Rigden and Jedrzejas. 2003). These two GAGs, HA and chondroitin are structurally similar except for an epimer change (Figure 21). HA is composed of repeating glucuronic acid and N-acteylglucosamine dissacharide units while chondroitin is composed is repeating glucuronic acid and N-acetylgalactosamine dissacharide units. Therefore, the structural difference is the positioning of one hydroxyl group in each dissacharide unit. *C.elegans* does synthesize chondroitin and therefore it was logical to test the ability of HYA-1 and OGA-1 for chondroitin degradation.

Chondroitin is much smaller in size than HA and cannot be embedded within a polyacrylamide gel; therefore an alternative method to assay chondroitinase activity was required. A novel *in vitro* assay was developed specifically for this objective (section 2.11). This assay consisted of mixing total protein lysate samples with commercially available chondroitin in a pH specific buffer. Samples were incubated at 20°C overnight prior to separation by polyacrylamide electrophoresis in a Tris-tricine buffer system. The gels were exposed to a protease digest to decrease protein staining which can obscure visualization of the chondroitin product. Activity is assessed by a decrease in intensity of the resulting chondroitin band for each sample representing a reduction in chondroitin present. Chondroitinase ABC (Sigma) was utilized as a positive control for this

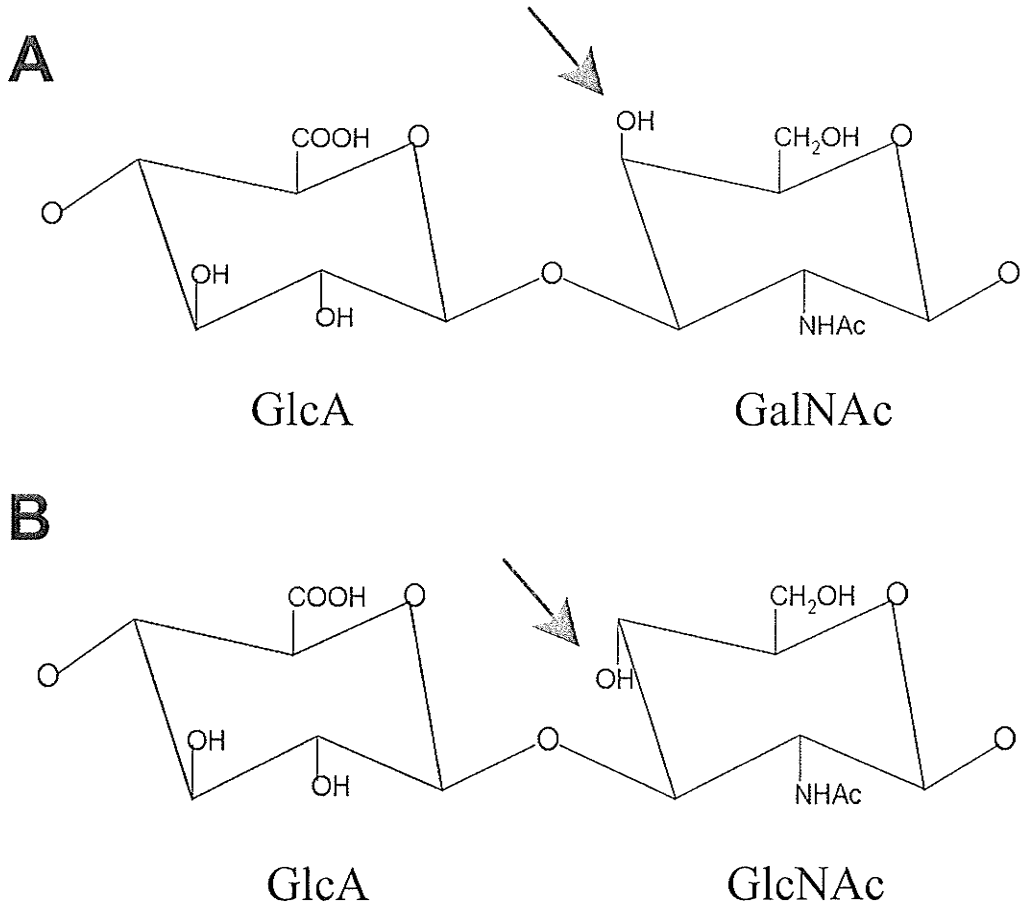

Figure 21: Structures of hyaluronan and chondroitin. (A) Chondroitin is composed of glucuronic acid (left) and N-acetylgalactosamine (right) with a beta 1-3 linkage. The hydroxyl group on carbon 3 of N-acetylgalactosamine is positioned up (arrow). (B) Hyaluronan is composed of glucuronic acid (left) and N-acetylglucosamine (right) with a beta 1-3 linkage. The hydroxyl group on carbon 4 is positioned down (arrow).

experiment. Chondroitinase ABC degrades chondroitin sulphate A and chondroitin sulphate C with reduced efficiencies for chondroitin sulphate B, chondroitin and HA at 40%, 20% and 2% compared to chondroitin sulfates A and C activity (Sigma product info). At pH 3.7 (Figure 22), no activity was detected in *hya-1(dm12); oga-1(ok1207)* or *hya-1(dm12)* while complete clearing of chondroitin occurs in *oga-1(ok1207)* and wild type samples representing chondroitinase activity present in these samples due to HYA-1. At pH 7, no activity is detected for *hya-1(dm12); oga-1(ok1207)* or *hya-1(dm12)* with reduced activity detected in *oga-1(ok1207)* and wild type samples. At pH 8.8, no significant amount of activity was detected for any sample. The chondroitin band in the pH 3.7 gel was a slightly different shape then in pH 7 and pH 8.8 gels due to using smaller wells for loading samples in the gel.

3.16 Distribution pattern of chondroitin *in vivo*

Chondroitin is commonly found sulphated within organisms. One antibody is available for the unsulfated form of chondroitn however it is very expensive and not in the budget for this project. Instead, to explore the distribution pattern of chondroitin *in vivo* we developed a simple method of staining freeze/cracked animals prepared for immunofluorescence utilizing Alcian blue. Alcian blue is commonly used in histology to demonstrate the presence of both acidic and neutral mucosubstances. As previously discussed, *C.elegans* synthesizes only chondroitin and heparan sulfate. Of these two GAGs, chondroitin is documented to be the most abundant with only a small amount of heparan sulphate synthesized (Yamada et al. 1999). Specifically, the GAGs were quantified using chromatographic methods at a ratio of almost 250:1 ng GAG/ mg of total

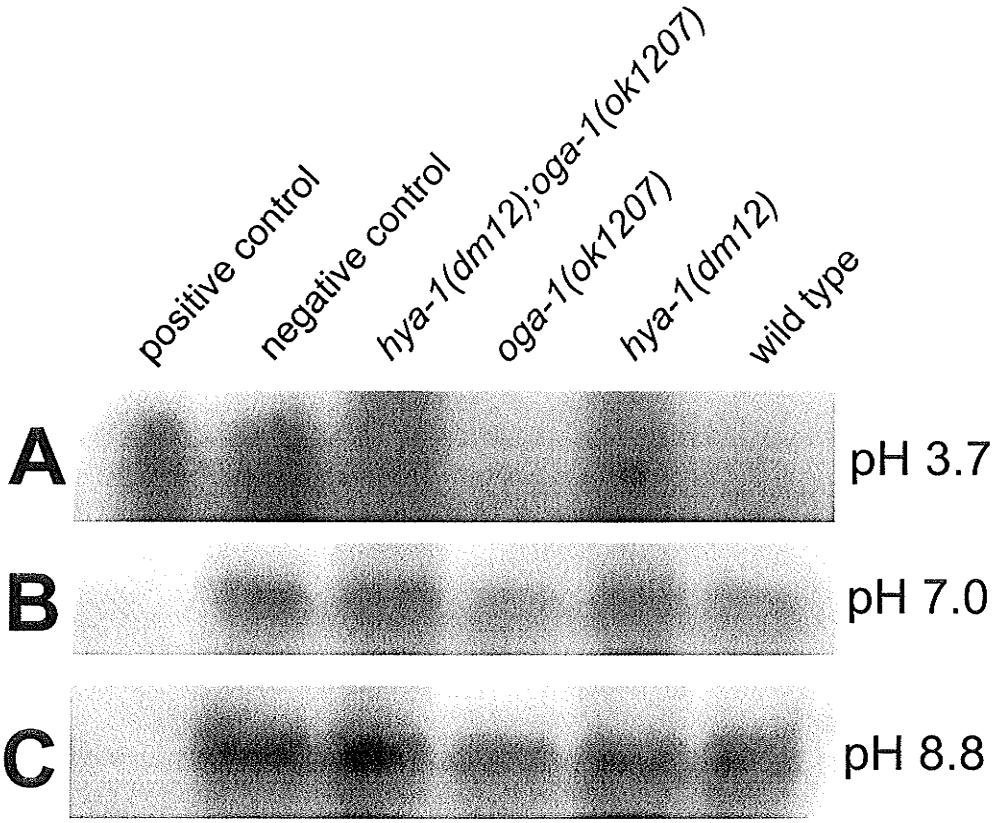

Figure 22: Analysis of chondroitin-degrading activity. Samples of total protein lysate (250 micrograms) were incubated with 7.5 micrograms of chondroitin at 20 degrees Celcius overnight at the specified pH. Samples were analyzed by polyacrylamide gel electrophoresis in a Tris-Tricine buffer system. Resulting gels were subjected to a protease digest. (A) At pH 3.7, no activity is detected in either *hya-1(dm12)* or *hya-1(dm12);oga-1(ok1207)* as assessed by chondroitin band intensity. Complete clearing of chondroitin occurs in wild type and *oga-1(ok1207)* representing chondroitinase activity present in these samples is due to the presence of HYA-1. (B) At pH 7.0, reduced activity is detected in wild type and *oga-1(ok1207)* and (C) at pH 8.8, no significant amount of activity is detected for any sample. Note: The chondroitin band in (A) is slightly different in shape then (B) and (C) because the samples were loaded onto the gel with smaller wells.

dried tissue in *C.elegans* (Toyoda, Kinoshita-Toyoda, and Selleck. 2000). Therefore any Alcian blue staining detected is most likely due to the presence of chondroitin.

This method revealed a relatively consistent pattern of staining among wild type animals (Figure 23). An even distribution of Alcian blue was exhibited throughout embryos on the slide. Young larval stage animals displayed staining in patches in both the anterior and posterior section of the animal. The anterior patch overlaps the proximal region of the pharynx and anterior section of the intestine with a distinct clear patch visible within this area. The intestinal lumen also distinctly displayed staining running the length of the animal. The posterior patch corresponds to an area which displays high *hya-1*::GFP expression. Older larval stage animals appeared to be stained in the region of migrating vulval cells. Adults clearly displayed staining throughout the germline, intestinal lumen and the anterior and posterior patches.

As the staining of wild type animals was informative, Alcian blue staining of *hya-1(dm12)* animals was also performed to determine if any observable change of pattern could be established. *hya-1(dm12)* animals also display staining in the anterior and posterior patches and the intestinal lumen as observed in wild type animals however the staining was more intense. Unlike wild type animals, *hya-1(dm12)* displays staining throughout the intestine and in the ventral nerve cord (Figure 24).

Chondroitin is previously reported to be synthesized in cells in the vulva, uterus and oocytes as interpreted from the detection of chondroitin synthase, *sqv-5*, within these cells (Hwang et al. 2003b). Additionally, chondroitin is required for the correct migration of gonadal distal tip cells, vulval morphogenesis (Suzuki et al. 2006) and cytokinesis and nuclear division during embryogenesis (Mizuguchi et al. 2003; Mizuguchi et al. 2004). Here we have directly shown Alcian blue staining (interpreted as the presence of

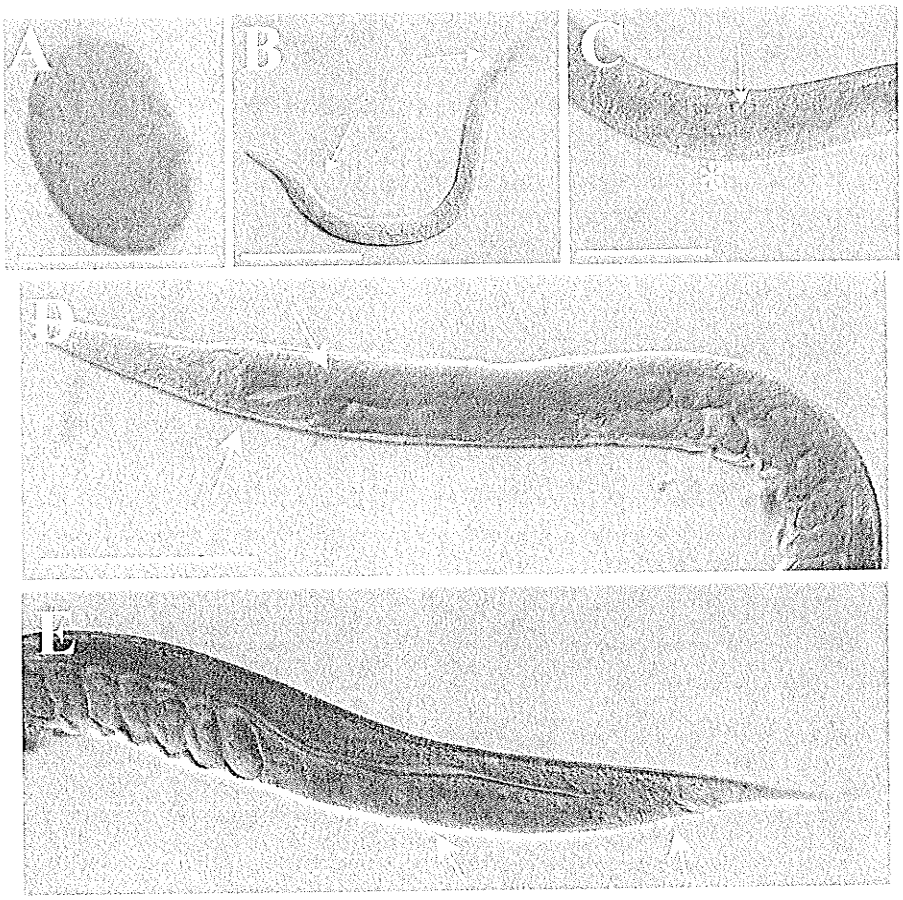

Figure 23: Wild type animals stained with Alcian blue to detect chondroitin *in vivo*. (A) A 100 cell stage embryo displays an even stain pattern all over. Scale bar represents 25 microns. (B) L1 stage animal displays the anterior and posterior stain patch pattern as well as staining of the intestinal lumen. Scale bar represents 50 microns. (C) An L3 animal displays distinct staining in the intestinal lumen (arrow) and in the area of vulval cells (*). Scale bar represents 40 microns. (D) Gravid adult animal displays staining of the germline as visible in the anterior gonad arm and the anterior patch as well as (E) the posterior germline and the posterior patch. Scale bar in (D) represents 40 microns in (D) and (E).

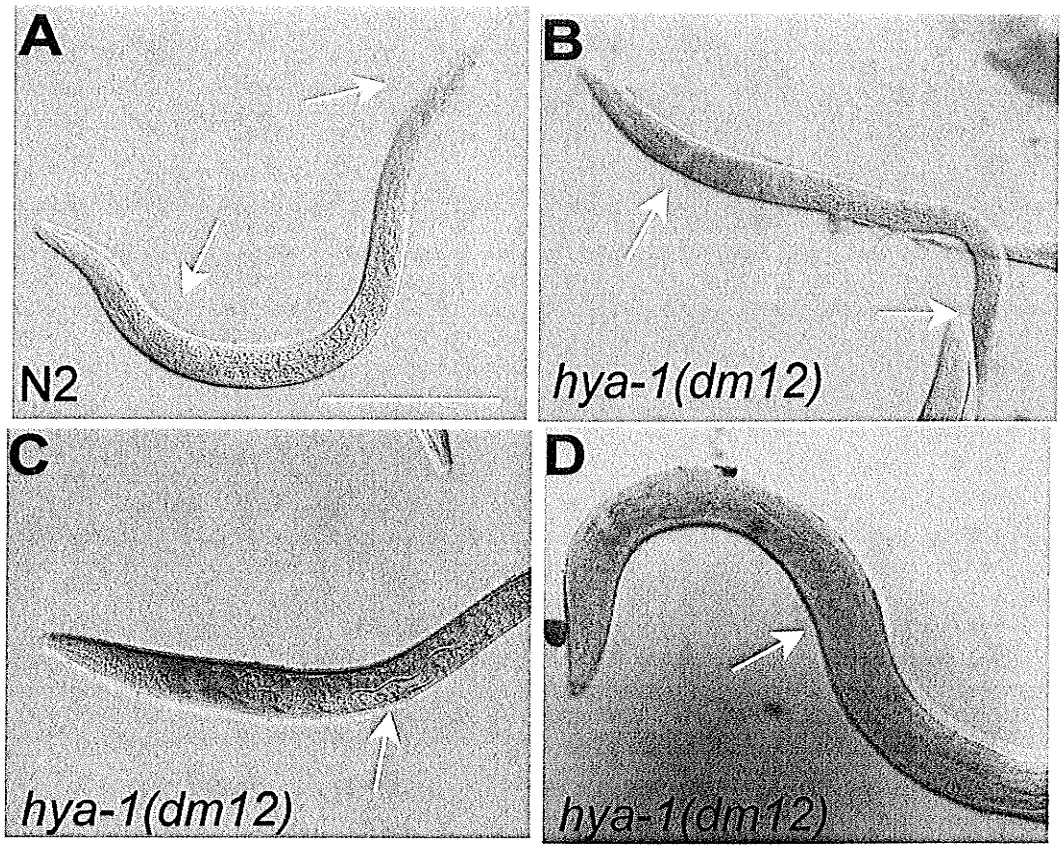

Figure 24: Alcian blue staining of *hya-1(dm12)*. (A) Wild type animal at L1 stage stained with Alcian blue to compare intensity of staining with that observed in *hya-1(dm12)*. (B) *hya-1(dm12)* L1 stage animal displays increased intensity in the anterior and posterior patches of staining also present in wild type animals. (C) The ventral nerve cord is distinctly stained in an L1 stage *hya-1(dm12)* animal. (D) Intestinal staining is visualized throughout the body of *hya-1(dm12)*. Dark spots seen on animal in (D) are artifacts. Scale bar in (A) represents 50 microns. Animals are oriented such that anterior is left, posterior is right, ventral is down and dorsal is up.

chondroitin) in the vulva, gonad and oocytes consistent with the expression of chondroitin synthase. Additionally we show Alcian blue staining in the intestine, ventral nerve cord and possibly the nerve ring where chondroitin has not previously been reported.

In *C.elegans*, lysosomes are specifically localized to intestinal cells (Hermann et al. 2005). Perhaps the chondroitin detected within the intestine in *hya-1(dm12)* animals is due to an accumulation within lysosomes. In mutants defective in lysosomal biosynthesis, lysosomal material accumulated within the intestinal lumen and was expelled during defecation (Hermann et al. 2005). Furthermore, many lysosomal storage disorders in humans result in neurological abnormalities (Online Mendelian Inheritance in Man (OMIM) database) suggesting an important role for lysosomes within neurons. Alternatively, chondroitin may be required in the ECM directly surrounding neurons as a component of the specialized ECM reported for PLM neurons (Emtage et al. 2004).

In summary, it appears that chondroitin is normally present in the intestinal lumen, vulval cells, germline and the anterior and posterior patches presented in Figure 23. In the absence of *hya-1*, it appears that the amount of chondroitin increases in these regions. As well, chondroitin appears to accumulate in two novel locations, the ventral nerve cord and the intestine.

4. DISCUSSION

The studies presented here were designed to explore the role of a hyaluronidase family member *in vivo* using a less complex model than a mammal. Mammals have at least six genes encoding hyaluronidase, with a seventh hyaluronidase identified in mice. The protein products of the hyaluronidase family members display some overlap in expression patterns and produce only mild phenotypic changes in knock-out models. Therefore redundancy between hyaluronidases is proposed in mammals.

We propose that HYA-1 is a chondroitinase. Bioinformatic analysis predicts a glycosyl hydrolase function and shows strong conservation of many features required for catalytic function of hyaluronidase orthologues. Additionally, strong support for this conclusion is based on the lack of detectable chondroitinase activity in protein samples from a *hya-1* deletion strain. However this evidence results from an *in vitro* assay, and may not reflect the role of HYA-1 *in vivo*. We have detected an apparent GAG substrate accumulation *in vivo* in the *hya-1* deletion strain as well as defects in structures known to require chondroitin for normal morphology (the vulva). An alternative way to address this issue would be to clone and express recombinant HYA-1 protein for the chondroitinase assays to directly assess HYA-1 function, although this would also be an *in vitro* method. To directly assess the role of HYA-1 for chondroitin degradation *in vivo*, levels of chondroitin *in vivo* would have to be quantified through immunofluoresence with a chondroitin specific antibody, by Fluorophore-assisted carbohydrate electrophoresis (FACE) (Calabro et al. 2001) or other biochemical means.

Protein samples containing HYA-1 showed optimal chondroitinase activity at acidic pH, suggesting that HYA-1 is lysosomal. HYA-1 also contains a predicted signal sequence supporting the lysosomal subcellular localization. However this signal sequence

could also be responsible for a secreted HYA-1. Again, the *in vitro* chondroitinase assay does not represent the *in vivo* environment and HYA-1 was also active at neutral pH, albeit with reduced activity, suggesting that it may be secreted. Most hyaluronidases are presumed to be located within lysosomes. As well, *hya-1*::GFP expression was detected in the intestine which provides the majority of nutrient storage in *C.elegans*. Within the intestine there are also gut granules which are lysosome-related organelles. In the posterior region of the intestine in a *hya-1* deletion strain we observed increased Alcian blue staining that we propose represents an accumulation of chondroitin. Although the Alcian blue resolution was not sufficient to directly visualize staining of the gut granules, we have observed enlarged gut granules corresponding to the same region of the intestine. An alternative way to address this issue would be to generate a translational GFP reporter construct or perform immunofluoresence with an anti- HYA-1 antibody to directly detect subcellular localization of HYA-*1 in vivo*.

C.elegans has no HA-degrading activity. Evidence to support comes from an *in vitro* assay which produced no detectable activity from any of the protein samples. The zymogram method is an established method for detecting HA-degrading activity as well, the positive control showed activity at acidic pH. The samples utilized for the HA zymogram assay were prepared from the same batch of protein aliquots utilized for the chondroitinase assays therefore demonstrating that the method of preparation did not diminish over-all protein activity. *C.elegans* does not have a HA synthase gene and does not synthesize HA (Morio et al. 2003; Suzuki et al. 2006; Toyoda, Kinoshita-Toyoda, and Selleck. 2000; Yamada et al. 2002). The sequence similarity between hyaluronidase orthologues in *C.elegans* and humans, the lack of HA and HA-degrading activity and the detection of chondroitinase activity in *C.elegans* taken together provide support for the

theory that hyaluronidase in higher organisms evolved from a chondroitinase in lower organisms (reviewed in Stern, Asari, and Sugahara. 2006).

The human orthologue of the *oga-1* predicted protein product, MGEA5, has displayed HA-degrading activity *in vitro*. Therefore we performed RNAi assay to assess the possibility of redundancy between *hya-1* and *oga-1*. Although initial observations of RNAi assays suggested redundancy, assessment of *oga-1* and *hya-1* deletion strains as well as a *hya-1;oga-1* double deletion strain do not support a redundant role for *hya-1* and *oga-1*. The difference observed in the RNAi-induced knock-down of *oga-1* expression and the null deletion mutant *oga-1(ok1207)* may be attributed to the RNAi method itself, which often is not 100% effective (Kamath et al. 2001; Timmons and Fire. 1998). Therefore the phenotypes observed due to RNAi may not be as severe as a null mutant. Thus, RNAi of *oga-1* did not reveal the full Egl phenotype, so the RNAi of *oga-1* in the *hya-1* null mutant produced a more severe phenotype than RNAi of *oga-1* alone, essentially falsely displaying redundancy between *oga-1* and *hya-1*.

For the *hya-1* and *oga-1* null mutants, the Egl phenotypes observed were transient and the Sqv phenotype displayed incomplete penetrance with variable severity. The assessment of penetrance may be skewed due to an insufficient sample size to completely represent the population. However other deletion strains for lysosomal enzymes have also displayed a lack of phenotypic change (Hujova et al. 2005). To address the issue of redundancy, the phenotypic analyses could be redesigned with more stringent guidelines. For example, the Egl phenotype may be scored based on egg-laying frequencing, staging of embryos within the uterus and upon exiting of the uterus, however this would be extremely consuming.

It is interesting to note that *hya-1* and *sqv* mutants display similar phenotypes. *hya-1* deletion mutants display Egl and Sqv phenotypes as well as protruding mature vulvas which are also displayed in *sqv* mutants (Bulik et al. 2000; Hwang and Horvitz. 2002a; Hwang and Horvitz. 2002b; Hwang et al. 2003a; Hwang et al. 2003b), although to a lesser degree. SQV-1-8 proteins are involved in chondroitin synthesis, thus chondroitin is required for vulval morphogenesis. RNAi assays for chondroitin proteoglycans CPG-1 and CPG-2 expressed together display a synergistic effect creating an embryonic lethal phenotype similar to mutants deficient in chondroitin synthase (SQV-5) (Olson et al. 2006). HYA-1 is a chondroitinase which suggests it is required for the remodelling of the extracellular matix for cell migration during vulval development. To address this issue, a chondroitin proteoglyan could be tagged for visualization *in vivo* and then the proteoglycan localization could be documented to observe possible turnover.

Hya-1 is expressed in the intestine, anal sphincter, amphid neurons in the head and the PLM neurons in the tail of *C.elegans* as detected utilizing a transcriptional reporter construct. This is an indirect method of detection, observing the expression of an exogenous protein. RNA *in situ* methods would directly detect the transcriptional product of *hya-1*. Immunofluorescence is an additional method to directly detect HYA-1, however the generation of an anti-HYA-1 antibody is a long complicated process with no guarantee that antisera raised to the antigen would bind HYA-1 *in vivo*. GFP transcriptional reporter constructs are commonly used in *C.elegans* and a catalogue of optimized vectors for generating transcriptional and translational reporter constructs in *C.elegans* is readily available (FIRE vectors, http://www.addgene.org/pgvec1?f=c&cmd=showcol&colid=1).

Oga-1 is broadly expressed throughout many tissues in *C.elegans* unlike the restricted expression pattern of *hya-1*. *oga-1* expression was detected in vulval cells and

neurons in the head, the same as *hya-1*. However, *oga-1* expression detected in the pharynx, tail neurons, spermatheca, distal tip cell, body wall muscles, excretory canal, rectal muscle and seam cell does not correspond with *hya-1* expression.

We propose *hya-1(dm12)* is a null allele. Sequencing results revealed the deletion included the nucleotides encoding the initiator methionine as well as spanning almost the entire catalytic glycosyl hydrolase domain, which is the only catalytic domain present. It is very unlikely that *hya-1(dm12)* results in a mutated protein. In *hya-1(dm12)* the initiator methionine is deleted, furthermore, the chondroitinase activity assays clearly display a loss of function in samples from *hya-1(dm12).* An alternative was to address this would be to perform RT-PCR and western blot analysis to determine if *hya-1(dm12)* is transcribed or if protein is translated in the *hya-1* deletion strain.

In conclusion, we propse that HYA-1 is a chondroitinase localized to the lysosome and active at acidic pH in *C.elegans.*

5. APPENDIX

5.1 Primer list

Primer	Sequence	Position of 5' base pair Relative to A in ATG	Primer Direction
AHT22-O	AACTGCCTGGACCCCTAACT	2161	forward
AHT22-P	GAGCCAACGTCACCAAAAAT	3841	reverse
AHT22-E	TGAACCGTTTCGGACTATGG	-327	forward
AHT22-F	TTGGATCACTTTCATTCTGAGC	488	reverse
AHT22-G	GAACGGATGTTGTGTGGATGG	151	forward
AHT22-H	TCAGTGTCCGACTTTTGTCC	1128	reverse
AHT22-I	CTCGAAGCTCACTTGATTCAGG	654	forward
AHT22-J	CACGCCCTTCACATCTCTCC	2174	reverse
AHT22-K	CTGCCTACTTTACTTTTTCC	-1183	forward
AHT22-X	CGAATTTATTCTAAGGAACAAGG	-1150	forward
AHT22-S	GCTCCCACATAGGTCTGAAC	765	reverse
DM12-1	GAGGAAAAAGAGGCGAAGGGCG	-215	forward
DM12-2	ACTCTCAGGGTTGGTCAATGC		
DM12-A	CGTAACTGGTTGGGACTCTCA	1310	forward
DM12-B	ACTCTCAGGGTTGGTCAATGC	1330	reverse
AHT22-MSC	CACACAATGGCCATCTTATGTTGGC	-11	reverse
AHT22-Q	TCCACCAACAAAATGCTGATCTA	412	reverse
AHT22-R	GAAGGATATGACTAACCTGGGGT	524	reverse
AHT22-Y	AGTCTGAAATTGTCGGACTCC	-1314	forward
AHT22-SPH	GATCTGATCTATGCGCATGCAC	-849	forward
A	TCATGCACAAACATCCGAAGCTCG	-1320	forward
D	GTGACATCTGGAATGACTTGAGG	1747	reverse
MGEA-1	TGCATTCTGCATAAGCCACC	2321	forward
MGEA-2	GGATCTTCCTAAATGCCG	2111	forward
MGEA-3	TAGGAAATATCCACGCGACC	3532	forward
MGEA-4	GAACCTTGAATGGAACATTGGCC		forward
MGEA-A2	GGTGCTGATGCTTGAGC	639	reverse
MGEA-B2	GTTTCAGTTGAACATGCAGTC	474	reverse
MGEA-C	CGAATTTCAGGCTTCTACGG	309	reverse
MGEA-D	GACTGTGAACACGATGGAGC	-13	reverse
CC8F1	GATCTGATCTATGCTCATGC		
CC8R1	GGGTAAGTTTTCCGTATGTT		

5.2 Vulval Measurements

5.2 Vulval measurements (in microns)

Wild type				***oga-1***				***hya-1***				***double***			
Height Utse	Toroids	Width Toroids	Worm	Height Utse	Toroids	Width Toroids	Worm	Height Utse	Toroids	Width Toroids	Worm	Height Utse	Toroids	Width Toroids	Worm
22.0	11.0	24.2	71.5	24.2	15.4	25.3	72.6	24.2	12.1	26.4	0.0	26.4	13.2	29.7	71.5
27.5	11.0	23.1	82.5	25.3	15.4	26.4	77.0	24.2	14.3	26.4	66.0	17.6	8.8	24.2	74.8
22.0	13.2	27.5	78.1	22.0	15.4	26.4	72.6	22.0	12.1	27.5	70.4	19.8	9.9	22.0	
25.3	13.2	28.6	79.2	24.2	15.4	23.1	71.5	22.0	11.0	24.2	71.5	19.8	8.8	24.2	75.9
26.4	13.2	28.6	75.9	22.0			84.7	16.5	8.8	22.0	60.5	23.1	12.1	24.2	64.9
18.7	11.0	23.1	77.0	0.0	11.0	16.5	50.6	25.3	11.0	26.4	72.6	23.1	13.2	24.2	66.0
23.1	11.0	26.4	73.7	16.5	6.6	18.7	70.4	30.8	16.5	25.3	73.7	19.8	11.0	24.2	61.6
22.0	9.9	25.3	67.1	16.5	8.8	23.1	68.2	25.3	12.1	24.2	64.9	20.9	12.1	24.2	56.1
22.0	11.0	25.3	66.0	19.8	12.1	26.4	71.5	27.5	15.4	24.2	0.0	19.8	11.0	31.9	64.9
24.2	12.1	25.3	70.4	19.8	13.2	20.9	72.6	22.0	9.9	22.0	61.6	20.9	12.1	24.2	64.9
23.1	12.1	24.2	79.2	19.8	8.8	17.6	69.3	22.0	8.8	22.0	64.9	22.0	11.0	23.1	69.3
19.8	11.0	26.4	73.7	22.0	12.1	27.5	71.5	19.8	7.7	22.0	60.5	18.7	9.9	22.0	60.5
27.5	20.9	33.0	69.3	20.9	11.0	22.0	63.8	12.1	7.7	16.5	66.0	17.6	5.5	18.7	69.3
27.5	15.4	27.5	70.4	17.6	12.1	24.2	62.7	22.0	11.0	23.1	64.9	22.0	12.1	24.2	0.0
22.0	11.0	27.5	66.0	22.0	12.1	23.1	71.5	20.9	9.9	24.2	63.8	23.1	11.0	23.1	69.3
30.8	12.1	27.5	63.8	22.0	13.2	26.4	78.1	20.9	8.8	24.2	66.0	22.0	11.0	23.1	61.6
20.9	11.0	27.5	66.0	20.9	12.1	23.1	63.8	24.2	11.0	22.0		22.0	13.2	22.0	62.7
24.2	11.0	22.0	79.2	16.5	11.0	23.1	67.1	18.7	9.9	18.7	62.7	16.5	8.8	16.5	0.0
27.5	20.9	30.8	75.9	25.3	9.9	24.2	69.3	22.0	7.7	19.8	68.2	22.0	11.0	27.5	0.0
				22.0	12.1	27.5	0.0	22.0	9.9	27.5	0.0	24.2	12.1	22.0	0.0
								22.0	11.0	22.0	0.0	0.0	12.1	22.0	0.0
								27.5	13.2	27.5	0.0	20.9	12.1	31.9	56.1
								18.7	11.0	22.0	61.6	22.0	14.3	30.8	56.1
												22.0	9.9	22.0	67.1
												20.9	11.0	23.1	67.1
Mean	24.0	12.7	26.5	72.9	19.9	12.0	23.2	69.9	22.2	10.8	23.2	58.8	20.9	10.8	23.9	55.2
Std Dev	3.2	3.1	2.7	5.6	5.6	2.5	3.2	7.0	4.0	2.5	2.8	21.7	2.4	1.9	3.4	25.9

7. REFERENCES

Ackley, B. D., J. R. Crew, H. Elamaa, T. Pihlajaniemi, C. J. Kuo, and J. M. Kramer. "The NC1/endostatin Domain of Caenorhabditis Elegans Type XVIII Collagen Affects Cell Migration and Axon Guidance." *The Journal of Cell Biology* 152, no. 6 (Mar 19 2001): 1219-1232.

Banerji, S., J. Ni, S. X. Wang, S. Clasper, J. Su, R. Tammi, M. Jones, and D. G. Jackson. "LYVE-1, a New Homologue of the CD44 Glycoprotein, is a Lymph-Specific Receptor for Hyaluronan." *The Journal of Cell Biology* 144, no. 4 (Feb 22 1999): 789-801.

Bargmann, C.I., Chemosensation in *C.elegans* (October 25, 2006), *WormBook*, ed. The *C.elegans* Research Community, WormBook, doi/10/1895/wormbook.1.123.1, http://www.wormbook.org.

Beauvais, D. M., and A. C. Rapraeger. "Syndecans in Tumor Cell Adhesion and Signaling." *Reprod.Biol.Endocrinol.* 2 (Jan 7 2004): 3.

Beech, D. J., A. K. Madan, and N. Deng. "Expression of PH-20 in Normal and Neoplastic Breast Tissue." *The Journal of Surgical Research* 103, no. 2 (Apr 2002): 203-207.

Bertrand, P., N. Girard, C. Duval, J. d'Anjou, C. Chauzy, J. F. Menard, and B. Delpech. "Increased Hyaluronidase Levels in Breast Tumor Metastases." *International Journal of Cancer.Journal International Du Cancer* 73, no. 3 (Nov 4 1997): 327-331.

Bono, P., E. Cordero, K. Johnson, M. Borowsky, V. Ramesh, T. Jacks, and R. O. Hynes. "Layilin, a Cell Surface Hyaluronan Receptor, Interacts with Merlin and Radixin." *Experimental Cell Research* 308, no. 1 (Aug 1 2005): 177-187.

Brenner, S. "The Genetics of Caenorhabditis Elegans." *Genetics* 77, no. 1 (May 1974): 71-94.

Bulik, D. A., G. Wei, H. Toyoda, A. Kinoshita-Toyoda, W. R. Waldrip, J. D. Esko, P. W. Robbins, and S. B. Selleck. "Sqv-3, -7, and -8, a Set of Genes Affecting Morphogenesis in Caenorhabditis Elegans, Encode Enzymes Required for Glycosaminoglycan Biosynthesis." *Proceedings of the National Academy of Sciences of the United States of America* 97, no. 20 (Sep 26 2000): 10838-10843.

C. elegans Sequencing Consortium. "Genome Sequence of the Nematode C. Elegans: A Platform for Investigating Biology." *Science (New York, N.Y.)* 282, no. 5396 (Dec 11 1998): 2012-2018.

Calabro, A., R. Midura, A. Wang, L. West, A. Plaas, and V. C. Hascall. "Fluorophore-Assisted Carbohydrate Electrophoresis (FACE) of Glycosaminoglycans."

Osteoarthritis and Cartilage / OARS, Osteoarthritis Research Society 9 Suppl A (2001): S16-22.

Cassada, R. C., and R. L. Russell. "The Dauerlarva, a Post-Embryonic Developmental Variant of the Nematode Caenorhabditis Elegans." *Developmental Biology* 46, no. 2 (Oct 1975): 326-342.

Chalfie, M., and J. Sulston. "Developmental Genetics of the Mechanosensory Neurons of Caenorhabditis Elegans." *Developmental Biology* 82, no. 2 (Mar 1981): 358-370.

Chang, N. S. "Transforming Growth Factor-beta1 Blocks the Enhancement of Tumor Necrosis Factor Cytotoxicity by Hyaluronidase Hyal-2 in L929 Fibroblasts." *BMC Cell Biology* 3 (Apr 3 2002): 8.

Cherr, G. N., A. I. Yudin, and J. W. Overstreet. "The Dual Functions of GPI-Anchored PH-20: Hyaluronidase and Intracellular Signaling." *Matrix Biology : Journal of the International Society for Matrix Biology* 20, no. 8 (Dec 2001): 515-525.

Cheung, W. F., T. F. Cruz, and E. A. Turley. "Receptor for Hyaluronan-Mediated Motility (RHAMM), a Hyaladherin that Regulates Cell Responses to Growth Factors." *Biochemical Society Transactions* 27, no. 2 (Feb 1999): 135-142.

Cinar, H. N., K. L. Richards, K. S. Oommen, and A. P. Newman. "The EGL-13 SOX Domain Transcription Factor Affects the Uterine Pi Cell Lineages in Caenorhabditis Elegans." *Genetics* 165, no. 3 (Nov 2003): 1623-1628.

Comtesse, N., D. Heckel, E. Maldener, B. Glass, and E. Meese. "Probing the Human Natural Autoantibody Repertoire using an Immunoscreening Approach." *Clinical and Experimental Immunology* 121, no. 3 (Sep 2000): 430-436.

Csoka, A. B., S. W. Scherer, and R. Stern. "Expression Analysis of Six Paralogous Human Hyaluronidase Genes Clustered on Chromosomes 3p21 and 7q31." *Genomics* 60, no. 3 (Sep 15 1999): 356-361.

Daly, M. C., R. H. Xiang, D. Buchhagen, C. H. Hensel, D. K. Garcia, A. M. Killary, J. D. Minna, and S. L. Naylor. "A Homozygous Deletion on Chromosome 3 in a Small Cell Lung Cancer Cell Line Correlates with a Region of Tumor Suppressor Activity." *Oncogene* 8, no. 7 (Jul 1993): 1721-1729.

Deguine, V., M. Menasche, P. Ferrari, L. Fraisse, Y. Pouliquen, and L. Robert. "Free Radical Depolymerization of Hyaluronan by Maillard Reaction Products: Role in Liquefaction of Aging Vitreous." *International Journal of Biological Macromolecules* 22, no. 1 (Feb 1998): 17-22.

Duggirala, R., J. Blangero, L. Almasy, T. D. Dyer, K. L. Williams, R. J. Leach, P. O'Connell, and M. P. Stern. "Linkage of Type 2 Diabetes Mellitus and of Age at Onset to a Genetic Location on Chromosome 10q in Mexican Americans." *American Journal of Human Genetics* 64, no. 4 (Apr 1999): 1127-1140.

Eastman, C., H. R. Horvitz, and Y. Jin. "Coordinated Transcriptional Regulation of the Unc-25 Glutamic Acid Decarboxylase and the Unc-47 GABA Vesicular Transporter by the Caenorhabditis Elegans UNC-30 Homeodomain Protein." *The Journal of Neuroscience : The Official Journal of the Society for Neuroscience* 19, no. 15 (Aug 1 1999): 6225-6234.

Emtage, L., G. Gu, E. Hartwieg, and M. Chalfie. "Extracellular Proteins Organize the Mechanosensory Channel Complex in C. Elegans Touch Receptor Neurons." *Neuron* 44, no. 5 (Dec 2 2004): 795-807.

Epstein, H. F., D. L. Casey, and I. Ortiz. "Myosin and Paramyosin of Caenorhabditis Elegans Embryos Assemble into Nascent Structures Distinct from Thick Filaments and Multi-Filament Assemblages." *The Journal of Cell Biology* 122, no. 4 (Aug 1993): 845-858.

Fares, H., and I. Greenwald. "Genetic Analysis of Endocytosis in Caenorhabditis Elegans: Coelomocyte Uptake Defective Mutants." *Genetics* 159, no. 1 (Sep 2001a): 133-145.

Fares, H., and I. Greenwald. "Regulation of Endocytosis by CUP-5, the Caenorhabditis Elegans Mucolipin-1 Homolog." *Nature Genetics* 28, no. 1 (May 2001b): 64-68.

Forsythe, M. E., D. C. Love, B. D. Lazarus, E. J. Kim, W. A. Prinz, G. Ashwell, M. W. Krause, and J. A. Hanover. "Caenorhabditis Elegans Ortholog of a Diabetes Susceptibility Locus: Oga-1 (O-GlcNAcase) Knockout Impacts O-GlcNAc Cycling, Metabolism, and Dauer." *Proceedings of the National Academy of Sciences of the United States of America* 103, no. 32 (Aug 8 2006): 11952-11957.

Francis, G. R., and R. H. Waterston. "Muscle Organization in Caenorhabditis Elegans: Localization of Proteins Implicated in Thin Filament Attachment and I-Band Organization." *The Journal of Cell Biology* 101, no. 4 (Oct 1985): 1532-1549.

Frost, G. I., G. Mohapatra, T. M. Wong, A. B. Csoka, J. W. Gray, and R. Stern. "HYAL1LUCA-1, a Candidate Tumor Suppressor Gene on Chromosome 3p21.3, is Inactivated in Head and Neck Squamous Cell Carcinomas by Aberrant Splicing of Pre-mRNA." *Oncogene* 19, no. 7 (Feb 17 2000): 870-877.

Gengyo-Ando, K., and S. Mitani. "Characterization of Mutations Induced by Ethyl Methanesulfonate, UV, and Trimethylpsoralen in the Nematode Caenorhabditis Elegans." *Biochemical and Biophysical Research Communications* 269, no. 1 (Mar 5 2000): 64-69.

Gleason, J. E., H. C. Korswagen, and D. M. Eisenmann. "Activation of Wnt Signaling Bypasses the Requirement for RTK/Ras Signaling during C. Elegans Vulval Induction." *Genes & Development* 16, no. 10 (May 15 2002): 1281-1290.

Godin, D. A., P. C. Fitzpatrick, A. B. Scandurro, P. C. Belafsky, B. A. Woodworth, R. G. Amedee, D. J. Beech, and B. S. Beckman. "PH20: A Novel Tumor Marker for

Laryngeal Cancer." *Archives of Otolaryngology--Head & Neck Surgery* 126, no. 3 (Mar 2000): 402-404.

Golden, J. W., and D. L. Riddle. "The Caenorhabditis Elegans Dauer Larva: Developmental Effects of Pheromone, Food, and Temperature." *Developmental Biology* 102, no. 2 (Apr 1984a): 368-378.

Golden, J. W., and D. L. Riddle. "A Pheromone-Induced Developmental Switch in Caenorhabditis Elegans: Temperature-Sensitive Mutants Reveal a Wild-Type Temperature-Dependent Process." *Proceedings of the National Academy of Sciences of the United States of America* 81, no. 3 (Feb 1984b): 819-823.

Gottlieb, S., and G. Ruvkun. "Daf-2, Daf-16 and Daf-23: Genetically Interacting Genes Controlling Dauer Formation in Caenorhabditis Elegans." *Genetics* 137, no. 1 (May 1994): 107-120.

Hanna-Rose, W., and M. Han. "COG-2, a Sox Domain Protein Necessary for Establishing a Functional Vulval-Uterine Connection in Caenorhabditis Elegans." *Development (Cambridge, England)* 126, no. 1 (Jan 1999): 169-179.

Hanover, J. A., M. E. Forsythe, P. T. Hennessey, T. M. Brodigan, D. C. Love, G. Ashwell, and M. Krause. "A Caenorhabditis Elegans Model of Insulin Resistance: Altered Macronutrient Storage and Dauer Formation in an OGT-1 Knockout." *Proceedings of the National Academy of Sciences of the United States of America* 102, no. 32 (Aug 9 2005): 11266-11271.

Hautmann, S. H., V. B. Lokeshwar, G. L. Schroeder, F. Civantos, R. C. Duncan, R. Gnann, M. G. Friedrich, and M. S. Soloway. "Elevated Tissue Expression of Hyaluronic Acid and Hyaluronidase Validates the HA-HAase Urine Test for Bladder Cancer." *The Journal of Urology* 165, no. 6 Pt 1 (Jun 2001): 2068-2074.

Heckel, D., N. Comtesse, N. Brass, N. Blin, K. D. Zang, and E. Meese. "Novel Immunogenic Antigen Homologous to Hyaluronidase in Meningioma." *Human Molecular Genetics* 7, no. 12 (Nov 1998): 1859-1872.

Heldin, P. "Importance of Hyaluronan Biosynthesis and Degradation in Cell Differentiation and Tumor Formation." *Brazilian Journal of Medical and Biological Research = Revista Brasileira De Pesquisas Medicas e Biologicas / Sociedade Brasileira De Biofisica ... [Et Al.]* 36, no. 8 (Aug 2003): 967-973.

Hermann, G. J., L. K. Schroeder, C. A. Hieb, A. M. Kershner, B. M. Rabbitts, P. Fonarev, B. D. Grant, and J. R. Priess. "Genetic Analysis of Lysosomal Trafficking in Caenorhabditis Elegans." *Molecular Biology of the Cell* 16, no. 7 (Jul 2005): 3273-3288.

Hersh, B. M., E. Hartwieg, and H. R. Horvitz. "The Caenorhabditis Elegans Mucolipin-Like Gene Cup-5 is Essential for Viability and Regulates Lysosomes in Multiple Cell

Types." *Proceedings of the National Academy of Sciences of the United States of America* 99, no. 7 (Apr 2 2002): 4355-4360.

Hill, R. J., and P. W. Sternberg. "The Gene Lin-3 Encodes an Inductive Signal for Vulval Development in C. Elegans." *Nature* 358, no. 6386 (Aug 6 1992): 470-476.

Hresko, M. C., B. D. Williams, and R. H. Waterston. "Assembly of Body Wall Muscle and Muscle Cell Attachment Structures in Caenorhabditis Elegans." *The Journal of Cell Biology* 124, no. 4 (Feb 1994): 491-506.

Hudson, M. L., T. Kinnunen, H. N. Cinar, and A. D. Chisholm. "C. Elegans Kallmann Syndrome Protein KAL-1 Interacts with Syndecan and Glypican to Regulate Neuronal Cell Migrations." *Developmental Biology* 294, no. 2 (Jun 15 2006): 352-365.

Hujova, J., J. Sikora, R. Dobrovolny, H. Poupetova, J. Ledvinova, M. Kostrouchova, and M. Hrebicek. "Characterization of Gana-1, a Caenorhabditis Elegans Gene Encoding a Single Ortholog of Vertebrate Alpha-Galactosidase and Alpha-N-Acetylgalactosaminidase." *BMC Cell Biology* 6, no. 1 (Jan 27 2005): 5.

Hutter, H., I. Wacker, C. Schmid, and E. M. Hedgecock. "Novel Genes Controlling Ventral Cord Asymmetry and Navigation of Pioneer Axons in C. Elegans." *Developmental Biology* 284, no. 1 (Aug 1 2005): 260-272.

Hwang, H. Y., and H. R. Horvitz. "The Caenorhabditis Elegans Vulval Morphogenesis Gene Sqv-4 Encodes a UDP-Glucose Dehydrogenase that is Temporally and Spatially Regulated." *Proceedings of the National Academy of Sciences of the United States of America* 99, no. 22 (Oct 29 2002a): 14224-14229.

Hwang, H. Y., and H. R. Horvitz. "The SQV-1 UDP-Glucuronic Acid Decarboxylase and the SQV-7 Nucleotide-Sugar Transporter may Act in the Golgi Apparatus to Affect Caenorhabditis Elegans Vulval Morphogenesis and Embryonic Development." *Proceedings of the National Academy of Sciences of the United States of America* 99, no. 22 (Oct 29 2002b): 14218-14223.

Hwang, H. Y., S. K. Olson, J. R. Brown, J. D. Esko, and H. R. Horvitz. "The Caenorhabditis Elegans Genes Sqv-2 and Sqv-6, which are Required for Vulval Morphogenesis, Encode Glycosaminoglycan Galactosyltransferase II and Xylosyltransferase." *Journal of Biological Chemistry* 278, no. 14 (Apr 4 2003a): 11735-11738.

Hwang, H. Y., S. K. Olson, J. D. Esko, and H. R. Horvitz. "Caenorhabditis Elegans Early Embryogenesis and Vulval Morphogenesis Require Chondroitin Biosynthesis." *Nature* 423, no. 6938 (May 22 2003b): 439-443.

Kamath, R. S., M. Martinez-Campos, P. Zipperlen, A. G. Fraser, and J. Ahringer. "Effectiveness of Specific RNA-Mediated Interference through Ingested Double-

Stranded RNA in Caenorhabditis Elegans." *Genome Biology* 2, no. 1 (2001): RESEARCH0002.

Kim, E., D. Baba, M. Kimura, M. Yamashita, S. Kashiwabara, and T. Baba. "Identification of a Hyaluronidase, Hyal5, Involved in Penetration of Mouse Sperm through Cumulus Mass." *Proceedings of the National Academy of Sciences of the United States of America* 102, no. 50 (Dec 13 2005): 18028-18033.

Kimble, J. E., and J. G. White. "On the Control of Germ Cell Development in Caenorhabditis Elegans." *Developmental Biology* 81, no. 2 (Jan 30 1981): 208-219.

Kimura, K. D., H. A. Tissenbaum, Y. Liu, and G. Ruvkun. "Daf-2, an Insulin Receptor-Like Gene that Regulates Longevity and Diapause in Caenorhabditis Elegans." *Science (New York, N.Y.)* 277, no. 5328 (Aug 15 1997): 942-946.

Kitagawa, H., N. Egusa, J. I. Tamura, M. Kusche-Gullberg, U. Lindahl, and K. Sugahara. "Rib-2, a Caenorhabditis Elegans Homolog of the Human Tumor Suppressor EXT Genes Encodes a Novel alpha1,4-N-Acetylglucosaminyltransferase Involved in the Biosynthetic Initiation and Elongation of Heparan Sulfate." *The Journal of Biological Chemistry* 276, no. 7 (Feb 16 2001): 4834-4838.

Kitagawa, H., T. Izumikawa, T. Uyama, and K. Sugahara. "Molecular Cloning of a Chondroitin Polymerizing Factor that Cooperates with Chondroitin Synthase for Chondroitin Polymerization." *The Journal of Biological Chemistry* 278, no. 26 (Jun 27 2003): 23666-23671.

Koga, M., and Y. Ohshima. "Drosophila MAP Kinase Kinase Suppresses the Vulvaless Phenotype of Lin-3, Let-23 and Lin-45 Mutations in Caenorhabditis Elegans." *Mechanisms of Development* 53, no. 1 (Sep 1995): 15-22.

Lathrop, W. F., E. P. Carmichael, D. G. Myles, and P. Primakoff. "CDNA Cloning Reveals the Molecular Structure of a Sperm Surface Protein, PH-20, Involved in Sperm-Egg Adhesion and the Wide Distribution of its Gene among Mammals." *The Journal of Cell Biology* 111, no. 6 Pt 2 (Dec 1990): 2939-2949.

Lehman, D. M., D. J. Fu, A. B. Freeman, K. J. Hunt, R. J. Leach, T. Johnson-Pais, J. Hamlington, T. D. Dyer, R. Arya, H. Abboud, H. H. Goring, R. Duggirala, J. Blangero, R. J. Konrad, and M. P. Stern. "A Single Nucleotide Polymorphism in MGEA5 Encoding O-GlcNAc-Selective N-Acetyl-Beta-D Glucosaminidase is Associated with Type 2 Diabetes in Mexican Americans." *Diabetes* 54, no. 4 (Apr 2005): 1214-1221.

Lepperdinger, G., B. Strobl, and G. Kreil. "HYAL2, a Human Gene Expressed in Many Cells, Encodes a Lysosomal Hyaluronidase with a Novel Type of Specificity." *Journal of Biological Chemistry* 273, no. 35 (Aug 28 1998a): 22466-22470.

Lepperdinger, G., B. Strobl, and G. Kreil. "HYAL2, a Human Gene Expressed in Many Cells, Encodes a Lysosomal Hyaluronidase with a Novel Type of Specificity." *The Journal of Biological Chemistry* 273, no. 35 (Aug 28 1998b): 22466-22470.

Lerman, M. I., and J. D. Minna. "The 630-Kb Lung Cancer Homozygous Deletion Region on Human Chromosome 3p21.3: Identification and Evaluation of the Resident Candidate Tumor Suppressor Genes. the International Lung Cancer Chromosome 3p21.3 Tumor Suppressor Gene Consortium." *Cancer Research* 60, no. 21 (Nov 1 2000): 6116-6133.

Lesley, J., V. C. Hascall, M. Tammi, and R. Hyman. "Hyaluronan Binding by Cell Surface CD44." *The Journal of Biological Chemistry* 275, no. 35 (Sep 1 2000): 26967-26975.

Li, Y., M. Rahmanian, C. Widstrom, G. Lepperdinger, G. I. Frost, and P. Heldin. "Irradiation-Induced Expression of Hyaluronan (HA) Synthase 2 and Hyaluronidase 2 Genes in Rat Lung Tissue Accompanies Active Turnover of HA and Induction of Types I and III Collagen Gene Expression." *American Journal of Respiratory Cell and Molecular Biology* 23, no. 3 (Sep 2000): 411-418.

Lin, G., and R. Stern. "Plasma Hyaluronidase (Hyal-1) Promotes Tumor Cell Cycling." *Cancer Letters* 163, no. 1 (Feb 10 2001): 95-101.

Lokeshwar, V. B., B. L. Lokeshwar, H. T. Pham, and N. L. Block. "Association of Elevated Levels of Hyaluronidase, a Matrix-Degrading Enzyme, with Prostate Cancer Progression." *Cancer Research* 56, no. 3 (Feb 1 1996): 651-657.

Lokeshwar, V. B., D. Rubinowicz, G. L. Schroeder, E. Forgacs, J. D. Minna, N. L. Block, M. Nadji, and B. L. Lokeshwar. "Stromal and Epithelial Expression of Tumor Markers Hyaluronic Acid and HYAL1 Hyaluronidase in Prostate Cancer." *The Journal of Biological Chemistry* 276, no. 15 (Apr 13 2001): 11922-11932.

Lokeshwar, V. B., G. L. Schroeder, R. I. Carey, M. S. Soloway, and N. Iida. "Regulation of Hyaluronidase Activity by Alternative mRNA Splicing." *Journal of Biological Chemistry* 277, no. 37 (Sep 13 2002): 33654-33663.

Lubas, W. A., D. W. Frank, M. Krause, and J. A. Hanover. "O-Linked GlcNAc Transferase is a Conserved Nucleocytoplasmic Protein Containing Tetratricopeptide Repeats." *The Journal of Biological Chemistry* 272, no. 14 (Apr 4 1997): 9316-9324.

Madan, A. K., Y. Pang, M. B. Wilkiemeyer, D. Yu, and D. J. Beech. "Increased Hyaluronidase Expression in More Aggressive Prostate Adenocarcinoma." *Oncology Reports* 6, no. 6 (Nov-Dec 1999a): 1431-1433.

Madan, A. K., K. Yu, N. Dhurandhar, C. Cullinane, Y. Pang, and D. J. Beech. "Association of Hyaluronidase and Breast Adenocarcinoma Invasiveness." *Oncology Reports* 6, no. 3 (May-Jun 1999b): 607-609.

Markovic-Housley, Z., G. Miglierini, L. Soldatova, P. J. Rizkallah, U. Muller, and T. Schirmer. "Crystal Structure of Hyaluronidase, a Major Allergen of Bee Venom." *Structure (London, England : 1993)* 8, no. 10 (Oct 15 2000): 1025-1035.

McClain, D. A., W. A. Lubas, R. C. Cooksey, M. Hazel, G. J. Parker, D. C. Love, and J. A. Hanover. "Altered Glycan-Dependent Signaling Induces Insulin Resistance and Hyperleptinemia." *Proceedings of the National Academy of Sciences of the United States of America* 99, no. 16 (Aug 6 2002): 10695-10699.

McGhee, J.D. The *C.elegans* intestine (March 27, 2007), *WormBook*, ed. The *C.elegans* Research Community, WormBook, doi/10.1895/wormbook.1.133.1, http://www.wormbook.org.

Merz, D. C., G. Alves, T. Kawano, H. Zheng, and J. G. Culotti. "UNC-52/perlecan Affects Gonadal Leader Cell Migrations in C. Elegans Hermaphrodites through Alterations in Growth Factor Signaling." *Developmental Biology* 256, no. 1 (Apr 1 2003): 173-186.

Minniti, A. N., M. Labarca, C. Hurtado, and E. Brandan. "Caenorhabditis Elegans Syndecan (SDN-1) is Required for Normal Egg Laying and Associates with the Nervous System and the Vulva." *Journal of Cell Science* 117, no. Pt 21 (Oct 1 2004): 5179-5190.

Mizuguchi, S., K. H. Nomura, K. Dejima, K. Nomura, K. Sugahara, H. Kitagawa, T. Uyama, S. Mitani, and K. Gengyo-Ando. "Chondroitin Sugars in Embryonic Cell Division of the Nematode C. Elegans." *Tanpakushitsu Kakusan Koso.Protein, Nucleic Acid, Enzyme* 49, no. 2 (Feb 2004): 141-147.

Mizuguchi, S., T. Uyama, H. Kitagawa, K. H. Nomura, K. Dejima, K. Gengyo-Ando, S. Mitani, K. Sugahara, and K. Nomura. "Chondroitin Proteoglycans are Involved in Cell Division of Caenorhabditis Elegans." *Nature* 423, no. 6938 (May 22 2003): 443-448.

Moerman, D.G. and Williams, B.D. Sarcomere assembly in *C.elegans* muscle (January 16, 2006), *WormBook*, ed. The *C.elegans* Research Community, WormBook, doi/10.1895/wormbook.1.81.1, http://www.wormbook.org.

Morio, H., Y. Honda, H. Toyoda, M. Nakajima, H. Kurosawa, and T. Shirasawa. "EXT Gene Family Member Rib-2 is Essential for Embryonic Development and Heparan Sulfate Biosynthesis in Caenorhabditis Elegans." *Biochemical and Biophysical Research Communications* 301, no. 2 (Feb 7 2003): 317-323.

Myint, P., D. J. Deeble, P. C. Beaumont, S. M. Blake, and G. O. Phillips. "The Reactivity of various Free Radicals with Hyaluronic Acid: Steady-State and Pulse Radiolysis Studies." *Biochimica Et Biophysica Acta* 925, no. 2 (Aug 13 1987): 194-202.

Natowicz, M. R., M. P. Short, Y. Wang, G. R. Dickersin, M. C. Gebhardt, D. I. Rosenthal, K. B. Sims, and A. E. Rosenberg. "Clinical and Biochemical Manifestations of

Hyaluronidase Deficiency." *The New England Journal of Medicine* 335, no. 14 (Oct 3 1996): 1029-1033.

Newman, A. P., G. Z. Acton, E. Hartwieg, H. R. Horvitz, and P. W. Sternberg. "The Lin-11 LIM Domain Transcription Factor is Necessary for Morphogenesis of C. Elegans Uterine Cells." *Development (Cambridge, England)* 126, no. 23 (Dec 1999): 5319-5326.

Novak, U., S. S. Stylli, A. H. Kaye, and G. Lepperdinger. "Hyaluronidase-2 Overexpression Accelerates Intracerebral but Not Subcutaneous Tumor Formation of Murine Astrocytoma Cells." *Cancer Research* 59, no. 24 (Dec 15 1999): 6246-6250.

Olson, S. K., J. R. Bishop, J. R. Yates, K. Oegema, and J. D. Esko. "Identification of Novel Chondroitin Proteoglycans in Caenorhabditis Elegans: Embryonic Cell Division Depends on CPG-1 and CPG-2." *The Journal of Cell Biology* 173, no. 6 (Jun 19 2006): 985-994.

Pham, H. T., N. L. Block, and V. B. Lokeshwar. "Tumor-Derived Hyaluronidase: A Diagnostic Urine Marker for High-Grade Bladder Cancer." *Cancer Research* 57, no. 4 (Feb 15 1997): 778-783.

Ponta, H., L. Sherman, and P. A. Herrlich. "CD44: From Adhesion Molecules to Signalling Regulators." *Nature Reviews.Molecular Cell Biology* 4, no. 1 (Jan 2003): 33-45.

Rai, S. K., F. M. Duh, V. Vigdorovich, A. Danilkovitch-Miagkova, M. I. Lerman, and A. D. Miller. "Candidate Tumor Suppressor HYAL2 is a Glycosylphosphatidylinositol (GPI)-Anchored Cell-Surface Receptor for Jaagsiekte Sheep Retrovirus, the Envelope Protein of which Mediates Oncogenic Transformation." *Proceedings of the National Academy of Sciences of the United States of America* 98, no. 8 (Apr 10 2001): 4443-4448.

Rea, S., and T. E. Johnson. "A Metabolic Model for Life Span Determination in Caenorhabditis Elegans." *Developmental Cell* 5, no. 2 (Aug 2003): 197-203.

Rhiner, C., S. Gysi, E. Frohli, M. O. Hengartner, and A. Hajnal. "Syndecan Regulates Cell Migration and Axon Guidance in C. Elegans." *Development (Cambridge, England)* 132, no. 20 (Oct 2005a): 4621-4633.

Rhiner, C., S. Gysi, E. Frohli, M. O. Hengartner, and A. Hajnal. "Syndecan Regulates Cell Migration and Axon Guidance in C. Elegans." *Development (Cambridge, England)* 132, no. 20 (Oct 2005b): 4621-4633.

Rigden, D. J., and M. J. Jedrzejas. "Structures of Streptococcus Pneumoniae Hyaluronate Lyase in Complex with Chondroitin and Chondroitin Sulfate Disaccharides. Insights into Specificity and Mechanism of Action." *The Journal of Biological Chemistry* 278, no. 50 (Dec 12 2003): 50596-50606.

Roden, L., P. Campbell, J. R. Fraser, T. C. Laurent, H. Pertoft, and J. N. Thompson. "Enzymic Pathways of Hyaluronan Catabolism." *Ciba Foundation Symposium* 143 (1989): 60-76; discussion 76-86, 281-5.

Rogalski, T. M., G. P. Mullen, J. A. Bush, E. J. Gilchrist, and D. G. Moerman. "UNC-52/perlecan Isoform Diversity and Function in Caenorhabditis Elegans." *Biochemical Society Transactions* 29, no. Pt 2 (May 2001): 171-176.

Sampson, P. M., C. L. Rochester, B. Freundlich, and J. A. Elias. "Cytokine Regulation of Human Lung Fibroblast Hyaluronan (Hyaluronic Acid) Production. Evidence for Cytokine-Regulated Hyaluronan (Hyaluronic Acid) Degradation and Human Lung Fibroblast-Derived Hyaluronidase." *The Journal of Clinical Investigation* 90, no. 4 (Oct 1992): 1492-1503.

Sharma-Kishore, R., J. G. White, E. Southgate, and B. Podbilewicz. "Formation of the Vulva in Caenorhabditis Elegans: A Paradigm for Organogenesis." *Development (Cambridge, England)* 126, no. 4 (Feb 1999): 691-699.

Simske, J. S., and S. K. Kim. "Sequential Signalling during Caenorhabditis Elegans Vulval Induction." *Nature* 375, no. 6527 (May 11 1995): 142-146.

Soltes, L., M. Stankovska, G. Kogan, P. Gemeiner, and R. Stern. "Contribution of Oxidative-Reductive Reactions to High-Molecular-Weight Hyaluronan Catabolism." *Chemistry & Biodiversity* 2, no. 9 (Sep 2005): 1242-1245.

Spicer, A. P., and J. A. McDonald. "Characterization and Molecular Evolution of a Vertebrate Hyaluronan Synthase Gene Family." *The Journal of Biological Chemistry* 273, no. 4 (Jan 23 1998): 1923-1932.

Stern, R. "Hyaluronan Metabolism: A Major Paradox in Cancer Biology." *Pathologie-Biologie* 53, no. 7 (Sep 2005): 372-382.

Stern, R. "Devising a Pathway for Hyaluronan Catabolism: Are we there Yet?" *Glycobiology* 13, no. 12 (Dec 2003): 105R-115R.

Stern, R., A. A. Asari, and K. N. Sugahara. "Hyaluronan Fragments: An Information-Rich System." *European Journal of Cell Biology* 85, no. 8 (Aug 2006): 699-715.

Stern, R., and M. J. Jedrzejas. "Hyaluronidases: Their Genomics, Structures, and Mechanisms of Action." *Chemical Reviews* 106, no. 3 (Mar 2006): 818-839.

Sternberg, P. W., and H. R. Horvitz. "Pattern Formation during Vulval Development in C. Elegans." *Cell* 44, no. 5 (Mar 14 1986): 761-772.

Sternberg,P.W., Vulval development (June 25, 2005), *WormBook*, ed. The *C.elegans* Research Community, WormBook, doi/10.1895/wormbook.1.6.1, http://www.wormbook.org.

Sulston, J. E., and J. G. White. "Regulation and Cell Autonomy during Postembryonic Development of Caenorhabditis Elegans." *Developmental Biology* 78, no. 2 (Aug 1980): 577-597.

Suzuki, N., H. Toyoda, M. Sano, and K. Nishiwaki. "Chondroitin Acts in the Guidance of Gonadal Distal Tip Cells in C. Elegans." *Developmental Biology* (Aug 22 2006).

Timmons, L., and A. Fire. "Specific Interference by Ingested dsRNA." *Nature* 395, no. 6705 (Oct 29 1998): 854.

Toole, B. P. "Hyaluronan in Morphogenesis." *Seminars in Cell & Developmental Biology* 12, no. 2 (Apr 2001): 79-87.

Toole, B. P., and J. Gross. "The Extracellular Matrix of the Regenerating Newt Limb: Synthesis and Removal of Hyaluronate Prior to Differentiation." *Developmental Biology* 25, no. 1 (May 1971): 57-77.

Toyoda, H., A. Kinoshita-Toyoda, and S. B. Selleck. "Structural Analysis of Glycosaminoglycans in Drosophila and Caenorhabditis Elegans and Demonstration that Tout-Velu, a Drosophila Gene Related to EXT Tumor Suppressors, Affects Heparan Sulfate in Vivo." *The Journal of Biological Chemistry* 275, no. 4 (Jan 28 2000): 2269-2275.

Treusch, S., S. Knuth, S. A. Slaugenhaupt, E. Goldin, B. D. Grant, and H. Fares. "Caenorhabditis Elegans Functional Orthologue of Human Protein h-Mucolipin-1 is Required for Lysosome Biogenesis." *Proceedings of the National Academy of Sciences of the United States of America* 101, no. 13 (Mar 30 2004): 4483-4488.

Triggs-Raine, B., T. J. Salo, H. Zhang, B. A. Wicklow, and M. R. Natowicz. "Mutations in HYAL1, a Member of a Tandemly Distributed Multigene Family Encoding Disparate Hyaluronidase Activities, Cause a Newly Described Lysosomal Disorder, Mucopolysaccharidosis IX." *Proceedings of the National Academy of Sciences of the United States of America* 96, no. 11 (May 25 1999): 6296-6300.

Udabage, L., G. R. Brownlee, S. K. Nilsson, and T. J. Brown. "The Over-Expression of HAS2, Hyal-2 and CD44 is Implicated in the Invasiveness of Breast Cancer." *Experimental Cell Research* 310, no. 1 (Oct 15 2005a): 205-217.

Udabage, L., G. R. Brownlee, M. Waltham, T. Blick, E. C. Walker, P. Heldin, S. K. Nilsson, E. W. Thompson, and T. J. Brown. "Antisense-Mediated Suppression of Hyaluronan Synthase 2 Inhibits the Tumorigenesis and Progression of Breast Cancer." *Cancer Research* 65, no. 14 (Jul 15 2005b): 6139-6150.

Wells, L., K. Vosseller, and G. W. Hart. "A Role for N-Acetylglucosamine as a Nutrient Sensor and Mediator of Insulin Resistance." *Cellular and Molecular Life Sciences : CMLS* 60, no. 2 (Feb 2003): 222-228.

Wisniewski, H. G., M. H. Sweet, and R. Stern. "An Assay for Bacterial and Eukaryotic Chondroitinases using a Chondroitin Sulfate-Binding Protein." *Analytical Biochemistry* 347, no. 1 (Dec 1 2005): 42-48.

Yamada, S., Y. Okada, M. Ueno, S. Iwata, S. S. Deepa, S. Nishimura, M. Fujita, I. Van Die, Y. Hirabayashi, and K. Sugahara. "Determination of the Glycosaminoglycan-Protein Linkage Region Oligosaccharide Structures of Proteoglycans from Drosophila Melanogaster and Caenorhabditis Elegans." *Journal of Biological Chemistry* 277, no. 35 (Aug 30 2002): 31877-31886.

Yamada, S., I. Van Die, D. H. Van den Eijnden, A. Yokota, H. Kitagawa, and K. Sugahara. "Demonstration of Glycosaminoglycans in Caenorhabditis Elegans." *FEBS Letters* 459, no. 3 (Oct 15 1999): 327-331.

Zhang, S., M. C. Chang, D. Zylka, S. Turley, R. Harrison, and E. A. Turley. "The Hyaluronan Receptor RHAMM Regulates Extracellular-Regulated Kinase." *The Journal of Biological Chemistry* 273, no. 18 (May 1 1998): 11342-11348.

Zhang, H., and P. A. Martin-DeLeon. "Mouse Spam1 (PH-20) is a Multifunctional Protein: Evidence for its Expression in the Female Reproductive Tract." *Biology of Reproduction* 69, no. 2 (Aug 2003): 446-454.

Zhou, B., J. A. Weigel, L. Fauss, and P. H. Weigel. "Identification of the Hyaluronan Receptor for Endocytosis (HARE)." *The Journal of Biological Chemistry* 275, no. 48 (Dec 1 2000): 37733-37741.